# REMEDIATION OF CRUDE OIL POLLUTED SOIL WITH COW DUNG AND *Pennisetum purpureum* ZINC OXIDE NANOPARTICLES

**BY**

**ENEMUGWEM, RACHEL ITONGNTE (B.Sc, PGD (UNIPORT); M.Sc (FUTO)**

**(REG NUMBER: 20184143058)**

**A DISSERTATION SUBMITTED TO THE POSTGRADUATE SCHOOL,**

**FEDERAL UNIVERSITY OF TECHNOLOGY, OWERRI.**

**IN PARTIAL FULFILMENT OF THE REQUIREMENTS FOR THE AWARD OF DOCTOR OF PHILOSOPHY (Ph.D) DEGREE IN**

**ENVIRONMENTAL BIOCHEMISTRY.**

**FEBRUARY, 2025**

## CERTIFICATION

This is to certify that this research work titled "**Remediation of Crude Oil Polluted Soil with Cow Dung and *Pennisetum purpureum* Zinc Oxide Nanoparticles**" was carried out by Enemugwem, Rachel Itongnte (Reg. number 20184143058) in partial fulfilment for the award of degree of Doctor of Philosophy (Ph.D) in Environmental Biochemistry in the Department of Biochemistry, Federal University of Technology, Owerri.

Professor C. S. Alisi
(Supervisor)

11/03/25
Date

Professor C. O. Ujowundu
(Supervisor)

11/03/2025
Date

Dr. C. I. Iheme
(Supervisor)

11/03/25
Date

Professor L. A. Nwaogu
Head, Department of Biochemistry

Date

Professor C. S. Alisi
Dean, School of Biological Sciences

11/03/25
Date

Professor (Mrs) J. N Nwosu
Dean, School of Post Graduate Studies

Date

Prof Lawrence Uhuo

External Examiner

23/01/25
Date

## DEDICATION

This work is dedicated to God almighty for His immense love towards me.

## ACKNOWLEDGEMENTS

I am forever grateful to my supervisor Prof. C. S. Alisi for helping me start and finish this programme and his contributions to this project work. I also appreciate my co-supervisors Prof. C. O. Ujowundu and Dr. C.I. Iheme for their contributions to the success of this study.

I wish to appreciate my Head of Department Professor L. A. Nwaogu, my lecturers Prof. K.M.E. Iheanacho, Prof. C. O. Ibegbulem, Prof. A. C. Ene, Prof. R. N. Nwaoguikpe, Dr. C. U. Igwe, Dr. (Mrs) F. N. Ujowundu, Dr. (Mrs.) D. I. Ukairo, Dr. Chioma Ezirim and my friends Dr. Nmadike Ezeji, Dr. Stanley Ogbonna and Dr. Uche Olunkwa in the Department of Biochemistry FUTO.

I humbly thank my beloved husband Dr. Ekejiuba Christopher and my children Onyinyechi, Christabel and ChrisBen for according me the love, support and opportunity to study.

My heartfelt thanks go to my beloved parents Professor and Mrs. John Enemugwem, my siblings and their family Engr. Horace Enemugwem, Mrs. Keturah Chikwe, Mrs. Sylverline Opuada Hart, Dr. Rogers Enemugwem, Miss InemeAwaji Fingesi, Miss Vydah Harold and my inlaws Mr and Mrs. Okechukwu Ekejiuba, Mr Nnamdi Ekejiuba, Mr Chizoba Ekejiuba and Miss Jane Ekejiuba for standing by me.

My heartfelt appreciation goes to my friends Mrs. Catherine Baridakara, Mrs. Nuka, Dr. (Mrs.) Gift Lucky, Mrs Barisi Felix, Dr. Famuyibo Dickson and Dr. Sudor Nwiyor in Kenule Beeson Saro-Wiwa Polytechnic, Bori for their encouragement and motivation throughout my PhD journey.

I would like to express my deepest gratitude to the Tertiary Education Trust Fund (TETFund) for their financial support in my Ph.D program.

I am grateful to God Almighty for his grace and mercies which saw me through this programme.

## TABLE OF CONTENT

**CHAPTER THREE**
**MATERIALS & METHODS**

**CHAPTER FOUR**
**RESULTS AND DISCUSSION**



**CHAPTER FIVE**
**CONCLUSION AND RECOMMENDATION**

## LIST OF TABLES

## LIST OF FIGURES

## ABSTRACT

This study investigated the remediation of crude oil polluted soil with cow dung and *Pennisetum purpureum* zinc oxide (ZnO) nanoparticles. Zinc oxide nanoparticles were synthesised using an aqueous leaf extract of *Pennisetum purpureum* and cow dung. The ZnO nanoparticles were characterized by ultraviolet–visible spectroscopy (UV–Vis), Fourier transform infrared spectroscopy (FTIR), X-Ray diffraction (XRD) and transmission electron microscopy (TEM). The phytochemical properties of *Pennisetum purpureum*, cow dung and ZnO nanoparticles were assessed using gas chromatography mass spectrometry (GC-MS). One kilogram soil was polluted invitro with 100 mL Bonny light crude oil. This study was carried out for 42 days. The concentrations of polycyclic aromatic hydrocarbons (PAHs), heavy metals, Benzene, Toluene, Ethylbenzene and Xylene (BTEX), total organic carbon (TOC), total petroleum hydrocarbon (TPH), nitrogen, phosphorous, pH, total heterotrophic bacteria (THB) and total hydrocarbon utilizing bacteria (THUB) count were determined in unpolluted, polluted and remediated soil using standard analytical methods. The major bioactive compounds in *Pennisetum purpureum* were linoleic acid (18.89%), cis-13-octadecenoic acid (15.74%), 1,2-benzisothiazole (6.69%), 11-octadecenoic acid (5.53%), oleic acid (5.01%), the major bioactive compounds in cow dung were trans-13-octadecenoic acid (12.03%), 8, 11 – octadecadienoic acid (8.29%), 9-octadecanoic acid (8.11%), cycloeisane (7.43%). UV–vis spectra showed absorption peaks at 367nm (3.38 eV) for cow dung ZnO nanoparticles and 370nm (3.35 eV) for *Pennisetum purpureum* ZnO nanoparticles. FTIR analyses identified functional groups (C-O, O-H, CH, C≡C, C=C, N-O) and chemical bond formations in *Pennisetum purpureum* and cow dung ZnO nanoparticles. XRD results revealed ZnO nanoparticle's crystalline structure, phase composition and average particle size of 23.37nm (*Pennisetum purpureum* ZnO nanoparticles) and 18.17nm (cow dung ZnO nanoparticles). The TEM images showed that the biosynthesised ZnO nanoparticles were spherical in shape with an average mean particle size of 3.47nm for cow dung ZnO and 15.21nm for *Pennisetum purpureum* ZnO nanoparticles at 100nm magnification. The remediation of crude oil polluted soil with cow dung and *Pennisetum purpureum* ZnO nanoparticles was dose dependent (20g and 40g). The pH of the polluted soil was acidic and alkaline in treated soil. There was a significant reduction ($p<0.05$) in the concentrations of heavy metal (As, Cr, Hg, Zn, Ni), nitrogen, zinc, phosphorous, PAH, BTEX, TOC, TPH on the crude oil polluted soil treated with cow dung and *Pennisetum purpureum* ZnO nanoparticles because of the photocatalytic activity of the ZnO nanoparticles on the pollutants. Total heterotrophic bacterial and total hydrocarbon utilizing bacteria count increased progressively during the 42 days study period. The higher concentrations (40g) of the nanoparticles were more efficient for soil remediation than lower concentrations (20g). The results from this study showed that cow dung and *Pennisetum purpureum* ZnO nanoparticles are photocatalysts and has the potential to degrade pollutants and reduce the clean - up time.



**Key words**: "Nanoparticles, zinc oxide (ZnO), cow dung, *Pennisetum purpureum,* Crude oil"

# CHAPTER ONE

# INTRODUCTION

## 1.1 Background of Study

Crude oil is a naturally occurring flammable liquid composed of aromatic, aliphatic hydrocarbons and other heterocyclics in varied concentrations. It is found in very large quantities as deposits in rocks beneath the earth's lithosphere. Crude oil is a complex mixture of predominantly carbon and hydrogen in varying molecular weights, though it also contains some nitrogen, oxygen and sulphur (Norman, 2001).

The high request for petroleum products in form of gas oil, cooking gas, engine lubricating oil, aviation fuel increases its production and eventually results in oil spills and hydrocarbon pollution of environments (Resinger, 1995). In Nigeria, Niger Delta has witnessed several instances of oil spills in some communities like Uzere and Olomoro in Isoko South Local Government Area, Owhe-Ologbo and Erumukohwarian in Ugehili North, Ogoni, Andoni in Rivers State and also Bayelsa State. Most mangrove swamps and marsh land areas have recorded oil contamination which causes slow rate of germination of plants and reduces soil fertility (Eboh, 1995).

It has been reported that 1.7 to 8.8 million metric tons of petroleum hydrocarbon escape into water bodies and soil every year or annually. Hydrocarbon contamination (especially polycyclic aromatic hydrocarbons (PAHs)) of fresh water and soil attract public attention because polycyclic aromatic hydrocarbons are toxic, carcinogenic and mutagenic (Clemente, Anazawa & Durrant, 2001).

Nanotechnology is now considered to be a proven state-of-the-art technology with important roles in pharmaceutical, mechanical, food processing industries power generation, optics, drug delivery, and environmental sciences (Ramsden, 2016). The development of nanotechnology and the use of nanomaterials is an innovative strategy for treating pollutants in soil, groundwater and wastewater (Vazquez-Núnez, Molina-Guerrero, Pena-Castro, Fernández-Luqueno & de la

Rosa-Álvarez, 2020). In the advent of nanotechnology, many nanoscale devices have been developed using numerous methods, such as physical, chemical, and green approaches (Albrecht, Evans & Durrant, 2006). A nanoparticle is a small particle that ranges between 1 to 100 nanometres in size (Sabouri, Amiri & Khatarrin, 2022). It has gained a lot of attention due to properties like the smaller size, high surface to volume ratio, higher strength, excellent delivery, catalytic properties.

Zinc oxide has certain remarkable features such as sensitivity, selectivity and chemical/thermal stability. When compared to other metal oxide nanoparticles, zinc oxide (ZnO) nanomaterials are not only inexpensive but also non-toxic (harmless/safe) and environmentally benign (Kalpana et al., 2018). Currently, there has been significant interest in the clean and cost-effective synthesis of zinc oxide nanoparticles and exploration of their uses as an active media in many device applications.

Green synthesis is an emerging field dedicated to the development and improvement of nanoparticle production in an effective, eco-friendly and non-hazardous manner. Green synthesis researchers are increasingly developing new nanoparticles to treat a wide range of environmental contaminants, heavy metals and organic pollutants. The presence of remarkable natural bioactive components in aqueous extract of plants, animal waste and microbes have medicinal characteristics such as anticancer, antioxidant, anti-inflammatory properties and also serve as surfactant, stabilizers, capping and coating agent in nanoparticle synthesis (Senthamarai, 2022). Therefore, scientists are exploring various plant extracts, flowering, fruiting parts, microbial and cellular components for the green synthesis of the nanoparticles.

## 1.2 Statement of Problem

Crude oil is a quick and easily accessible source of energy. Its leakage and spill during extraction and transportation has posed danger to the environment because of its content of mutagenic and carcinogenic compounds. The toxicity, mutagenic and carcinogenic nature may affect human

health and the ecosystem. The conventional methods of remediation have been used for decades and have shown great results, but have also shown drawbacks due to the use of hazardous chemicals, high cost, long-term treatment, difficulty in reducing the concentration of pollutants to the regulated levels. In this study cow dung and *Pennisetum purpureum* zinc oxide nanoparticles were used to remediate crude oil polluted soil.

### 1.3 Objective of Study

The main objective of this work was to synthesize cow dung and *Pennisetum purpureum* zinc oxide nanoparticles and remediate crude oil polluted soil with the synthesized zinc oxide nanoparticles.

The specific objectives of this research work were to:

a. Synthesize zinc oxide nanoparticles using aqueous extracts of cow dung.
b. Synthesize zinc oxide nanoparticles using aqueous extracts of *Pennisetum purpureum*.
c. Characterize cow dung zinc oxide nanoparticles using various dispersion methods such as UV - visible spectroscopy, Fourier-transform infrared spectroscopy (FTIR), Transmission electron microscopy (TEM), X-ray diffraction (XRD).
d. Characterize *Pennisetum purpureum* zinc oxide nanoparticles using various dispersion methods such as UV - visible spectroscopy, Fourier-transform infrared spectroscopy (FTIR), Transmission electron microscopy (TEM), X-ray diffraction (XRD).
e. Determine the phytochemical properties of *Pennisetum purpureum* and *Pennisetum purpureum* zinc oxide nanoparticles.
f. Determine the phytochemical properties of cow dung and cow dung zinc oxide nanoparticles.
g. Remediate crude oil polluted soil with cow dung zinc oxide nanoparticles.
h. Remediate crude oil polluted soil with *Pennisetum purpureum* zinc oxide nanoparticles.

i. Determine the physicochemical properties of unpolluted and crude oil polluted soil.

j. Determine the physicochemical properties of the remediated soil by cow dung zinc oxide nanoparticles.

k. Determine the physicochemical properties of the remediated soil by *Pennisetum purpureum* zinc oxide nanoparticles.

l. Determine the heavy metal concentration, benzene, toluene, ethyl benzene and xylene (BTEX), total petroleum hydrocarbon (TPH), polycyclic aromatic hydrocarbon (PAH), total heterotrophic bacteria (THB) count, total hydrocarbon utilizing bacteria (THUB) count in unpolluted, polluted and remediated soil.

## 1.4 Justification of the Study

Crude oil contamination is one of the major environmental problems affecting aquatic and terrestrial environment. Conventional methods of soil remediation have been in use for decades and have shown great results, but have also shown drawbacks due to the use of hazardous chemicals, high cost, long-term treatment, difficulty in reducing the concentration of pollutants to the regulated levels (Schrick, Hydutsky, Blough & Mallouk, 2004). Nanoremediation has the potential to reduce the costs of clean-up of large-scale contaminated sites, reduce clean up time, minimize pollutant concentrations and its ecofriendly. Nanoparticles have been used to remediate contaminated soil. (Vu & Mulligan, 2022). Zinc oxide nanostructures exhibit high catalytic efficiency, as well as strong adsorption ability, it has been successfully used as an adsorbent and photocatalyst in environmental remediation process because they exhibit photocatalytic activity under irradiation of sunlight. The presence of biomolecules in elephant grass and cow dung aqueous extracts were responsible for the reduction, capping and stabilization of the nanoparticles (Rana, Yadav & Jagadevan, 2020). This present study is on remediation of crude oil polluted soil with cow dung zinc oxide nanoparticles and *Pennisetum purpureum* zinc oxide nanoparticles.

## 1.5 Scope of the Study

Zinc oxide nanoparticles were synthesized using aqueous extract of cow dung and *Pennisetum purpureum* (Leaf). The synthesized cow dung zinc oxide nanoparticle and *Pennisetum purpureum* zinc oxide nanoparticles were characterized by UV spectroscopy, Fourier-transform infrared spectroscopy (FTIR), Transmission electron microscopy (TEM), X-ray diffraction (XRD).

Physicochemical properties such as heavy metal, benzene, toluene, ethyl benzene and xylene (BTEX), total petroleum hydrocarbon (TPH), polycyclic aromatic hydrocarbon (PAH) concentrations, total heterotrophic bacteria (THB) count, total hydrocarbon utilizing bacteria (THUB) count in unpolluted, polluted and remediated soil were determined using standard analytical techniques.

# CHAPTER TWO

# LITERATURE REVIEW

## 2.1 Elephant Grass (*Pennisetum purpureum*)

Elephant grass (*Pennisetum purpureum* Schumach) is a major tropical grass and one of the highest yielding tropical grasses. It can be grown under a wide range of conditions (dry or wet conditions) (Mannetje, 1992; FAO, 2015).

Elephant grass is a rhizomatous, robust, tufted perennial grass. The leaves are flat, linear and hairy at the base, up to 1-5 cm wide and 100-120 cm long (DAFF, 2014).

Elephant grass is a very important forage in the tropics and it is suited to feed cattle, buffaloes and elephants. It is made into hay or silage and mainly used in cut-and-carry systems ("zero grazing") to livestock (FAO, 2015). The culms can be used to make fences, and the whole plant is used for thatch. It is also considered a potential second-generation energy source crop in the USA (EPA, 2013).

*Pennisetum purpureum* have several environmental applications. It can be used to make mulch, soil erosion control, weed controller and in Africa, it has been used as a trap plant in push-pull management strategies to fight against stemborers in maize crops (Khan, Wadhams & Mumuni, 2007).

*Pennisetum purpureum* have been used in phytoremediation studies, it can degrade high concentration of pollutants (Das & Chandran, 2017; Boonmeerati & Sampanpanish, 2021). Many studies that reported the use of *Pennisetum purpureum* in phytoremediation were restricted to the treatment of inorganic pollutants, few studies have investigated the use of the plant in phytoremediation of petroleum hydrocarbon contaminated soil (Kang, Seo, Saito, Suzuki & Ishii, 2015; Osmana, Roslana, Ibrahima & Hassana, 2020).

## 2.2 Cow Dung

Cow dung is the undigested residue of plant matter which has passed through the cow gut and the resultant faecal matter is rich in minerals. The colour ranges from greenish to blackish, often darkening soon after exposure to air (Garg & Mudgal, 2007).

Diverse group of microorganisms that may be beneficial to humans are harboured in cow dung. Microorganisms that are capable of degrading hydrocarbon pollutants, have been isolated and identified from cow dung. These organisms include; *Micrococcus sp., Pseudomonas sp., Bacillus sp., Enterobacter sp., Aspergillus sp., Proteus klebsiella, Rhizopus and Penicillium*. Therefore, cow dung is an effective, eco-friendly, economical and bioremediation agent which can lead to complete mineralization of hydrocarbon (Neethu, Dubey, Kaswala & Patel, 2019).

The major chemical compounds present in the cow dung extract are tetraethylene glycol (17.57%), palmitic Acid (16.21%), 2-Ethoxyethyl methyl phthalate (17.40%), 2-Propanol, oleic acid (5.13%), phosphate (5.41%), Myristic acid (5.57%), phthalic acid, 3-chlorophenyl methyl ester (4.52%), hexadecanoic acid (2.44%) and stearic acid (2.26%). Most of these compounds are reported as useful component in nanoparticle synthesis and perform various functions like stabilizers and coating agents in nanoparticle synthesis (Dong et al*.,* 2016).

## 2.3 Crude Oil

Crude oil is a naturally occurring flammable liquid composed of aromatic, aliphatic hydrocarbons and other heterocyclics in varied concentrations. It is found in very large quantities as deposits in rocks beneath the Earth's lithosphere. Crude oil is a complex mixture of predominantly carbon and hydrogen in varying molecular weights, though it also contains some nitrogen, sulphur, and oxygen (Norman, 2001). It consists of three major distinctive categories: naphthenes, paraffins and aromatics (Varjani, Rana, Jain, Bateja & Upasani, 2018).

Bonny light crude oils are classified as light crude oils, with aromatic hydrocarbons of at least 45% of the total hydrocarbons. Given the relatively higher solubility of the aromatic hydrocarbons in water, less water–soluble crude oils and higher toxicity of light crude oil than the heavier, (Orisakwe, Akumka, Njan & Afonne, 2004; Ezike, Igugo, Uwadiegwu & Felix, 2019). The lipophilicity of these crude oil components confer on them the intrinsic properties of energy inhibitors and electron uncouplers with the biological membrane being the major target sites of their adverse effects (Orisakwe et al., 2004).

### 2.3.1 Significance of crude oil in modern times

Crude oil provides fuel for various means of transportation on sea, land and air. It provides electricity generation. It is also a feedstock for the chemical industries, in the manufacturing of plastics, detergents, cosmetics, insecticides, road construction materials, paints and fertilizers (Das & Chandran, 2011).

### 2.3.2 Crude oil pollution and the consequences, especially in the Niger Delta

Nigeria's petroleum is free of sulphur and classified mostly as "light" and "sweet". Nigeria is the largest producer of sweet oil in organization of the petroleum exporting countries. The second largest oil and gas producer in Africa after Angola is Nigeria. Crude oil from the Niger Delta basin comes in two types: heavy and light, the lighter has 36 of API gravity while the heavier has 20–25 of API gravity. Both types are low in sulphur and paraffinic (David, 1995).

The advent of crude oil production has negatively impacted the Niger Delta region due to unprecedented oil spillage which has made the region one of the most polluted in the world ( UNEP, 2017).

Half of all oil spills occur due to pipeline and tanker accidents and corrosion (50%), other causes include oil production operations (21%), sabotage (28%) and 1% of the spills being accounted for by non-functional or inadequate production equipment ( Nwilo & Badejo, 2001 ).

There are no consistent figures of the quantity of crude oil spilled in the Niger delta, it is believed that since 1958 an estimated 13 million barrels (1.5 million tons) of crude oil have been spilled from over 7000 oil spill incidents; a yearly average of about 240,000 barrels (UNDP, 2006), Inconsistency in the quantity of crude oil spilled has been attributed to a number of reasons, including security concerns limiting access, difficulty in accessing some spill sites due to swamp conditions and remoteness, some spills occurring away from community locations, high volatility of the Nigerian crude oil, a long time-lag between the initiation of a spill and its detection, causing an estimated 50% to evaporate within 24-48 h; intentional company and government under-reporting and inadequate government oversight (Steiner, 2010).

Crude oil spill reduces soil fertility and quality of food crops (Osuji & Nwoye, 2007), smother economic trees and outrightly reducing their yield or killing them (Edema, Obadoni, Erheni & Osakwuni, 2009) oil spills also reduces the quality of food crops (Nwaoguikpe, 2011; Osam, Wegwu & Uwakwe, 2011), bio-accumulation of heavy metals in the surviving food crops like pumpkin and cassava (Nkwoocha & Duru, 2010).

Oil spillage has impact on the ecosystem and may constitute ecocide (Okon, 2017). Immense tracts of the mangrove forests, which are especially susceptible to oil because it is stored in the soil and released during inundations, have been destroyed. Oil spills in populated areas often spread out over a wide area, destroying aquacultures and crops through contamination of the groundwater and soils. In the impacted communities, crude oil spill also resulted in the reduction of the quantity and quality of food available to households. This could result in 24% increase in the prevalence of childhood malnutrition and several hunger pangs. These situations were said to be exacerbated in the Niger delta region by the near total absence of outside relief effort, such that members of the impacted communities were often left unassisted by the government and the oil company (Ordinioha & Sawyer, 2008). The health implications, childhood malnutrition and hunger are obvious (Rice, Sacco, Hyder & Black, 2000). The implication of the

exchange of sex for financial and other gratifications that is common in Niger delta communities in a period of lack are not well recognized (Nwauche & Akani, 2001). This exchange has been linked to the high prevalence of teenage pregnancy, abortion (Anochie & Ikpeme, 2001), sexually transmitted infections (Federal Ministry of Health Nigeria, 2003) and HIV/AIDS in the region (Federal Ministry of Health Nigeria, 2010). One fifth of the oil spills were attributed to third party activity and therefore did not attract any form of compensation to the impacted communities according to a clause in the Nigeria's oil pipeline act that was designed to discourage sabotage. It is surprising that medical care and material relief were seen as "compensation" and therefore denied to members in the affected communities. Members of the communities often kill and eat the fish from the polluted river and also bear the full cost of resultant health problem. Considering the acute and long-term effects of exposure to the oil spill, it is not good for innocent members of the communities to face the situation alone; the least they should receive are material relief and immediate and long-term medical treatment, the world standard for persons exposed to potentially carcinogenic environmental hazards. This formed the basis of the public health recommendations in the Ogoni UNEP report. (UNEP, 2011) and should be the standard practice throughout Nigeria.

### 2.4 Heavy Metals

Heavy metals are metals that have high densities (4.5 $g.cm^{-3}$), they are good electrical and thermal electrical conductivity materials in solid and liquid states, and they are not transparent and gloss in opalescence (Ociepa-Kubicka & Ociepa, 2012). They show toxic properties caused by their ability to accumulate in tissues and organs. These elements can get through the skin, inhaled and consumed with plant and animal products. Some of the heavy metals ( Zn, As, Cd, Hg, Cu) can cause immediate acute poisoning, others (As, Zn, Cd, Cr, Cu, Hg, Pb, Sn, Co, Ni, Mn, Se, Fe & Ag) cause chronic conditions (Kostrz & Satora, 2017).

The sources of heavy metals in plant and soil are mainly natural, including geologic sources such as rock formation, transported sediments by winds and soils while the artificial sources include industrial sources that supply the heavy metals to the soil and air causing contamination of the environment. It is expected that the heavy metal concentration varied considerably with the polluted, contaminated and industrial areas, depending on the wind speed and directions (Ahrens, 2005).

Nanoremediation is cost effective and ecofriendly, this technique uses nanoparticles to detoxify heavy metal contaminants in the soil, water and other environments. This remediation technique has proven to be effective in the removal of heavy metals by absorbing, reducing the toxic valence to a stable metallic state and catalyzing the reaction (Gil-Díaz et al., 2016).

## 2.5 Polycyclic Aromatic Hydrocarbons

Polycyclic aromatic hydrocarbons are organic compounds comprised of two or more condensed aromatic rings (Speight, 2006). Physically, they are described as colourless, white, or pale yellow solids with varying melting and boiling points (Abdel-Shafy & Mansour, 2015). Chemically polycyclic aromatic hydrocarbons comprise of two or more benzene rings bonded in linear angular or cluster arrangements and are found in many petroleum mixtures (Arey & Atkinson, 2003). In addition, they have low vapour pressure, very low aqueous solubility, light sensitivity, heat resistance; heat conductivity, emit ability, corrosion resistance, and physiological action (Akyuz & Cabuk, 2010). Polycyclic aromatic hydrocarbons containing up to six fused aromatic rings are often known as ‘‘small” polycyclic aromatic hydrocarbons, and those containing more than six aromatic rings are called ‘‘large” polycyclic aromatic hydrocarbons. The major source of polycyclic aromatic hydrocarbons is crude petroleum however; they are predominantly introduced to the environment through natural and anthropogenic combustion processes (Speight, 2006).

## 2.6 Benzene, Toluene, Ethyl Benzene and Xylene (BTEX)

The chemicals of benzene, toluene, ethyl benzene and xylene occur naturally in crude oil and can be found in sea water in the vicinity of natural gas and petroleum deposits. Benzene, toluene, ethyl benzene and xylene compounds are created and used during the processing of petroleum products, cosmetics, inks, adhesives and pharmaceutical products. Leakage of gasoline from underground storage tanks causes groundwater contamination which is primarily due to the presence of benzene, toluene, ethyl benzene and xylene. The organic chemicals of petroleum products are able to enter the soil and groundwater systems and cause serious pollution problems because of their polarity and very soluble characteristics. Benzene, toluene, ethyl benzene and xylene compounds are among the most abundantly produced chemicals in the world (Naraboyina & Rastogi, 2014).

## 2.7 Bioremediation

Bioremediation is the use of specific microorganisms or plants to degrade, detoxify, mineralize or transform harmful substances innocuous state. These organisms are known for their biochemical and physical affinity to hydrocarbons among other pollutants. Various types of bacteria, fungi, archaea, algae and some species of plants are all able to break down specific toxic waste products into safer constituents. Bioremediation is classified by the organism responsible for remediation with three major subdivisions: microbial remediation, mycoremediation and phytoremediation (Shukla, Anurakti, Srivastava & Sudhakar, 2017).

Bioremediation technology is thought to be effective and inexpensive (Nwankwegu, Orji & Onwosi, 2016). Biodegradation by natural microbiological communities is one of the main mechanisms by which oil contaminants can be removed from the environment. it is cheaper than other treatment methods (Ron & Rosenberg, 2014). Several researchers have reported several factors affecting the biodegradation rate of oil (Jahangeer & Kumar, 2013). An important need for successful bioremediation is the existence of microorganisms with suitable metabolic capacity.

If microorganisms are found, optimum growth rates and microbial degradation of hydrocarbons can be maintained by providing sufficient nutrient and oxygen concentrations and a pH (6-9). The physiochemical properties of the oil are significant factors for the success of bioremediation (Eze, Onwuakor & Orok, 2014). The techniques taken for the bioremediation of oil pollutants are the addition of surfactants, microorganisms (eligible to degrade hydrocarbons), modification of the environment by adding fertilizers (N and P) or other substrates and aerating the contaminated site (composting and bulking) (biostimulation) (Ikuesan, 2017). Surfactants were utilized to elevate the unsolvable organic matter bioavailability. The incorporation of chemical oxidation and biological remediation should be cost effective, where the primary chemical operation transforms contaminants into low toxic substances and compounds that can be biodegraded (Rufino, de Luna, Takaki & Sarubbo, 2014).

The two major approaches to enhance bioremediation are bioaugmentation and biostimulation provided that environmental factors are maintained at optimal range.

Factors that affect bioremediation are pH, temperature, redox reaction potential, oxygen, moisture and other molecules present, nutrient availability, soil composition, solubility of pollutant ( Zulfa, Samir, Dhabia , Saeed & Nabil, 2017).

Three main types of bioremediation used for petroleum spills include microbial remediation, phytoremediation, and mycoremediation.

### 2.7.1 Microbial bioremediation

Microbial bioremediation uses anaerobic and aerobic properties of microorganisms to respire and ferment compounds transforming toxins into innocuous compounds. These microorganisms reduce, ferments and demobilize the constituents of oil spills over time, and create innocuous compounds. Bioremediation techniques involve using these mechanisms to reduce pollutant concentrations (Azubuike, Chikere & Okpokwasili, 2016). These

microorganisms require enzymes for the breakdown of petroleum, and very specific nutrient compositions to work successfully (Das & Chandran, 2010).

Microbial degradation is the major mechanism for the elimination of used petroleum products from the environment (Atlas & Bartha, 1992). Many microbial ecologists have recognised various microbial species that are effective degrader of hydrocarbons in natural environments. Many of these microbial consortia have been isolated and identified from heavily contaminated areas. However, bacteria play the vital role in hydrocarbon degradation. The driving force for petroleum biodegradation is the ability of microorganisms to utilize hydrocarbons to satisfy their cells growth and energy needs. A large number of studies report that low molecular weight alkanes are degraded more rapidly. In many ecosystems, there is adequate indigenous microorganisms capable of biodegradation in a favourable environmental condition (Capelli, Busalmen & De Sanchez, 2004; Kim, Choi, Sin & Oh, 2005). There are several advantages relying on indigenous microorganisms rather than adding microorganisms to degrade hydrocarbons. Firstly, natural populations of these microorganisms are adapted for survival and proliferation in that environment. Secondly, the ability to utilize hydrocarbons is distributed among a diverse microbial population. This population occurs in natural ecosystems independently or in combination and metabolizes various hydrocarbons. Nutrient availability, especially of phosphorus and nitrogen seems to be the most limiting factors. It was confirmed that these nutrients enhance growth of microorganisms which leads to more rapid decomposition of contaminants (Chaineau, Rougeux, Yepremian & Oudot, 2005).

### 2.7.2 Phytoremediation

Phytoremediation is a process in which plants are used to sequester toxins and hydrocarbons into plant tissue from contaminated soils. This technique relies on the use of plant interactions (physical, biochemical, biological, chemical and microbiological) in polluted sites to mitigate the toxic effects of pollutants. Depending on pollutant type (elemental or organic), there are several

mechanisms (accumulation or extraction, degradation, filtration, stabilization and volatilization) involved in phytoremediation. Elemental pollutants (toxic heavy metals and radionuclides) are mostly removed by extraction, transformation and sequestration. On the other hand, organic pollutants (hydrocarbons and chlorinated compounds) are predominantly removed by degradation, rhizoremediation, stabilization and volatilization, with mineralization being possible when some plants such as willow and alfalfa are used (Meagher 2000; Kuiper, Lagendijk, Bloemberg & Lugtenberg, 2004).

Plants secrete sugars, enzymes, and oxygen from roots which provide necessary substrates for rhizobia and associated rhizosphere microbes to stimulate degradation of organic pollutants (Gerhardt, Huang, Glick & Greenberg, 2009). Studies have demonstrated the bioaccumulation abilities of various plants with rhizobia associations in particular *Chromolaena odorata* were able to remove 80% of petroleum and heavy metal toxins from soils (Atagana, 2010). While more commonly used on terrestrial environments, contaminated marine environments also benefit from plants based bioremediation through the use of various algae and macrophytes. Phytoremediation is most effective when used in conjunction with microbial remediation and Mycoremediation (Vouillamoz & Milke, 2001; Alarcon, Davies, Autenrieth & Zuberer, 2008).

### 2.7.3 Mycoremediation

Mycoremediation techniques make use of pollutant tolerant fungi which sequester or denature environmental toxins particularly heavy metals. Toxins are sequestered into highly absorbent molecules such chitin and glucan which are found in fungal cell walls (Shukla & Srivastava, 2017) *Saccharomyces cerevisiae* (baker's yeast) can be used to remediate heavy metal contaminated marine ecosystems, with 80% to 90% success in the case of arsenic. Soil contaminated with crude oil displays toxic levels of various heavy metals such

as lead, zinc and magnesium. Application of mycoremediation techniques to crude contaminated soils have shown significant reductions of heavy metal concentrations (Maduekwe, Nwachukwu & Joel, 2016).

## 2.8 Nanotechnology

Nanotechnology is the branch of science that comprises the synthesis, engineering, and utilization of materials whose size ranges from 1 to 100 nm, known as nanomaterials (Hasan, 2015).

### 2.8.1 Nanoparticles

A nanoparticle is a small particle that ranges between 1 to 100 nanometres in size. Undetectable by the human eye, nanoparticles can exhibit significantly different physical and chemical properties to their larger material counterparts. It can be of different shapes, sizes, and structures (TWI, 2004).

### 2.8.2 Physicochemical properties of nanoparticles

Nanoparticles are very important because they have superior physicochemical and biological characteristics. These nanoparticle materials are mechanically strong, magnetic, optically active, catalytic and chemically reactive, larger surface-to-volume ratio due to their small size (1–100 nm) which results in increased surface reactivity. This special characteristic allows them to be used in a variety of applications from material science to biotechnology (Kaur & Roy, 2021),

### 2.8.3 Nanoparticle synthesis

Nanoparticle synthesis refers to methods for creating nanoparticles.

The nanoparticles are classified into different classes such as inorganic nanoparticles, organic nanoparticles, ceramic nanoparticles and carbon base nanoparticles. The inorganic nanoparticles are further classified into metal nanoparticles and metal oxide nanoparticles. Similarly, carbon base nanoparticles classified into Fullerene, Carbon nanotubes, Graphene, Carbon nanofiber and

carbon black Nanoparticles are also classified on the basis of dimension such as one dimension nanoparticles, two dimension nanoparticles and three-dimension nanoparticles. The nanoparticles are synthesized by using two approaches like top-down approach and bottom-up approach (Altammar, 2023).

The three main methods for the synthesis of nanomaterials are physical, biological and chemical methods

#### 2.8.3.1 Physical method

Physical methods depend in their working principle to produce nanomaterials on the use of thermal energy, radiation on energy, and mechanical pressure forces, which results in the condensation, dissolution, evaporation or abrasion of the materials. Physical methods for producing nanomaterials are distinguished from chemical methods in that they are environmentally friendly, do not cause pollution, produce homogeneous nanoparticles and chemical solvents are never used in these methods (Kumari et al., 2023)**.** Nanomaterials are usually produced by physical methods from fragmentation of bulk materials in top-down methods (Baig, Kammakakam & Falath, 2021).

The present review provides an overview of the different physical techniques used in the generation of nanomaterials, such as mechanical ball milling, inert gas condensation (IGC), physical vapors deposition (PVD), laser ablation, laser pyrolysis, electrospinning, ion sputtering, pulsed wire discharge, and Arc discharge method.

#### 2.8.3.2 Chemical methods

Nanomaterials or nanostructures can be synthesized by a variety of techniques such as spray pyrolysis, thermal decomposition, molecular beam epitaxy, chemical vapor deposition, and laser ablation, chemical precipitation, hydrothermal method, pyrolysis, chemical vapour deposition, sol gel process. These types of preparations suffer from high energy demand and also involve toxic and hazardous chemicals, which may lead to biological risks. This method of synthesis of

nanoparticles can lead to formation of toxic byproduct chemicals and its non-ecofriendly (Hudlikar, Joglekar, Dhaygude & Kodam, 2012; Singhal, 2011).

#### 2.8.3.3 Biological method (Green synthesis)

Biological methods are becoming the most preferred methods as they are often single step, clean, safe and cost effective. Green synthesis procedures involve the plant based synthesis of nanoparticles. Green synthesis techniques make use of somewhat pollutant-free chemicals for synthesis of nanostructures. It embraces the use of ecofriendly and safe solvents such as water, natural extracts. So biological approaches using microorganisms and plants or plant extracts for synthesis of metal nanoparticles have been suggested as safe alternatives to chemical methods. In biogenic synthesis of nanoparticles, several biological systems including bacteria, fungi, and yeast have been used safely (Alagumuthu & Kirubha, 2012). In present times "green" method in the synthesis of nanoparticles has greatly become a topic of interest because the conventional chemical methods are expensive and require the use of chemical compounds/organic solvents as reducing agents which are toxic as well (Mason, Vivekanandhan, Misra & Mohanty, 2012). Green chemistry reduces pollution risk at source level and it is enhanced to prevent waste rather than treat or clean up waste after it is formed. The principle focuses on choice of reagents which are ecofriendly. Although physical and chemical methods are quick and easier for nanoparticles synthesis the biogenic technique is better and ecofriendly (Reed & Hutchison, 2000).

## 2.9 Zinc Oxide Nanoparticles

The biological synthesis of nanoparticles is an innovative approach and eco-friendly process. Synthesis of nanoparticles from microbes and plant extract are reported in various literatures (Barman, 2013). The presence of various types of biomolecules (phytochemicals) in plant and microbial extracts are responsible for the reduction, capping and stabilization of the nanoparticles (Rana, Vadav & Jagadevan, 2020).

Zinc oxide is a metal oxide compound classified as an n-type groups II-VI semiconductor materials. The stability of zinc oxide is examined at room temperature with a wide bandgap value of 3.37 eV. Recently, this material has the potential in electronic and optical applications. The wide bandgap energy of zinc oxide has attracted researchers to modify its optical property in absorbing visible light. Zinc oxide is commonly synthesized in the form of nanostructures due to its large surface area. Among various metal oxide nanostructures, zinc oxide has a stable hexagonal wurtzite phase at room temperature. Additionally, zinc oxide has been reported for several applications such as photocatalysis, electrode loading on conductive glass, and their UV-shielding applications (Priyanka, Kamakhya, Saikat & Susruta, 2021).

Zinc oxide nanoparticle is nontoxic and stand out as one of the most versatile materials, due to their diverse properties, functionalities, and applications (agriculture, medicine, remediation, cosmetics), it can be used as photocatalytic degradation materials of environmental pollutants (Ryu et al., 2003). Zinc oxide nanostructures exhibit high catalytic efficiency, strong antimicrobial actions against some bacteria and fungi. As far as synthesis of zinc oxide nanoparticles is concerned, they can be synthesized by chemical methods but green synthesis of zinc oxide nanoparticle is much safer and environment friendly because it does not lead to formation of toxic byproduct chemicals.

Zinc oxide nanoparticles have been synthesized by an environmentally eco-friendly method utilizing extracts from various plants such as, *Aloe vera* leaf, *Lemon grass* leaves, *Garcinia xanthochymus*, *Artocarpus gomezianus*, *Cassia fistula*, *Carica papaya*, *Solanum nigrum*, *Agathosma betulina*, *Moringa oleifera*, *Vitex negundo* L, *Tribulus terrestris*, *Pongamia pinnata*, *Azadirachta indica* L, *Asphalathus linearis*, and *Plectranthus amboinicus* extract (Priyanka et al., 2021).

Sutradhar and Saha (2016) used tomato extract to synthesize zinc oxide nanoparticles. The presence of phytochemicals in tomato functioned as a natural capping and reducing agent. Phenols and protein in tomato plays a crucial role in reducing zinc oxide, flavonoids and flavones present in the extract act as the capping and reducing agent for synthesizing zinc oxide nanoparticle.

### 2.9.1 Mechanism of zinc oxide nanoparticles formation

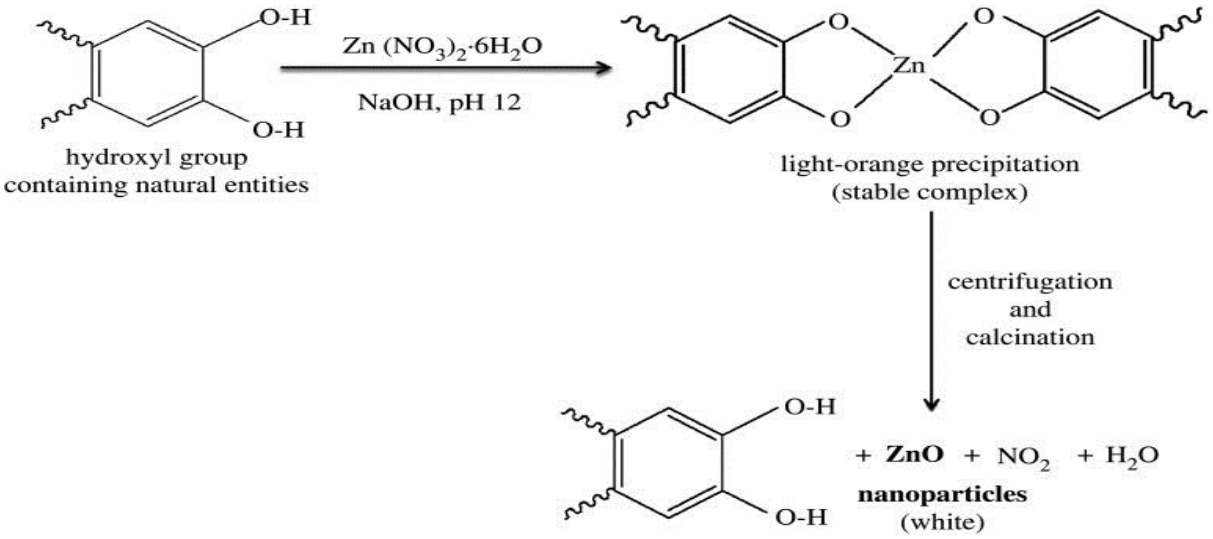


Figure 2.1. Proposed mechanism of zinc oxide nanoparticles formation (Rahman et al., 2022).

## 2.10 Applications of Nanoparticles

### 2.10.1. Applications in drugs and medications

Nano-sized inorganic particles display unique, physical and chemical properties and represent an increasingly important material in the development of novel nano devices which can be used in numerous biological, physical, pharmaceutical and biomedical applications (Loureiro, Azoia, Gomes & Cavaco-Paulo, 2016).

Nanoparticles have the ability to deliver drugs in the optimum dosage range, resulting in increased therapeutic efficiency of the drugs, improved patient compliance and weaken side effects (Alexis, Pridgen, Molnar, & Farokhzad, 2008). Iron oxide nanoparticles such as magnetite ($Fe_3O_4$) or its oxidized form maghemite ($Fe_2O_3$) are the most commonly employed for biomedical

applications. The selection of nanoparticles for achieving efficient contrast for biological, photo thermal therapeutic and cell imaging applications is based on the optical properties of nanoparticles. Polymers have been used in drug delivery for delivery of drugs to the target site thus increasing the therapeutic benefit, while minimizing side effects (Qu et al., 2016).

### 2.10.2. Applications in manufacturing and materials

Nanocrystalline materials provide very interesting substances for material science since their properties deviate from respective bulk material in a size dependent manner. Manufactured nanoparticles display physicochemical characteristics that induce unique mechanical, electrical, optical and imaging properties that are extremely looked for in certain applications within the commercial, medical, and ecological sectors (Todescato et al., 2016).

### 2.10.3. Applications in the environment

Natural nanoparticles play an important role due to high surface to mass ratio in solid/water partitioning of contaminants which can be adsorbed to the surface of nanoparticles, co-precipitated during the formation of natural nanoparticles or trapped by aggregation of nanoparticles which had contaminants adsorbed to their surface. The interaction of contaminants with nanoparticles is dependent on the nanoparticle characteristics, such as size, composition, morphology, porosity, aggregation/disaggregation and aggregate structure (Swadeshmukul, Peng & Rovelyn, 2001).

Nanotechnology applications in the environment falls into three categories:

i. Environmentally benign sustainable products (pollution prevention or green chemistry).
ii. Remediation of materials contaminated with hazardous substances and
iii. Sensors for environmental stages (Tratnyek & Johnson, 2006).

Superparamagnetic iron oxide nanoparticles are an effective sorbent material for toxic soft material. Photodegradation by nanoparticles is also a very common practice and many

nanomaterials are utilized for this purpose. ZnO/ NiO nanoparticles modified silica was used for photodegradation purposes. The high surface area of nanoparticles facilitates the efficient photodegradation reaction (Rogozea et al., 2017).

### 2.10.4. Applications in energy harvesting

Nanoparticles are used to generate energy from electrochemical water splitting and photoelectrochemical due to their large surface area, catalytic nature, and optical behaviour. Nanoparticles are used in energy storage applications to reserve the energy into different forms at nanoscale level. Nanogenerators are created recently, which can convert the mechanical energy into electricity using piezoelectric, which is an unconventional approach to generate energy (Wang & Chang, 2015).

## 2.11 Nanoremediation

Nanoremediation is the use of nanoparticles for environmental remediation. It is being explored to treat ground water, wastewater, soil, sediment, or other contaminated environmental materials (EPA, 2012) . It is cost-effective and eco-friendly approach that uses nanoparticles to detoxify contaminants in the soil and other environments (Baragano, Forjan, Welte & Gallego, 2020).

### 2.11.1 Mechanism of Nanoremediation

Once a nanoparticle contacts a contaminant, it may degrade the contaminant to less harmful compounds through a redox reaction, complexation or adsorption to the contaminant to immobilize it (Sanchez et al., 2011).

During photocatalytic degradation, the contaminant is adsorbed on the surface of the catalyst (zinc) and then it is exposed to ultraviolet light illumination to excite valence electrons so the electrons may transfer to the conduction band from the valence band; during the process, a positive hole ($H^+$) is lifted inside the valence band. The positive holes and free electrons will react on the

surface of the photocatalyst along with adsorbed water molecules, the positive holes will react with water to produce $OH^-$ radicals and the free electrons reduce the dissolved oxygen to superoxide anion $O_2^-$ radicals. These light-generated radicals degrade the contaminants into less harmful compounds (Su, Dong, Zhang, Du & XU, 2013)

# CHAPTER THREE

# MATERIALS & METHODS

## 3.2 Materials

Bonny light crude oil, soil, elephant grass, cow dung, water bath (Grant, England), hot air oven (Gallenpkam, England), Bench centrifuge (Clay adams, USA), beakers, digital weighing balance (Mettler PT 320-Wagen, Switzerland), funnel, measuring cylinder, pH meter (Hanna, HI 98106), plastic containers (reactor), Fourier transform infrared (Shimadzu Corp, Japan), magnetic stirrer (Lensor, USA), No 1 Whatman Filter paper, High resolution transmission electron microscope (HR TEM Model Tecnai G2 Stwin (200kv)), Gas Chromatography (Thermo Scientific Co, Ultra Ver. 5.0, Japan), Atomic Absorption Spectrophotometer (GBC Xplorer AAS, Australia), thermometer, Rotary evaporator (Buchi Rotavapour Switzerland), hand glove, nose mask, trowel and nylon bag, X-ray diffractometer (Rigaku Int. Corp, Tokyo, Japan) UV-Vis Spectrophotometer (Genesys Uv-Vis spectrophotometer, prove 30) .

### 3.1.2 Chemicals / Reagents

All chemicals and reagents used in this study were of analytical grades and includes sodium hydroxide, hydrochloric acid (HCl) and sodium hexametaphosphate, dichloromethane, zinc acetate dihydrate, Deionized water, macconkey agar, nutrient agar, peptone water, sodium hydroxide, methanol, $HNO_3$, $H_2SO_4$, $HClO_4$, $K_2Cr_2O_7$, and ferrous ammonium sulphate.

## 3.2 Methodology

## 3.2 Sample Collection

### 3.2.1 Bonny light crude oil

Bonny light crude oil from Port Harcourt refinery, Rivers State. Nigeria was used in polluting the soil.

### 3.2.2 Soil

Seven kilograms soil sample was collected from University of Port Harcourt, Abuja campus, Rivers State, Nigeria. These were obtained using a 22-cm hand-dug soil auger and put in labelled clean polyethylene bags. The soil sample was air dried for two weeks.

### 3.2.3 Cow dung

Five kilogrammes of cow dung were collected from University of Port Harcourt, Faculty of Agriculture, Abuja campus, Rivers State, Nigeria. The cow dung was put into a clean ziplock bag. It was sun dried for two weeks and preserved in an air tight container.

### 3.2.4 Plant

Fresh leaves of Elephant grass (*Pennisetum purpureum* Schumach*)* were harvested from University of Port Harcourt, Rivers State and was identified and authenticated by Dr. Wisdom Barade (WNB85), a plant taxonomist. The voucher number (KSPT/2023/317) was obtained from the Herbarium of Kenule Beeson Saro-Wiwa Polytechnic, Bori, Rivers State. Nigeria.

## 3.3 Extract Preparation for Phytochemical Studies.

### 3.3.1 Elephant grass (*Pennisetum purpureum)*

The fresh leaves of *Pennisetum purpureum* were separated from the stems, washed with clean running tap water three times and rinsed with distilled water to remove dust particle and air-dried at room temperature for two weeks. The dried leaves were ground into powder using a mechanical grinder. One hundred grammes of the leaf powder was weighed and soaked in 500 mL of distilled water in a conical flask. This was covered, shaken every 30 minutes for 6 h and allowed to stand for about 48 h. The solution was shaken and filtered using Whatman number 1 filter paper. The filtrate was evaporated to dryness using a rotary evaporator (Model type 349/2, Corning Ltd). The extract was stored at 4 $^{o}$C (Nwaogu, Alisi, Ibegbulem & Igwe, 2007).

Percentage yield $= \frac{weight\ of\ extract \times 100}{weight\ of\ starting\ material}$ Equation 3.1

### 3.3.2 Cow dung

One hundred grammes of the cow dung powder was weighed and soaked in 500 mL of distilled water in a conical flask. This was covered, shaken every 30 min for 6 h and then allowed to stand for 48 h. The solution was shaken and filtered using Whatman number 1 filter paper. The filtrate was evaporated to dryness using a rotary evaporator (Model type 349/2, Corning Ltd). The extract was stored at 4 $^{o}$C (Nwaogu, Alisi, Ibegbulem & Igwe, 2007).

## 3.4 Phytochemical Studies

The crude aqueous extract of *Pennisetum purpureum*, cow dung*, Pennisetum purpureum* zinc oxide and cow dung zinc oxide nanoparticles were analyzed for the quality and quantity of the volatile phytochemicals present in it using GC-MS technique. The GC-MS was performed on a Thermo Scientific Co, Thermo GC-TRACE Ultra Ver. 5.0, thermo MS DSQ II. Experimental conditions of GC-MS include; BS-MS dimension: 30 Mts, ID: 0.25 mm, Film thickness: 0.25 µm. The flow rate of the mobile phase was set at 1.0 mL/min (carrier gas: helium). In the gas chromatography the oven temperature was initially 40 °C and raised to 150 °C at 10 °C/min. The temperature was raised again to 230 °C/min at the rate 5 °C/min and the process continued till it remained constant at 280 °C at the rate of 20 °C/min which was held for 8 minutes. The injector port temperature remained constant at 280 °C and detector temperature was 250 °C.

The crude extract (1 g) was reconstituted in 1 mL of methanol. Then, 2 µl of the extract was injected into the port and vaporized down the column with helium as the carrier gas at the flow rate of 1 mL/min and the results were compared to Wiley Spectral Library Search Program. Interpretation of the mass spectrum of the constituents of the extract was carried out in comparison with the database of the National Institute of Standard and Technology (NIST).

## 3.5 Synthesis of Zinc Oxide Nanoparticles (Green Synthesis Approach) for *Pennisetum purpureum* Zinc Oxide Nanoparticles and Cow Dung Zinc Oxide Nanoparticles

Zinc oxide nanoparticles were biosynthesized using the modified method of Sabir, Arshad & Chaudhari (2014). Zinc acetate dihydrate was used as the precursor while the aqueous extract of cow dung and *Pennisetum purpureum* was used as the reducing agent. The zinc oxide nanoparticles were biosynthesized using aqueous extracts of cow dung or *Pennisetum purpureum*. Fifty milliliters of aqueous extract (*Pennisetum purpureum* or cow dung) was added to 50 mL of 0.1 M zinc acetate dihydrate solution in a beaker. The pH was adjusted to pH 12 by addition of 5 mL 0.2 M NaOH. A pale white aqueous solution was formed. The mixture was stirred using a magnetic stirrer for 2 h and kept in a water bath at 50 °C. A pale white precipitate was formed which indicated the presence of zinc oxide nanoparticles. The colloidal suspension was centrifuged at 10000 rpm for 15 min and the supernatant was discarded. Pellet was collected and washed with deionized water, followed by ethanol to make it free from impurities then oven dried overnight at 60 °C. A pale white powder of zinc oxide nanoparticles was obtained.

## 3.6 Characterization of Synthesized Nanoparticles.

The synthesised cow dung zinc oxide nanoparticles and *Pennisetum purpureum* zinc oxide nano particles were characterized by various dispersion methods such as UV spectroscopy, Fourier-transform infrared spectroscopy (FTIR), Transmission electron microscopy (TEM) and X-ray diffraction (XRD).

### 3.6.1 X-ray diffraction (XRD).

The sample was finely ground and homogenized. The powdered sample was prepared using the sample preparation block and compressed in the flat sample holder that was mounted on the sample stage in the xrd cabinet.

The sample was analyzed using the reflection-transmission spinner stage, using the Theta-Theta settings (Two-Theta starting position was 4 degrees and ends at 75 degrees). The tube current was 40 mA and the tension was 45 VA. A programmable divergent slit was used with a 5mm width mask and Gonio Scan was used.

The intensity of diffracted X-rays was recorded continuously as the sample and detector rotated through their respective angles. The peaks occurred when the mineral contained lattice planes with d-spacings appropriate to diffract X-rays at that value of θ (theta). At higher values of θ greater separation occurred. The combined peaks were treated as one. The 2 λ position of the diffraction peak was typically measured as the center of the peak at 80 % peak height.

The crystalline size was calculated using Debye Scherrer's equation

$$D=\frac{0.94\lambda}{\beta cos\theta} \qquad \text{Equation 3.2}$$

where 0.94 is Scherrer's constant, $\lambda$ is X-ray wavelength = 1.5406, $\theta$ is the Bragg diffraction angle, and $\beta$ is the peak full width of the diffraction line at half-maximum intensity (FWHM).

### 3.6.2 Transmission electron microscopy (TEM)

The sample was fixed, a secondary fixation was carried out using osmium tetroxide ($OsO_4$). After which the sample was freeze dried, ethanol and acetone were the solvents in this method. The sample was embedded and kept in an oven at 60 °C overnight to allow for setting a process called polymerization. After embedding, some materials were subjected to polishing to reduce scratches as well as other problems that can minimize the quality of the image. Ultrafine abrasives were used to give the specimen a mirror-like finish. The sample was sectioned into fine sections using a glass knife attached to ultramicrotome. The device has a trough that was filled with distilled water. The sections cut were collected in the device trough filled with distilled water, and then loaded on a carbon-coated copper grid by drop cast techniques to be viewed under the microscope by HR TEM Model Tecnai G2 Stwin (200kv). The size of each section was between 30 nm and

60 nm to get the best resolution. The staining of the specimens was done twice before dehydration and after sectioning. In this process, heavy metals like uranium, lead, or tungsten were used to increase the contrast between different structures in the specimen, and also to scatter the electron beams. Staining before hydration was done in block, while in staining after sectioning, the sample was exposed to an aqueous solution of the above metals.

### 3.6.3 Ultraviolet-visible absorption spectroscopy

This process was started by dispersing 0.01 g of zinc oxide nanoparticles in double-distilled water (DDW), then 2 mL in a quartz cuvette was taken and analysed by a Genesys Uv-vis spectrophotometer (prove 300) with a serial number (2130315791). The absorption spectrum was recorded from 200nm to 800 nm. The samples were measured during different time intervals between 0 to 6 h and after 24 h of incubation. The energy band gap was calculated from absorption wavelength using the equation ($hv = 1240/\lambda$).

### 3.6.4 Fourier transform infrared (FTIR)

Fourier transform infrared (FTIR) analysis of the dried zinc oxide nanoparticles was carried out by the KBr pellet method and the presence of the various vibrational modes in the synthesized nanoparticles was investigated. The functional groups involved in the biosynthesis of zinc oxide nanoparticles with a spectrum range of 4000–400 $cm^{-1}$ were determined.

## 3.7 Groupings and Treatments

Six empty clean plastic reactors labelled (A, B, C, D, E, F) were weighed.

One kilogramme of the soil sample was placed in each of the clean plastic reactor.

One hundred millilitre (100 mL) of Bonny light crude oil was poured in each reactor (B-F) containing one kilogram of the soil samples and mixed properly.

The soil samples were spiked with water uniformly to soften the soil and to enhance the biodegradation of the petroleum hydrocarbons.

After 2 weeks of soil stabilization cow dung zinc oxide nanoparticles and *Pennisetum purpureum* zinc oxide nanoparticles were added into the reactors with soil.

Reactor A: Unpolluted soil (CONTROL)

Reactor B: crude oil polluted soil without cow dung and *Pennisetum purpureum* zinc oxide nanoparticles (NEGATIVE CONTROL)

Reactor C: crude oil polluted soil and 20 g cow dung zinc oxide nanoparticles.

Reactor D: crude oil polluted soil and 40 g Cow dung zinc oxide nanoparticles

Reactor E: crude oil polluted soil and 20 g *Pennisetum purpureum* zinc oxide nano particles.

Reactor F: crude oil polluted soil and 40 g *Pennisetum purpureum* zinc oxide nano particles.

This study was carried out for 42 days.

Ten grams of soil samples were collected from each reactor once every two weeks (14 days) for a period of six weeks (42 days) for determination of the concentrations of heavy metals (As, Cr, Hg, Zn, Ni), benzene, toluene, ethyl benzene and xylene (BTEX), polycyclic aromatic hydrocarbon, physicochemical (Colour, pH, conductivity, moisture content, total organic carbon (TOC), total nitrogen, total potassium, phosphorous, total petroleum hydrocarbon), and microbial properties (total heterotrophic bacteria (THB) count, total hydrocarbon utilizing bacteria (THUB) count).

### 3.8 Determination of Nitrogen in Soil Kjeldahl Method

Total nitrogen analysis was done in three steps using Kjeldahl method (2021).

**Digestion**:

One gram of air-dried soil sample was weighed into a 100mL digestion tube. Two grams catalyst mixture (i.e copper sulphate pentahydrate and potassium sulphate) was added 3.5 mL of

concentrated $H_2SO_4$ was added and placed in the tube in a digester and the temperature was set to 390 $^0$C, the tubes were allowed to cool with tap water.

**Distillation and Titration**

Twenty millilitre (20 mL) of Boric acid solution was added to an Erlenmeyer flask. One hundred (100 mL) of condensate was distilled, twenty millilitre (20 mL) of water and twenty millilitre (20 mL) of NaOH solution were added. Three drops of bromocresol green indicator were added to the distillate and titrated with 0.01 M $H_2SO_4$. to the end point of the indicator.

$$N = \frac{m\ X\ 28.013\ X\ p}{132.14} \quad \text{Equation 3.3}$$

Where,

N = $(NH_4)_2SO_4$ was the N contained in the mass of $(NH_4)_2SO_4$ used, in milligrams.

m was the mass of $(NH_4)_2SO_4$ used, in milligrams.

p was the factor that considers the purity of $(NH_4)_2SO_4$ used for the control

28.013g was the mass of the N contained in one millimole of $(NH_4)_2SO_4$, in milligrams.

132.14mg was the mass of one millimole of $(NH_4)_2SO_4$, in milligrams.

## 3.9 Moisture Content

The moisture content (MC) of soil samples were determined following the method described by Association of Official Analytical Chemists (1990). Ten grammes of each soil sample was weighed into crucible and heated in an oven at 105ºC for 24 h to dry off water content. Thereafter, the dried soil samples were cooled in desiccator for 30 minutes. On cooling, the samples were reweighed to constant weight.

The percentage moisture content was calculated according to equation

$$\%\ \text{moisture content (MC)} = \frac{Weight\ of\ moist\ soil\ (M) - Weight\ of\ dry\ soil\ (D)}{Weight\ of\ dry\ soil\ (D)} \quad \text{Equation 3.4}$$

### 3.10 Soil pH

The pH of soil samples were determined following the method described by Association of Official Analytical Chemists (1990). The pH of soil before and during treatment was determined in the laboratory. Ten percent (w/v) of air dried soil suspension for each sample was prepared in de-ionized water, and allowed to settle for about 1 h. Thereafter, it was filtered through Whatman filter paper, while the pH of the filtrate was determined via calibrated pH meter (Hanna, HI 98106) (Venosa, 2001).

### 3.11 Determination of Phosphorus in Soil Sample (Ascorbic acid method)

Total phosphorous in the soil samples were determined by the method of Association of Official Analytical Chemists (1990). Ten grammes of soil was weighed into a beaker, 100mL of water was added and allowed to settle and filtered into a clean beaker using Whatman filter paper. The extracted phosphorus was measured calorimetrically based on the reaction with ammonium molybdate and development of the 'Molybdenum Blue' colour. The absorbance of the standards and samples were measured at wavelength 890 nm in a spectrophotometer.

### 3.12 Total Petroleum Hydrocarbon

#### 3.12.1 Extraction

The samples were extracted by ultrasonication USEPA Method $355^0$C (2007). Ten grammes of soil samples were homogenized with the same mass of anhydrous $Na_2SO_4$, 30 mL of a 1:1 dichloromethane (DCM)/*n*-hexane mixture was added to the homogenate, and the mixture was ultrasonicated for 45 min at 35 °C. The extracts were then filtered through a 0.45 μm glass microfiber filter, concentrated to 2 mL and cleaned-up in a silica gel (4.0 g) / alumina (2.0 g) packed column.

A volume of 30 mL each of dichloromethane (DCM) and *n*-hexane mixture was used to elute the total petroleum hydrocarbon from the column and the eluate was concentrated to 2 mL under a slow flowing stream of nitrogen gas.

### 3.12.1 Chromatographic analysis

The total petroleum hydrocarbon concentrations in the sample extracts were determined by gas chromatography with a flame ionization detector (GC-FID). The gas chromatographic column had an initial temperature of 70 °C, which was held for 20 min, and was then increased at 25 °C $min^{-1}$ to 150 °C, it was further raised to 200 °C at 3 °C $min^{-1}$ and finally increased to 300 °C at 2 °C $min^{-1}$. The temperature of the injection port, ion source, quadrupole and transfer line were 250, 230, 150 and 280 °C respectively. The sample was injected into the GC via a pulsed splitless mode with an injection volume of 1µl.

## 3.13 Polycyclic Aromatic Hydrocarbon

### 3.13.1 Extraction

The samples were extracted by ultrasonication USEPA Method $355^0$C (2007). Ten grammes of soil samples were homogenized with the same mass of anhydrous $Na_2SO_4$, 30 mL of a 1:1 dichloromethane (DCM)/*n*-hexane mixture was added to the homogenate, and the mixture was ultrasonicated for 45 min at 35 °C. The extracts were then filtered through a 0.45 µm glass microfiber filter, concentrated to 2 mL and cleaned-up in a silica gel (4.0 g) /alumina (2.0 g) packed column. A volume of 30 mL each of dichloromethane (DCM) and *n*-hexane mixture was used to elute the polycyclic aromatic hydrocarbons from the column and the eluate was concentrated to 2 mL under a slow flowing stream of nitrogen gas.

### 3.13.1 Chromatographic analysis

The polycyclic aromatic hydrocarbon concentrations in the sample extracts were determined by gas chromatography-mass spectrometry with an Agilent 6890 plus gas chromatograph (GC)

interfaced with an Agilent 5973 mass selective detector (Agilent Technologies, Santa Clara, USA). ADB-5 capillary column (30 m length × 0.25 µm film thickness × 0.25 mm i.d.) was used for separation of the PAHs. Pure helium, Nitrogen/Hydrogen gas at a flow velocity of 1mL/min and 30mL/mins was used as the carrier gas. The gas chromatographic column had an initial temperature of 70 °C, which was held for 20 min, and was then increased at 25 °C $min^{-1}$ to 150 °C; it was further raised to 200 °C at 3 °C $min^{-1}$ and finally increased to 300 °C at 2 °C $min^{-1}$. The temperature of the injection port, ion source, quadrupole and transfer line were 250, 230,150 and 280 °C respectively. The sample was injected into the GC via a pulsed splitless mode with an injection volume of 1µL.

### 3.14 Benzene, Toluene, Ethyl Benzene And Xylene (BTEX)

The concentrations of benzene, toluene, ethyl benzene and xylene (BTEX) in the soil samples were determined using GC/MS USEPA method 8240 (1884).

Five gramme of soil sample was weighed into a 20 mL headspace vial, 10 mL of methanol was thereafter added. This was incubated in the Headspace oven and injected directly into the inlet of the Gas chromatography system.

### 3.15 Heavy Metals

Heavy metal concentrations in the soil samples were determined by the method of Association of Official Analytical Chemists (2012). Two grams of dried soil sample was weighed into 100 mL beaker. Two millilitres of nitric acid, 6 mL HCl with 3 mL of peroxide was added into the beaker and allowed to stand overnight. The flask was swirled gently and placed on a hot plate at 105 $^{0}$C and heated to near dryness. After the digestion was complete, the digest was cooled, filtered through 541 Whatman filter paper into a volumetric flask and diluted to 50 mL with distilled water. The digested samples were analysed for heavy metals, using atomic absorption spectrophotometer. The metals analysed were potassium, chromium, mercury, zinc, nickel and Arsenic.

### 3.16 Total Organic Carbon

The determination of soil total organic carbon was based on the modified Walkley & Black chromic acid wet oxidation method (2019). The Walkley Black method was adopted for the analysis of the total organic carbon. One gramme of air dried soil samples were weighed into a 500 mL erlenmeyer flask, followed by the addition of 10 mL of 0.167 $K_2Cr_2O_7$ solution and 20 mL $H_2SO_4$ after the oxidation reaction, the unreacted Potassium chromate was then titrated with ferrous ammonium sulphate using three drops of diphenylamine indicator.

### 3.17 Conductivity

The conductivity of the soil samples was determined by the method of Association of Official Analytical Chemists (1990). Conductivity was determined using electrical conductivity meter. Ten grammes of air-dried soil suspension for each sample was prepared in de-ionized water, and allowed to settle for about one hour. Thereafter, it was filtered through Whatman filter paper. The conductivity probe was inserted into the filtrate and the conductivity of the soil sample was recorded.

### 3.18 Microbiological Analysis

#### 3.18.1 Sterilization

All glass wares were washed and dried. After drying the glass wares were sterilised in the hot air oven at 160 $^0$C for one hour.

#### 3.18.2 Total Heterotrophic Bacteria (THB) Count

Total heterotrophic bacteria (THB) count was performed on nutrient agar (Oxoid), using the spread plate method (Gradi, 1985).

The soil sample was mixed, and a suspension of 10g (dry weight equivalent) in 90mL of peptone water was prepared. One mL of the soil suspension was then diluted serially (ten-fold) and used in the estimation of aerobic heterotrophic bacterial by standard spread-plate dilution method described by Seeley and VanDemark (1981), in triplicate. Nutrient agar containing 0.015% (w/v)

nystatin (to inhibit fungi growth) was used for bacteria isolation and incubation was at $37^0$C for 24 h.

### 3.18.3 Preparation of Pure Culture

Pure culture was made by microbial isolation from the culture plate through subsequent sub cultures in several generations. The pure culture was used for characteristic tests such as Gram test and other biochemical tests for identification of bacterial isolates.

### 3.18.4 Total Hydrocarbon Utilizing Bacteria Count

Total hydrocarbon utilizing bacteria (THB) count was performed on mannitol agar (Oxoid), using the spread plate method (Gradi, 1985).

The soil sample was mixed, and a suspension of 10 g (dry weight equivalent) in 90 mL of peptone water was prepared. One mL of the soil suspension was then diluted serially (ten-fold) and used in the estimation of total hydrocarbon utilizing bacteria by standard spread-plate dilution method described by Seeley and VanDemark (1981), in triplicate. The percentage of hydrocarbon utilizers within the heterotrophic bacteria population was determined by oxidase and sugar fermentation test.

## 3.19 Statistical Analyses

Data generated was analysed using statistical tools such as one way analysis of variance (ANOVA). All analyses were done using Statistical Package for Social Sciences (SPSS) version 27.0 (IBM Statistics, UK).

Statistical significance of value was at 95% confidence level ($p \leq 0.05$) using Turkey and Duncan homogeneity of variance test. Results were presented as Mean ± Standard deviation.

Correlation Analysis of parameters was determined using Pearson correlation analysis.

# CHAPTER FOUR

# RESULTS AND DISCUSSION

## 4.0 Results

### 4.1 Phytochemical Constituents of Aqueous Extract of Cow Dung, *Pennisetum Purpureum*, Cow Dung Zinc Oxide Nanoparticles and *Pennisetum purpureum* Zinc Oxide Nanoparticles.

Gas chromatography mass spectrometry (GC-MS) analysis revealed phytochemical constituents in aqueous extract of *Pennisetum purpureum*, *Pennisetum purpureum* zinc oxide nanoparticles, cow dung and cow dung zinc oxide nanoparticles that have biological activities and useful components in nanoparticle synthesis.

Bioactive compounds were present in aqueous extract of *Pennisetum purpureum* with the major constituents being 9,12-octadecadienoic acid (linoleic acid) (18.89%), Cis-13-octadecenoic acid (15.74%), 1,2-benzisothiazole (6.69%), 11-octadecenoic acid (5.53%), oleic acid (5.01%). The major bioactive compounds in aqueous extracts of *Pennisetum purpureum* zinc oxide nanoparticles are hexadecanoic acid (15.25%), 1-octadene (13.16%), 11-octadecenoic acid (7.14%), cyclopentadecane (6.64%), the major constituents in aqueous extract of cow dung are trans-13-Octadecenoic acid (12.03%), 8, 11 – octadecadienoic acid (8.29%), 9-octadecanoic acid (8.11%) and cycloeisane (7.43%). The major bioactive constituents in aqueous extract of cow dung zinc oxide nanoparticles are alpha-endosulfan (67.99%), 4-trifluoroacetoxy tetradecane (10.18%), 1-octadecene (4.83%), 5-bromomethyl-2-chloropyridine (4.46%). A yield of 12% of aqueous extract of cow dung was obtained while 10% yield was obtained from aqueous extract of *Pennisetum purpureum*.

The phytochemical constituents of *Pennisetum purpureum* and *Pennisetum purpureum* zinc oxide nanoparticles are shown in Tables 4.1.1 and 4.1.2. The phytochemical constituents of cow dung and cow dung zinc oxide nanoparticles are shown in Tables 4.1.3 and 4.1.4.

Table 4.1.1: GC- MS Results of Phytochemical Composition of Aqueous Extract of *Pennisetum purpureum* zinc oxide nanoparticles.

| S/N | RETENTION TIME | NAME OF COMPOUND | PEAK AREA (%) | MOLECULAR WEIGHT | MOLECULAR FORMULA |
|---|---|---|---|---|---|
| 1. | 7.838 | Cyclohexane | 0.64 | 84.16 | $C_6H_{12}$ |
| 2. | 8.573 | Cetene<br>1-Hexadecanol<br>1-Dodecanol | 0.07 | 242.43 | $C_{16}H_{34}O$ |
| 3. | 8.616 | Pentafluoropropionoic acid, | 0.02 | 164.03 | $C_3HF_5O_2$ |
| 4. | 11.269 | 3-Hexadecene, (Z)-<br>Cyclo hexadecane | 0.19 | 226.45 | $C_{16}H_{32}$ |
| 5. | 11.795 | 1,3-Dimethyl-5-isobutylclohexane | 0.04 | 100.16 | $C_6H_{12}O$ |
| 6. | 13.280 | Cetene, 7-Hexadecene | 1.23 | 226.45 | $C_{16}H_{32}$ |
| 7. | 13.448 | Cetene | 1.03 | | $C_{16}H_{32}$ |
| 8. | 13.551 | Cyclohexadecane<br>1-Decanol | 1.03 | 226.44 | $C_{16}H_{32}$ |
| 9. | 14.467 | Cyclohexadecane<br>Cyclohexadecanol | 0.11 | 226.44 | $C_{16}H_{32}$ |
| 10. | 14.506 | Cyclohexadecane<br>Cetene | 0.10 | 224.44 | $C_{16}H_{32}$ |
| 11. | 14.545 | Oleic acid, Cetene<br>2-Dodecenal | 0.05 | 282.46 | $C_{18}H_{34}O_2$ |
| 12. | 14.579 | Pentadecafluorooctanoic acid | 0.07 | 414.06 | $C_3HF_5O_2$ |
| 13. | 14.926 | Cyclododecane<br>Propyl triacontyl ether<br>Triacontyl pentafluoro propionate | 0.13 | 182.34 | $C_{12}H_{28}$ |
| 14. | 14.977 | Propyl triacontyl ether,<br>Tridecane, 7-cyclohexyl | 0.09 | 582.92 | $C_{30}H_{63}O$ |
| 15. | 15.036 | Citronellal<br>Tetracosyl heptafluoro butyrate<br>Docosyl pentafloropropionate | 0.17 | 152.25 | $C_{10}H_{24}O$ |
| 16. | 15.146 | Cyclo dodecanol, 1-ethyl-<br>1-Hentetracontanol<br>Propyl tetracosyl ether | 0.09 | 182.34 | $C_{12}H_{24}O$ |
| 17. | 15.300 | Cetene<br>Pentadecafluoro octanoic acid, | 0.08 | 414.07 | $C_8HF_{15}O_2$ |

| | | | | | |
|---|---|---|---|---|---|
| 18. | 15.348 | Dotriacontyl pentafluoropropionate<br>Dotriacontyl heptafluorobutyrate<br>Decane | 0.06 | 142.28 | $C_{10}H_{22}$ |
| 19. | 15.475 | Acetic acid n-octadecyl ester, Hexacosyl propyl ethe ,Propyl triacontyl ether | 0.09 | 298.48 | $C_{20}H_{40}O_2$ |
| 20. | 15.509 | Disparlure<br>Heptadecyl heptafluorobutyrate<br>Pentadecafluoro octanoic acid, octadecyl ester | 0.02 | 286.53 | $C_{19}H_{30}O_2$ |
| 21. | 15.665 | 5-Octadecene, (E)-<br>Cyclohexadecane<br>9-Octadecene, (E)- | 0.05 | 254.45 | $C_{16}H_{32}$ |
| 22. | 15.772 | Dotriacontyl heptafluorobutyrate<br>Hexatriacontyl pentafluoropropionate<br>Triacontyl pentafluoropropionate | 0.49 | 594.12 | $C_{35}H_{65}F_5O_2$ |
| 23. | 15.801 | Hexadecyl propyl ether<br>Eicosyl propyl ether<br>Octacosyl propyl ether | 0.21 | 360.52 | $C_{19}H_{40}O$ |
| 24. | 15.834 | Tetrapentacontane,1,54-dibro 2-(tetradecyloxy)<br>Pentadecafluoroooctanoic acid, octadecyl ester<br>Ethanol, 2-(tetradecyloxy) | 0.15 | 686.05 | $C_{50}H_{10}O$ |
| 25. | 15.982 | Cis-vaccenic acid<br>Heptadecanoic acid | 0.36 | 284.38 | $C_{18}H_{34}O_2$ |
| 26 | 16.047 | 3-Chloropropionoic acid, heptadecyl ester<br>Ethanol, 2-(tetradecyloxyl)<br>Propyl tetradecyl ether | 0.38 | 46.07 | $C_2H_6O$ |
| 27. | 16.101 | 1-Nonadecene<br>Heptafluorobutyric acid, hexadecyl ester<br>Oleic acid | 0.39 | 268.48 | $C_{19}H_{38}$ |
| 28. | 16.148 | Cyclododecanol, 1-ethenyl-<br>Oleic acid<br>Tert-Hexadecane thiol | 0.36 | 182.36 | $C_{12}H_{25}0H$ |
| 29. | 16.169 | Cyclohexadecane<br>Oleic Acid | 0.25 | 182.36 | $C_{12}H_{25}0H$ |

| | | | | | |
|---|---|---|---|---|---|
| 30. | 16.213 | Acetic acid, 3,7,11,15 tetramethyl- hexadecyl ester<br>Pentadecafluoro-octanoic acid, octadecyl ester<br>Heptadecyl heptafluorobutyrate | 0.37 | 298.48 | $C_2H_4O_2$ |
| 31. | 16.237 | Heptafluorobutyric acid, pentadecyl ester<br>1-octadecene<br>Cyclotetradecane | 0.29 | 254.45 | $C_{18}H_{36}$ |
| 32. | 16.294 | Bromoacetic acid, octadecyl ester<br>Ethanol, 2-(tetradecyloxy)-<br>Pentadecafluorooctanoic, octadecyl ester. | 0.50 | 46.07 | $C_2H_6O$ |
| 33. | 16.344 | 9-Octadecene, (E)-<br>Cyclohexadecane<br>3-Octadecene | 0.83 | 254.47 | $C_{18}H_{36}$ |
| 34. | 16.821 | 1-Octadecene<br>Cyclotetradecane | 0.69 | 254.47 | $C_{18}H_{36}$ |
| 35. | 16.604 | Cyclododecanol, 1-ethenyl-<br>1-hexadeconol, acetate<br>9- octadecenoic acid | 0.47 | 172.33 | $C_{12}H_{24}O$ |
| 36. | 16.661 | 1-octadecene<br>Cyclotetradecane<br>2-piperidnone, n-(4 bromo-n-buty1) | 0.70 | 97.14 | $C_5H_9NO$ |
| 37. | 16.821 | 5-tetradecene, (2)-<br>Cyclo tetradecane<br>Propyl triacontyl ether | 0.78 | 520.94 | $C_{35}H_{72}O$ |
| 38. | 17.190 | Heptadecanoic acid, Heptadecyl ester<br>Cyclotetradecane<br>12-methyl-E,E-2,13-Octadecadien-1-01 | 1.17 | 270.47 | $C_{17}H_{34}O_2$ |
| 39. | 17.468 | Dotriacontyl pentafluoro propionate<br>Heptadecyl heptaflourbutyrate<br>5-octadecene, (E) | 1.87 | 472.01 | $C_{15}H_{23}FO_5$ |
| 40. | 17.630 | 1-octadecene<br>1-nconadecene | 13.16 | 282.44 | $C_{18}H_{36}$ |
| 41. | 17.754 | 1-octadecene<br>E-15-heptadecenal<br>1-octadecene | 1.45 | 282.44 | $C_{18}H_{36}$ |
| 42. | 17.780 | Cetene<br>1-octadecene | 7.79 | 224 | $C_{16}H_{32}$ |

| | | | | | |
|---|---|---|---|---|---|
| | | Cetene | | | |
| 43. | 17.940 | 1- octadecene<br>5-octadecene, (E)- | 2.11 | 272.44 | $C_{18}H_{36}$ |
| | | E – 15- Heptadecenal | | | |
| 44. | 18.521 | Cyclotetradecane<br>9- octadecenoic acid | 1.68 | 226.40 | $C_{18}H_{38}$ |
| 45. | 18.552 | Hexacosyl propyl ether<br>Heptadecanoic acid, heptadecyl ester. | 0.83 | 260.39 | $C_{17}H_{38}O_2$ |
| | | 17-pentariacontene | | | |
| 46. | 18.581 | Cyclohexadecane<br>Trans-4-aminocyclohexanol, Oleic acid | 0.63 | 282.46 | $C_{18}H_{34}O_2$ |
| 47. | 18.603 | Heptadecanoic acid, heptadecyl ester | 0.66 | 260.39 | $C_{17}H_{38}O_2$ |
| | | 17-pentatriacontene | | | |
| 48. | 18.742 | Cyclohexadecane<br>Cis-vaccenic acid | 2.01 | 226.45 | $C_{16}H_{32}$ |
| 49. | 18.906 | 1, 1 – bi cyclohexyl, 2-(2-methylpropyl), trans-<br>Decane, 2-cyclohexyl cyclohexane, (1-methylpropyl)- | 4.90 | 142.24 | $C_{10}H_{22}$ |
| 50. | 18.960 | Cyclododecanol, 1-ethenyl-3-eicosene, (E)-<br>Cyclohexane, 11-(1,2-dimethyl-1<br>2-ethanediyl) 613-,R*, R* ($^{+}/_{-}$) | 1.70 | 204.34 | $C_{12}H_{22}0$ |
| 51. | 19.066 | E-11(13, 13-dimethyl) tetratecen-1-0<br>1 acetate<br>Pentadecafluorooctanoic acid, octa decyl ester | 0.92 | 0.92 | $C_2\,H_4O_2$ |
| 52. | 19.130 | 2-Piperidinone, N- [4-bromo-n-butyl<br>Cyclododecanol, 1-ethenyl-<br>Pentadecafluorooctanoic acid, hexadecyl ester | 1.87 | 97.14 | $C_5H_9NO$ |
| 53. | 19.152 | 9-heptadecanone<br>n-6-Tetradecen-1-ol acetate | 2.69 | 246.40 | $C_{17}H_{34}O$ |
| 54. | 19.234 | Cyclododecanol, 1ethenyl -<br>1-octadecene, | 3.88 | 282.44 | $C_{18}H_{36}$ |
| 55. | 19.688 | 1-octadecene<br>6-octadecenoic acid<br>3-tetradecene, (E)- | 4.21 | 282.44 | $C_{18}H_{18}$ |

| | | | | | |
|---|---|---|---|---|---|
| 56. | 19.734 | Cyclopentadecane<br>2-chloropropionic acid, pentadecyl ester.<br>Trichloroacetic acid, pentadecyl ester. | 6.44 | 222.33 | $C_{15}H_{30}$ |
| 57. | 20.205 | Hexadecanoic acid, methyl ester<br>Pentadecanoic acid, 14-methyl-methyl ester | 15.25 | 256.42 | $C_{16}H_{32}O_2$ |
| 58. | 21.652 | 3-Eicosene, 9- Eicosene<br>5- Eicosene | 1.35 | 282.56 | $C_{20}H_{40}$ |
| 59. | 21.749 | 1-Octadecene<br>E-15-Heptadecenal | 0.61 | 282.44 | $C_{18}H_{36}$ |
| 60. | 23.439 | 11-Octadecenoic acid, methyl ester, methyl ester.<br>9-Octadecenoic acid, methyl ester, (E)-<br>9,12-Octadecadienoic acid (Z)-, methyl ester. | 7.14 | 272.44 | $C_{18}H_{34}O_2$ |
| 61. | 23.439 | 11-Octadecenoic acid, methyl ester<br>9-octadecenoic acid, methyl ester, (E)-<br>Cis-13-octadecenoic acid, methyl ester | 1.54 | 272.44 | $C_{18}H_{34}O_2$ |
| 62. | 24.037 | Methyl stearate<br>Heptadecanoic acid | 1.54 | 292.49 | $C_{19}H_{38}O_2$ |
| 63. | 25.349 | Trichloroacetic acid, pentadecyl ester.<br>1-Docosene<br>Trichloroacetic acid, tetradecyl ester | 0.19 | 168.30 | $C_{22}H_{44}$ |
| 64. | 30.715 | Diisooctyl phthalate<br>Bis (2-ethyl hexyl) phthalate | 0.48 | 390.56 | $C_{24}H_{38}O_4$ |
| 65. | 30.783 | Diisooctyl phthalate<br>Bis (2-ethyl hexyl) phthalate<br>Dicyclohexyl phthalate | 0.33 | 288.41 | $C_{24}H_{38}O_4$ |
| 66. | 34.949 | Squalene<br>Docosa-2,6,10,14,18-pentamethyl-,all-trans | 1.08 | 420.67 | $C_{30}H_{50}$ |
| 67. | 37.329 | Butyl-9-tetradecenoate<br>Oleic acid<br>Heptadecanoic acid, heptadecyl ester | 0.07 | 282.46 | $C_{18}H_{34}O_2$ |
| 68. | 37.407 | Octadec-9-enoic<br>9-Octadecenoic acid ( E)- | 0.02 | 272.44 | $C_{18}H_{34}O_2$ |

| | | | | | |
|---|---|---|---|---|---|
| | | 2-Chloropropionoic acid, Octadecyl | | | |
| 69. | 37.435 | Oleic acid | 0.02 | 272.44 | $C_{18}H_{34}O_2$ |
| 70. | 37.628 | Oleic acid<br>9-Octadecenoic acid ( E)-<br>Cis-vaccenic acid | 0.08 | 282.46 | $C_{18}H_{34}O_2$ |
| 71. | 37.797 | Heptadecanoic acid<br>1-Octadecene<br>1-Propyl 9-tetradecenoate | 0.06 | 282.46 | $C_{18}H_{36}$ |
| 72. | 37.910 | Oleic acid<br>1-propyl 9-tetradecenoate | 0.06 | 282.46 | $C_{18}H_{34}O_2$ |
| 73. | 37.934 | 9-Octadecenoic acid, (E)-<br>9-Octadecenoic acid,<br>9-Octadecenoic acid (Z)-, 2,3-dihydroxypropyl ester<br>Decyl oleate | 0.01 | 272.44 | $C_{18}H_{34}O_2$ |
| 74. | 38.464 | Cis-9-Tetradecenoic acid,<br>9-Octadecenoic acid | 1.81 | 272.44 | $C_{18}H_{34}O_2$ |

Table 4.1.2: GC- MS Results of Phytochemical Composition of Aqueous Extract of *Pennisetum purpureum*

| S/N | RETENTION TIME | NAME OF COMPOUND | PEAK AREA (%) | MOLECULAR WEIGHT (g/mole) | MOLCULAR FORMULAR |
|---|---|---|---|---|---|
| 1 | 8.403 | Ethyl 9-hexadecenoate, 7,11- hexadecadienal | 0.03 | 282.46 | $C_{18}H_{34}O_2$ |
| 2 | 8.740 | Oleic acid | 0.04 | 272.44 | $C_{18}H_{34}O_2$ |
| 3 | 9.552 | Undec -10-ynoic acid, | 0.04 | 182.26 | $C_{11}H_{18}O_2$ |
| 4 | 9.713 | 3, 11- tetradecadien -1-01 | 0.05 | 210.36 | $C_{14}H_{26}O$ |
| 5 | 20.225 | Hexadecanoic acid | 2.40 | 256.43 | $C_{16}H_{32}O$ |
| **6** | 21.578 | Hexadecanoic acid | 0.42 | 256.43 | $C_{16}H_{32}O$ |
| 7 | 22.015 | n- hexadecanoic acid | 0.71 | 256.28 | $C_{16}H_{32}O$ |
| 8 | 22.015 | n-hexadecanoic acid | 0.60 | 256.28 | $C_{16}H_{32}O$ |
| 9 | 22.942 | n-hexadecanoic acid | 0.03 | 256.28 | $C_{16}H_{32}O$ |
| 10 | 23.336 | 9,12-octadecadienoic acid (Linoleic acid), methyl ester | 18.89 | 280.4472 | $C_{18}H_{34}O_2$ |
| 11 | 23.467 | Cis-13-octadenoic acid 11-octadecenoic acid | 15.74 | 282.4614 | $C_{18}H_{34}O_2$ |
| 12 | 24. 0.63 | Methyl stearate Heptodecanoic acid, 16-methyl ester | 1.92 | 298.50 | $C_{19}H_{38}O_2$ |
| 13. | 25.249 | Cis –vaccenic acid 9-octadecenoic acid | 3.37 | 282.46 | $C_{18}H_{34}O$ |
| 14 | 25.249 | Oleic acid Cis vaccenic acid 9-octadecenoic acid | 2.85 | 282.46 | $C_{18}H_{34}O$ |
| 15. | 25.554 | 5-eicosene, (E)- | 0.69 | 268.50 | $CH_3$ ($CH_2$) |
| 16. | 25.671 | 3- Eicosene, (E) 9-Eicosene, (E)- Octadecanoic acid | 1.45 | 284.48 | $CH_3$ ($CH_2$) |
| 17. | 25.768 | Octadecanoic acid | 0.65 | 284.48 | $C_{18}H_{34}O_2$ |

| | | | | | |
|---|---|---|---|---|---|
| 18 | 30.854 | Methyl trans -9-(2-butylcy clopentyl) nonanoate<br>Docosanoic acid, methyl ester<br>Nonanoic acid, 9-hydroxy methyl ester | 0.15 | 372.60 | CH300 C (H2)6CH ($H_3$)$C_6$ $H_{10}$ CH |
| 19. | 30.890 | Tricosanoic acid<br>Dedecyl propyl ether<br>9-eicosenoic acid, (Z)- | 0.04 | 354.61 | $C_{23}$ $H_{46}$ $O_2$ |
| 19. | 33.891 | Eicosyl propyl ether<br>Propyl tetradecyl ether<br>9-eicosenoci acid (z) | 0.03 | 344.63 | $C_{23}$ $H_{48}O$ |
| 20. | 34.453 | 9-cotadecenoic acid, (E)-<br>Cis-vaccenic acid<br>Cis-13-octadecenoic acid | 0.02 | 282.47 | $CH_3(CH_2)7CH$ $2CH(CH_2)$, COOH |
| 21. | 34.492 | Oleic acid<br>Cis- vacenic acid<br>Trans-13-octadecenoic acid | 0.01 | 282.46 | $C_{18}H_{34}O_2$ |
| 22. | 34.569 | Oleic acid<br>Cis –vaccenic acid | 0.02 | 282.47 | $C_{18}H_{34}O$ |
| 23. | 34.695 | Oleic acid<br>Cis –vaccenic acid | 0.03 | 282.47 | $C_{18}H_{34}O$ |
| 24. | 34.757 | 13-octadecenal-Z- | 0.01 | 266.47 | $C_{18}H_{34}O$ |
| 25. | 34.792 | Oleic acid<br>6-octadecenoic acid, (z)-<br>9-eicosenoic acid, (Z)- | 0.01 | 282.47 | $C_{18}H_{34}O$ |
| 26. | 35.034 | 2-methyl-Z,Z-3,13-octadecatrienoyl<br>Cis -7, cis – 11-hexadecadien 1-yl acetate<br>Oleic acid | 0.27 | 270.45 | $C_{19}$ $H_{36}O$ |
| 27. | 35.068 | 2-methyl-z, z-3, 13- | 0.11 | 280.50 | $C_{19}H_{36}O$ |
| 28. | 35.108 | Octadecadienol<br>Oleic acid<br>2,6,10-dodeatrien -1-ol, 3,7,11-trimethyl-<br>Oleic acid<br>13-octadecenal, (z)- | 0.03 | 282.47 | $C_{18}H_{34}O$ |
| 29. | 35.130 | Oleic acid<br>1, 19-eiscodadiene<br>9-octadecenoic acid | 0.03 | 282.45 | $C_{18}H_{34}O$ |
| 30. | 35.152 | 9-octadecenoic acid<br>5-eicosene, (e)-<br>2-mathyl-z, z-3, 13-octadecatienol | 0.01 | 282.47 | $C_{18}H_{34}O$ |
| 31. | 35.152 | Oleic acid | 0.04 | 282.47 | $C_{18}H_{34}O$ |

| | | | | | |
|---|---|---|---|---|---|
| | | Cis -13-octadecenoic acid | | | |
| 32. | 35.384 | Oleic acid | 0.16 | 282.47 | $C_{18}H_{34}O$ |
| 33. | 35.448 | 1,2-benzizothiazole, 3-(hexahydro-1H-azepin-1-yl) Oleic acid Cis -13-octadecenoic | 0.08 | 282.47 | $C_{18}H_{34}O$ |
| 34. | 35.697 | Oleic acid Cis -13-octadecenoic acid Trans-13-octadecenoic acid | 0.01 | 282.47 | $C_{18}H_{34}O$ |
| 35. | 35.831 | Cis -7, cis -11-hexadeca dien-1-yl acetate Oleic acid | 1.16 | 282.47 | $C_{18}H_{34}O$ |
| 36. | 35.915 | 2-methyl-z, z-3,13-octadecadienol Oleic acid | 1.10 | 280.50 | $C_{19}H_{36}O$ |
| 37. | 35.945 | Oxirane, tridecyl trans-13-octadeconic acid erucic acid | 0.46 | 338.57 | $CH_3(CH_2)_7CH=CH(CH_2)_{11}COOH$ |
| 38. | 36.221 | 3-eicosene, (E)- 1,2benzisothiazole, 3-(hexahydro-1H-azepin-1-yl)-1,1-dioxide Oleic acid | 6.69 | 282.46 | $C_{18}H_{34}O_2$ |
| 39. | 36.244 | 2-Methyl-Z, Z-3,13-Octadienol Oleic acid n-propyl 11-octadecenoate | 0.76 | 280.50 | $C_{19}H_{36}O$ |
| 40. | 36.376 | Z-2-Octadecen-1-ol Oleic acid n-propyl 11-octadecenoic acid | 5.53 | 282.46 | $C_{18}H_{34}O_2$ |
| 41. | 36.437 | Oleic acid | 3.84 | 282.46 | $C_{18}H_{34}O_2$ |
| 42. | 36.480 | Oleic acid 9-Octadecenoic acid (Z)-2,3-dihydroxylpropyl ester | 1.78 | 282.46 | $C_{18}H_{34}O_2$ |
| 43. | 36.529 | Erucic acid | 2.19 | 338.57 | $C_{18}H_{34}O_2$ |

| | | | | | |
|---|---|---|---|---|---|
| | | n-propyl 11-octadecenoate<br>Oleic acid | | | |
| 44. | 36.568 | Erucic acid<br>Oleic acid | 1.72 | 282.47 | $C_{18}H_{34}O$ |
| | | Octadec-9-enoic acid | | | |
| 45 | 36.637 | Oleic acid | 2.29 | 282.47 | $C_{18}H_{34}O$ |
| | | Cis-7, cis-11-hexadecadien-1-yl actate | | | |
| 46. | 36.657 | 3-Eicosene,(E)-<br>Oleic acid | 1.11 | 282.47 | $C_{18}H_{34}O$ |
| | | Cis-vaccenic | | | |
| 47. | 36.688 | Oleic acid | 1.90 | 282.47 | $C_{18}H_{34}O$ |
| | | 14-pentadecenoic acid | | | |
| 48. | 36.732 | Erucic acid<br>Oleic acid | 0.78 | 282.47 | $C_{18}H_{34}O$ |
| | | Octadec-9-enoic acid | | | |
| 49. | 36.757 | Oleic acid | 1.68 | 282.47 | $C_{18}H_{34}O$ |
| | | 7,11-hexadecadienal | | | |
| 50. | 36.801 | Oleic acid | 1.26 | 280.50 | $C_{19}H_{36}O$ |
| | | 2-methyl-Z,Z-3,13-octadecadienol | | | |
| 51. | 36.995 | Oleic acid<br>Octadec-9-enoic acid | 0.55 | 282.47 | $C_{18}H_{34}O$ |
| 52. | 37.266 | Z,Z-3,13-Octadecadien- | 0.04 | 282.47 | $C_{18}H_{34}O$ |
| 53. | 37.293 | 1-ol actate<br>Oleic acid<br>E-9-Hexadecenal<br>Cis-7, cis-11-hexadecadien-1-yl acetate<br>Oleic acid<br>Octadec-9-enoic acid | 0.03 | 282.47 | $C_{18}H_{34}O$ |
| 54. | 37.323 | 1-Docosene<br>n-propyl 11-octadecenoate<br>Oleic acid | 0.04 | 282.47 | $C_{18}H_{34}O$ |
| 55. | 37.376 | E-9-Tetradecenal<br>Aspidospermidin-17-ol,1-acetyl-19,21-epoxy-15,16-dimethoxy-<br>Oleic acid | 0.07 | 198.31 | $C_{15}H_{21}O$ |
| 56. | 37.807 | Erucic acid<br>Oleic acid | 5.01 | 282.47 | $C_{18}H_{34}O$ |
| 58. | 37.882 | Oleic acid<br>2-methyl-Z,Z-3,13-octadecadienol | 1.32 | 280.50 | $C_{19}H_{36}O$ |
| 59. | 37.948 | 9-Eicosenoic acid, (Z)-<br>Z-2-Octadecen-1-ol<br>Oleic acid | 2.56 | 282.47 | $C_{18}H_{34}O$ |

| | | | | | |
|---|---|---|---|---|---|
| | | 1,19-Eicosadiene | | | |
| 60. | 38.015 | Oleic acid,Oxirane, tetradecyl 9-Octadecenoic acid (Z)-,2,3-dihydroxypropyl ester | 2.27 | 44.05 | $C_2H_4O$ |
| 61. | 38.122 | Oleic acid,Erucic acid | 1.25 | 282.47 | $C_{18}H_{34}O$ |
| 62. | 38.270 | 3-Eicosene,(E)- Oleic acid 1,14-Docosanediol 1,19-Eicosadiene | 2.47 | 282.47 | $C_{18}H_{34}O$ |

Table 4.1.3: GC- MS Results of Phytochemical Composition of Aqueous Extract of Cow dung

| S/N | RETENTION TIME | NAME OF COMPOUND | PEAK AREA (%) | MOLECULAR WEIGHT | MOLECULAR FORMULAR |
|---|---|---|---|---|---|
| 1 | 20.229 | Hexadecanoic acid, methyl ester, pentadecanoic acid. | 1.37 | 256.42 | $C_{16}$ $H_{32}$ $O_2$ |
| 2 | 21.584 | Decanoic acid, ethyl ester | 0.24 | 172.26 | $C_{10}$ $H_{20}$ $O_2$ |
| 3 | 21.670 | Chloropropionic acid, dichloro-acetic acid, tetradecyl ester | 0.05 | 232.42 | $C_{15}$ $H_{32}$ $O_2$ |
| 4 | 22.021 | Dodecyl propyl ether | 0.09 | 204.36 | $C_{15}$ $H_{32}$ O |
| 5 | 22.088 | Pentadecanoic acid | 0.03 | 242.40 | $C_{15}$ $H_{30}$ $O_2$ |
| 6 | 22.017 | 9,10-Epoxyoctadecan-1-ol | 0.04 | 296.45 | $C_{18}$ $H_{32}O_2$ |
| 7 | 23.317 | 8, 11 – Octadecadienoic acid, 9,12-Octadecadienoic acid | 8.29 | 280.42 | $C_{18}$ $H_{30}$ $O_2$ |
| 8 | 24.068 | Heptadecanoic acid, methyl stearate, Heptadecanoic acid, | 1.06 | 270.45 | $C_{17}$ $H_{34}$ $O_2$ |
| 9 | 24.701 | Ethyl-Oleate (E)-9-Octadecenoic acid ester trans-9-Octadecenoic acid | 0.18 | 282.46 | $C_{18}$ $H_{36}$ |
| 10 | 24.829 | Oleic acid | 0.01 | 282.46 | $C_{18}$ $H_{34}$ $O_2$ |
| 11 | 25.176 | 9-Octadecenoic acid, (E)-Cis-vaccenic acid, Cis-13-Ethyl Oleate (E) | 0.65 | 310.51 | $C_9$ $H_6$ $O_{60}$ |
| 12 | 25.198 | 13-Octadecadienol, 2Octyl-Cyclopropaneoctanal, 9, 12-Octadecadienoic acid | 0.13 | 294.43 | $C_{22}$ $H_{44}$ |
| 13 | 25.268 | (Z, Z) – cyclohexane, cyclopropaneoctanol | 1.15 | 84.16 | $C_7$ $H_6$ $O_2$ |
| 14 | 25.530 | Octadec-9-enoic acid, 9-Octadecenoic acid | 0.10 | 282.46 | $C_{20}$ $H_{40}$ |
| 15 | 25.604 | Undecyl ester octadec-9-enoic acid, dodecyl ester undec-10-ynoic acid | 0.21 | 182.29 | $C_{11}$ $H_{18}$ $O_2$ |
| 16 | 25.743 | Oleic acid, Octadecanoic acid, Cis-vaccenic acid | 0.32 | 282.46 | $C_{18}$ $H_{34}$ $O_2$ |
| 17 | 27.031 | Cycloeicosane, cyclopropaneoctanal, | 0.08 | 140.22 | $C_9$ $H_{16}$ O |
| 18 | 27.602 | 3-Pentyle-methyl ester, | 0.06 | 270.45 | $C_{17}$ $H_{34}$ $O_2$ |
| 19 | 27.626 | oxiraneun decanoic acid, Cis-methyl 7-methyl hexadecanoate Eicosanoic acid, 14-methyl-, methyl ester | 0.06 | 312.53 | $C_{20}$ $H_{40}$ $O_2$ |
| 20 | 28.656 | 2-Chloropropionic acid, pentadecyl ester, Octacosyl propyl ether | 0.01 | 466.87 | $C_{32}$ $H_{66}$ O |
| 21 | 28.688 | Heptadecanolide, -heptafluorobutyle ester | 0.03 | 268.44 | $C_{17}$ $H_{32}$ $O_2$ |

| | | | | | |
|---|---|---|---|---|---|
| 22 | 28.774 | Heptafluorobutyric acid, n-tetradecyl ester, Pentafluoropionic acid | 0.05 | 264.03 | $C_4 H_{70} O$ |
| 23 | 28.920 | Heptadecyl ester, Oleic Acid, Cis-Vacccenic acid | 0.02 | 256.42 | $C_{16} H_{32} O_2$ |
| 24 | 30.879 | Docosanoic acid, trans-9-(2-butylcyclopentyl) monanoate | 1.03 | 340.59 | $C_{22} H_{44} O_2$ |
| 25 | 31.112 | Tetradecanal Cis-Vaccenic acid, propyl tetradecyl ether | 0.08 | 282.46 | $C_{18} H_{34} O_2$ |
| 26 | 31.148 | E-15-Heptadecenal, 3-Octadecene | 0.07 | 252.48 | $C_{18} H_{36}$ |
| 27 | 31.217 | Hexacosyl propyl ether, Eicosyl propyl ether, Docosyl propyl ether | 0.04 | 433.82 | $C_{30} H_{61} O$ |
| 28 | 31.265 | Cis-13-Octadecenoic acid, Oleic Acid, 1-methyl ethenyi | 0.12 | 58.08 | $C_3 H_6 O$ |
| 29 | 31.325 | Cyclohexanol, 5-methyl-2-(i-methyl ethenyl) | 0.10 | 100.16 | $C_6 H_{12} O$ |
| 30 | 31.378 | 2, 3-dihydroxypropyl ester, Hexacosyl propyl ether | 0.12 | 488.86 | $C_{30} H_{610} C_{37}$ |
| 31 | 31.462 | Hexadecyl ester, 1-propyl, 9-tetradecenoate | 0.43 | 268.44 | $C_{17} H_{32} O_2$ |
| 32 | 31.510 | Decosyl propyl ether, Eicosyl Propyl ether | 0.16 | 352.64 | $C_{23} H_{48} O$ |
| 33 | 31.549 | Octadec-9-enoic acid, 6-Octadecenoic acid | 0.09 | 282.46 | $C_{18} H_{34} O_2$ |
| 34 | 31.603 | Prople triacontoyl Ether, Octacosyl propyl ether | 0.18 | 472.89 | $C_{33} H_{68} O$ |
| 35 | 31.662 | Cycloicosane, 13-Octadecadi-enol, 5-Eicosene | 0.25 | 280.54 | $C_{20} H_{40}$ |
| 36 | 31.739 | 1, 19 Eicosadiene, 8-Hexaecenal, undec-10-ynoic acid | 0.14 | 238.41 | $C_{16} H_{30} O$ |
| 37 | 31.863 | Cis-13-Octadecenoic acid, trans-13-Octadecenoic acid | 0.12 | 280.54 | $C_{20} H_4 O$ |
| 38 | 31.960 | 9-Octadecenoic acid, (E)-3-Ei-Cosene, (E)-Ei Cosene | 0.29 | 282.56 | $C_{120}H_{42}$ |
| 39 | 31.994 | Cycloeicossane, undec-10-ynoic acid | 0.19 | 182.26 | $C_{11} H_{18} O_2$ |
| 40 | 31.204 | 9-Octadeccenoic acid, Cis-13-Octadecenoic acid, Eicosyl propyl ether | 0.19 | 386.66 | $C_{22} H_{45} O_7$ |
| 41 | 32.370 | Octadec-9-enoic acid, 2-methyle-z Oleic acid | 0.39 | 282.46 | $C_{18} H_{34} O_2$ |
| 42 | 32.660 | Trans-13-Octadecenoic acid, Tetradecenoic acid | 0.49 | 226.36 | $C_{14} H_{26} O_2$ |
| 43 | 32.785 | Trans-13-Octadecenoic acid, 9-Tricosene | 0.60 | 322.61 | $C_{23} H_{46}$ |

| | | | | | |
|---|---|---|---|---|---|
| 44 | 32.920 | I-Nonadecene Oleic Acid, Acetoxybenzoic acid | 0.39 | 266.50 | $C_{19}$ $H_{38}$ |
| 45 | 33.201 | E-II-Hexadecenal, I-Octadecene, 13-Octadecenal | 0.82 | 238.41 | $C_{16}$ $H_{30}$ O |
| 46 | 33.354 | Erucic acid 9-Tricosene, Acetoxybenzoic acid | 2.87 | 340.57 | $C_{22}$ $H_{42}$ O |
| 47 | 33.643 | Cycloeicosane, Oleic acid, trans-13-octadecenoic acid | 7.43 | 280.54 | $C_{20}$ $H_{40}$ |
| 48 | 33.741 | 13-Octadecadien -1-olacetate, 2-methyl-z, 2-3, 13-Octadecadienol | 3.00 | 264.45 | $C_{18}$ $H_{32}$ O |
| 49 | 33.760 | Palmitoleic acid, z-8-methyl-9-tetradecenoic acid | 0.85 | 254.41 | $C_{16}$ $H_{30}$ $O_2$ |
| 50 | 34.179 | 2, 3 dihydropropyl ester, 9-Octadecenoic acid | 8.11 | 134.17 | $C_6$ $H_{14}$ $O_3$ |
| 51 | 34.260 | Cis – 7, Cis -11-Hexadecadien, - 1-yl acetate, 5-Eicosene, (E)-2-methyl-z, z-3. | 1.68 | 280.45 | $C_{18}$ $H_{32}$ $O_2$ |
| 52 | 34.283 | 1-Octadecene,I-Decosene | 1.05 | 308.59 | $C_{22}$ $H_{44}$ |
| 53 | 34.304 | 5-Eicosene, (E)-9-Octadecenoic acid (z)-, 2-hydroxy-I-(hydroxymethyl) | 1.02 | 280.54 | $C_{20}$ $H_{40}$ |
| 54 | 34.398 | I-Nonadecene, I-Docosene, Eurcic acid | 2.54 | 340.57 | $C_{22}$ $H_{42}$ $O_2$ |
| 55 | 34.500 | Trans-13-Octadecenoic acid, Octadec-9-enoic acid, Dichloroacetic acid | 12.03 | 128.94 | $C_2$ $H_2$ $Cl_2$ $O_2$ |
| 56 | 34.870 | Cis-9-Hexadecenal, Propyl carbonate Cis-13-Octadecenoic acid | 0.82 | 102.09 | $C_4$ $H_6$ $O_3$ |
| 57 | 34.997 | Undec-10-ynoic acid, 2, 10-Dode Cadien-1-01, 3, 7, 11-trimethyl | 0.43 | 166.31 | $C_{12}$ $H_{22}$ |
| 58 | 36.887 | I-Cyclohexylnonene, oleic acid, 2-methyl-z, z-3 | 0.02 | 208.38 | $C_{15}$ $H_{28}$ |
| 59 | 37.174 | 6-Octadecenoic acid, (z) – oleic acid | 0.02 | 282.46 | $C_{18}$ $H_{34}$ $O_2$ |
| 60 | 37.254 | Docosyl propyl ether, | 0.01 | 196.37 | $C_{15}H_{32}O$ |
| 61 | 37.345 | 9-Eicosene, (E) 2-Eicosene, (E), 13-Octadecadienol | 0.00 | 278.51 | $C_{20}$ $H_{38}$ |
| 62 | 37.379 | 6-Octadecenoic acid, Oleic acid | 0.04 | 282.46 | $C_{18}$ $H_{24}$ $O_2$ |
| 63 | 37.414 | 9-Octadecenal, (z)-Oleic acid, 2-methyl – z, z – 3. | 0.06 | 266.46 | $C_{18}$ $H_{34}$ O |
| 64 | 37.548 | 13.Octadecadienol, 13-Octadecenal, (z)-6-Octadecenoic acid, Heptafluorobytrio acid | 0.02 | 266.46 | $C_{18}$ $H_{34}$ O |

Table 4.1.4: GC- MS Results of Phytochemical Composition of Aqueous Extract of Cow dung ZnO nanoparticle

| S/N | RETENTION TIME | NAME OF COMPOUND | PEAK AREA (%) | MOLECULAR WEIGHT | MOLECULAR FORMULAR |
|---|---|---|---|---|---|
| 1 | 5.399 | 4-trifluoroacetoxy tetradecane, 3-Heptafluorobutyroxypentadecane | 10.18 | 114.15 | $C_5 H_{10} O_2$ |
| 2 | 8.817 | Caryophyllene Octadecene, 1-Chloro-Octadecane | 0.80 | 204.35 | $C_{15} H_{24}$ |
| 3 | 13.227 | 2-Tetradecane, (E)-9-Eicosene, (E)-Dichloroacetic acid, 4-hexadecyl ester | 1.06 | 278.51 | $C_{20} H_{38}$ |
| 4 | 13.432 | Hexadecane, 1-Octadecanesulphonyl chloride | 0.69 | 256.42 | $C_{16} H_{32} O_2$ |
| 5 | 17.432 | 1-Octadecene 9-Eicosene, (E)-5-Eicosene, 2-Tetradecene | 2.11 | 196.37 | $C_{14} H_{28}$ |
| 6 | 17.808 | 1-Octadecane sulphonyl chloride, carbonic acid, dodecyl vinyl ester, tetradecyl ester | 1.28 | 362.98 | $C_{18} H_{37} O_2$ |
| 7 | 19.850 | Silane, trichlorodecyl-1-octadecane sulphonyl chloride, octadecane. | 1.23 | 254.49 | $C_{18} H_{38}$ |
| 8 | 20.225 | Hexadecenoic acid, , pentadecanoic acid | 2.00 | 242.40 | $C_{15} H_{30} O_2$ |
| 9 | 21.637 | 1-Octadecene, Cydoeisocane, 3-Eicosene | 4.83 | 252.48 | $C_{18} H_{36}$ |
| 10 | 21.827 | Carbonic acid, Octadecyl prop-1-en-1-yl ester Hexadecyl prop-1-en-1-yl ester | 1.65 | 61.02 | $H_2 CO_3$ |
| 11 | 23.280 | alpha-endosulfan beta-endosulfan | 67.99 | 406.95 | $C_9 H_6 O_{60}$ |
| 12 | 25.392 | 1-Docosene,1-Nonadecene | 0.98 | 308.58 | $C_{22} H_{44}$ |
|  | 25.790 | 5-(bromomethyl)-2-chloropyridine, Acetoxybenzoic acid | 4.46 | 122.12 | $C_7 H_6 O_2$ |
| 14 | 28.807 | Pentacos-1-ene, Nonacos-1-ene, E-Eicosene | 0.72 | 280.53 | $C_{20} H_{40}$ |

### 4.1.2 Characterization of Cow Dung Zinc Oxide Nanoparticles

#### 4.1.2.1 UV–visible spectroscopy

The formation of zinc oxide nanoparticles was primarily characterized by ultraviolet–visible (UV–Vis) spectrophotometer.

The addition of the zinc acetate dihydrate and NaOH to the aqueous extract changed colour from light brown to white colour indicating the formation of zinc oxide nanoparticles for cow dung and dark brown color to off white for *Pennisetum purpureum* zinc oxide nanoparticles.

The absorption spectra of cow dung and *Pennisetum purpureum* synthesized zinc oxide nanoparticles are presented in Figure 4.1.1 and figure 4.1.2. From the obtained spectra, cow dung zinc oxide nanoparticles and *Pennisetum purpureum* zinc oxide nanoparticles showed absorbance peaks at 367nm and 370 nm, respectively, confirming the successful green synthesis of zinc oxide nanoparticles.

The energy band gap was calculated from wavelength using the equation (Eg (eV) =1240/$\lambda$(nm)). The calculated energy band gap value for cow dung zinc oxide nanoparticle was 3.38eV and 3.35eV for *Pennisetum purpureum* zinc oxide nanoparticle.

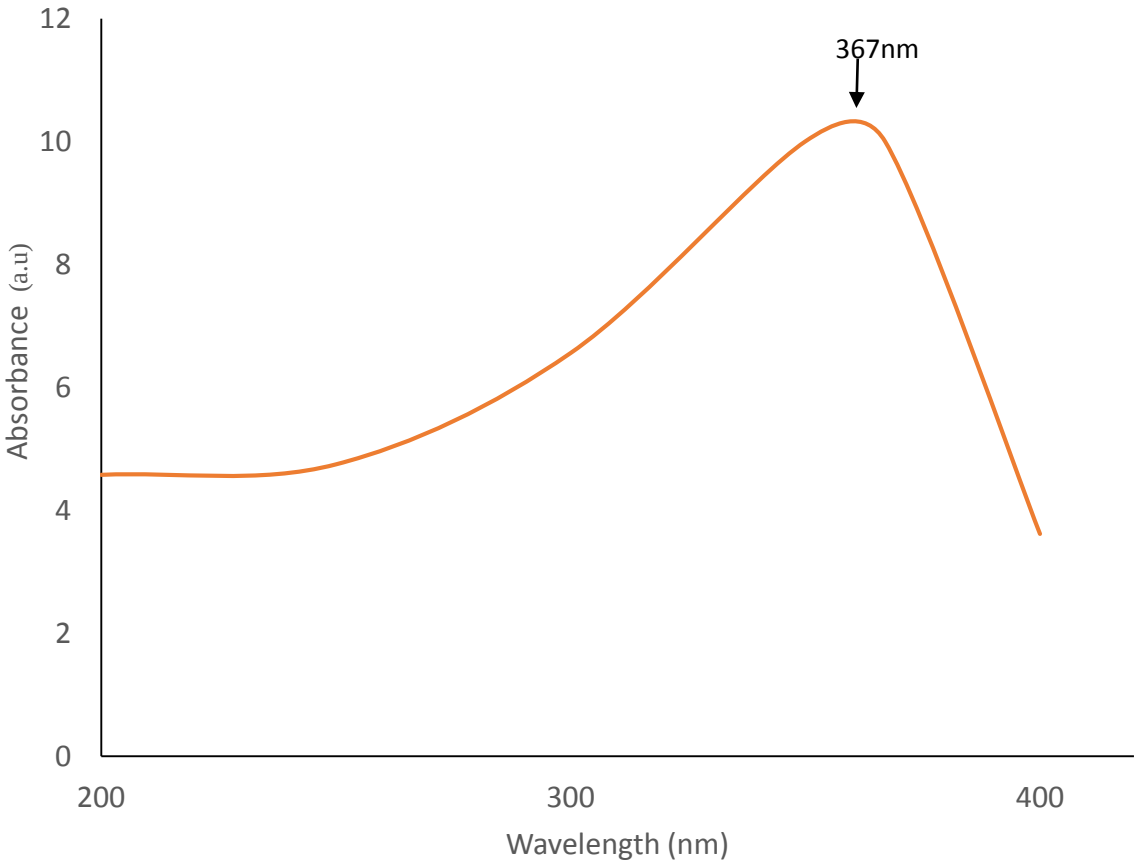


Figure 4.1.1 UV-visible absorption spectrum of zinc oxide nanoparticles synthesized from cow dung extract

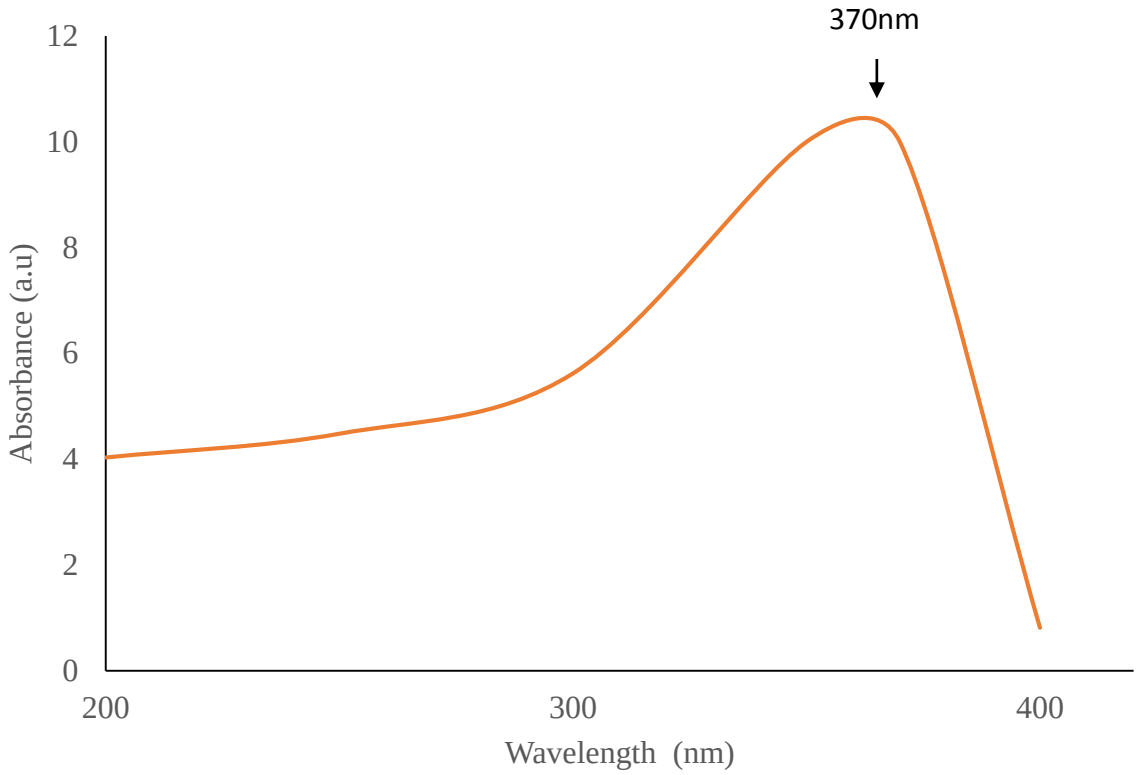


Figure 4.1.2 UV-visible absorption spectrum of zinc oxide nanoparticles synthesized from *Pennisetum purpureum* extract

### 4.1.2.2 Fourier Transform Infrared Spectroscopy of Cow Dung and *Pennisetum purpureum* Zinc Oxide Nanoparticles

The Fourier transform infrared spectroscopy (FTIR) results in figures 4.1.3 - 4.1.4 and Tables 4.1.5- 4.1.6 showed the presence of biomolecules and functional groups that capped the synthesized zinc oxide nanoparticles. The FTIR spectra of the synthesized zinc oxide nanoparticles were within the range of 4000 to 450cm$^{-1}$. The highly intense peak located at 3,365.8 cm$^{-1}$ (cow dung zinc oxide nanoparticles) and 3201 cm$^{-1}$ (*Pennisetum purpureum* zinc oxide nanoparticles) denoted the presence of OH group. The peaks located at 2102.2 cm$^{-1}$ (cow dung zinc oxide nanoparticles) and 2117 cm$^{-1}$ (*Pennisetum purpureum* zinc oxide nanoparticles) denoted the presence of C≡C (alkyne). The peaks located at 1349 cm$^{-1}$, 1558.0 cm$^{-1}$ (cow dung zinc oxide nanoparticles) and 1401.5cm$^{-1}$, 1543.1 cm$^{-1}$ (*Pennisetum purpureum* zinc oxide nanoparticles) showed the presence of N-O (Nitro). The peaks located at 1408.9 cm$^{-1}$ showed the presence of C=C (alkene) in cow dung zinc oxide nanoparticles and 1021.3 cm$^{-1}$, 1017.6 cm$^{-1}$ showed the presence of C-O (ether) in cow dung and *Pennisetum purpureum* zinc oxide nanoparticles.

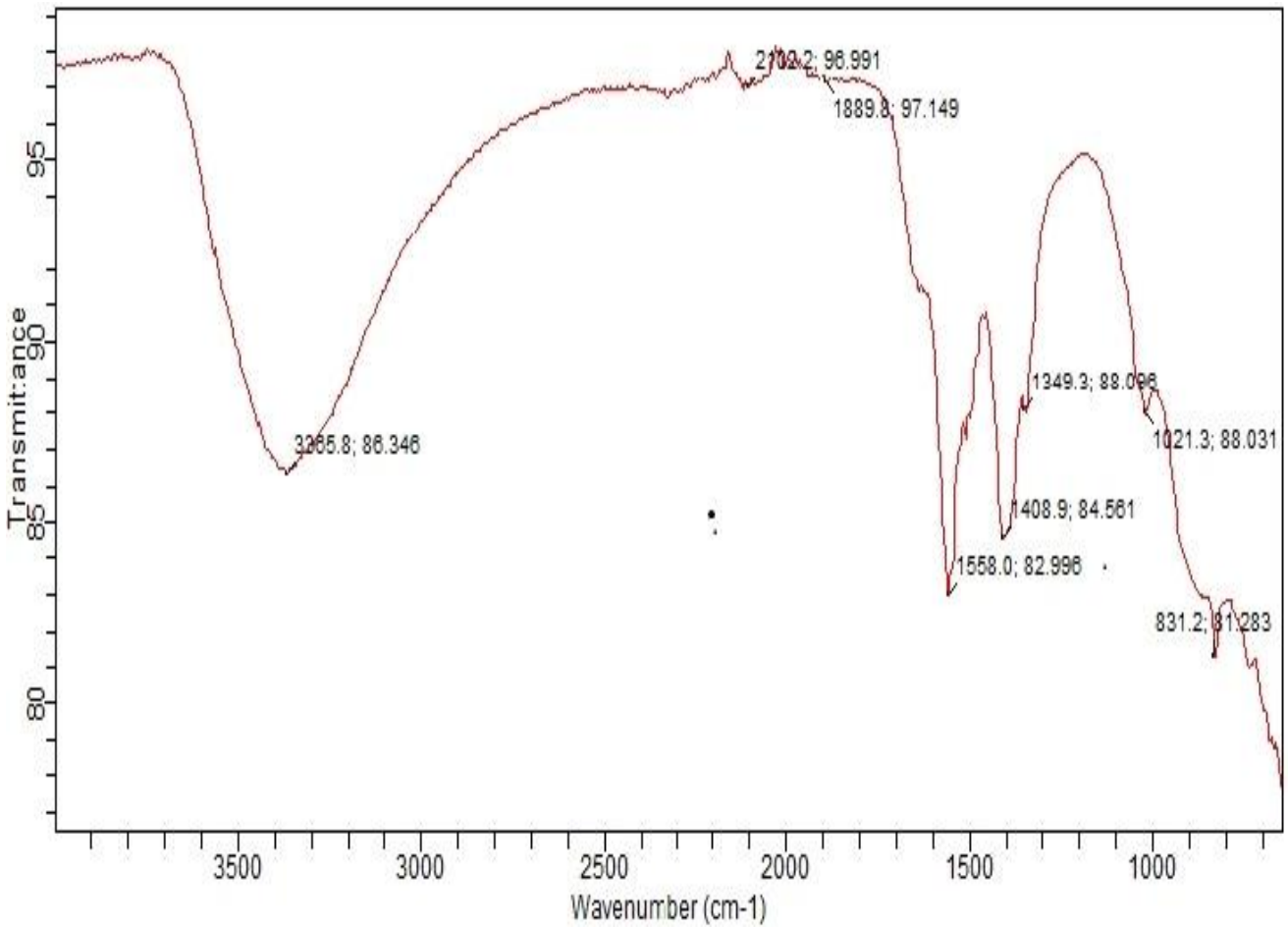


Figure 4.1.3: FTIR spectrum of cow dung zinc oxide nanoparticles.

**Table 4.1.5: FTIR result of cow dung zinc oxide nanoparticles**

| **Characteristic Absorption ($cm^{-1}$) Peak value** | **Bond** | **Functional group** |
|---|---|---|
| 1021.3 | C-O | Ether |
| 1408.9 | C=C | Alkene |
| 1349.3 | N-O | Nitro |
| 1558.0 | N-O | Nitro |
| 2102.2 | C≡C | Alkyne |
| 3365.8 | O-H | Alcohol |

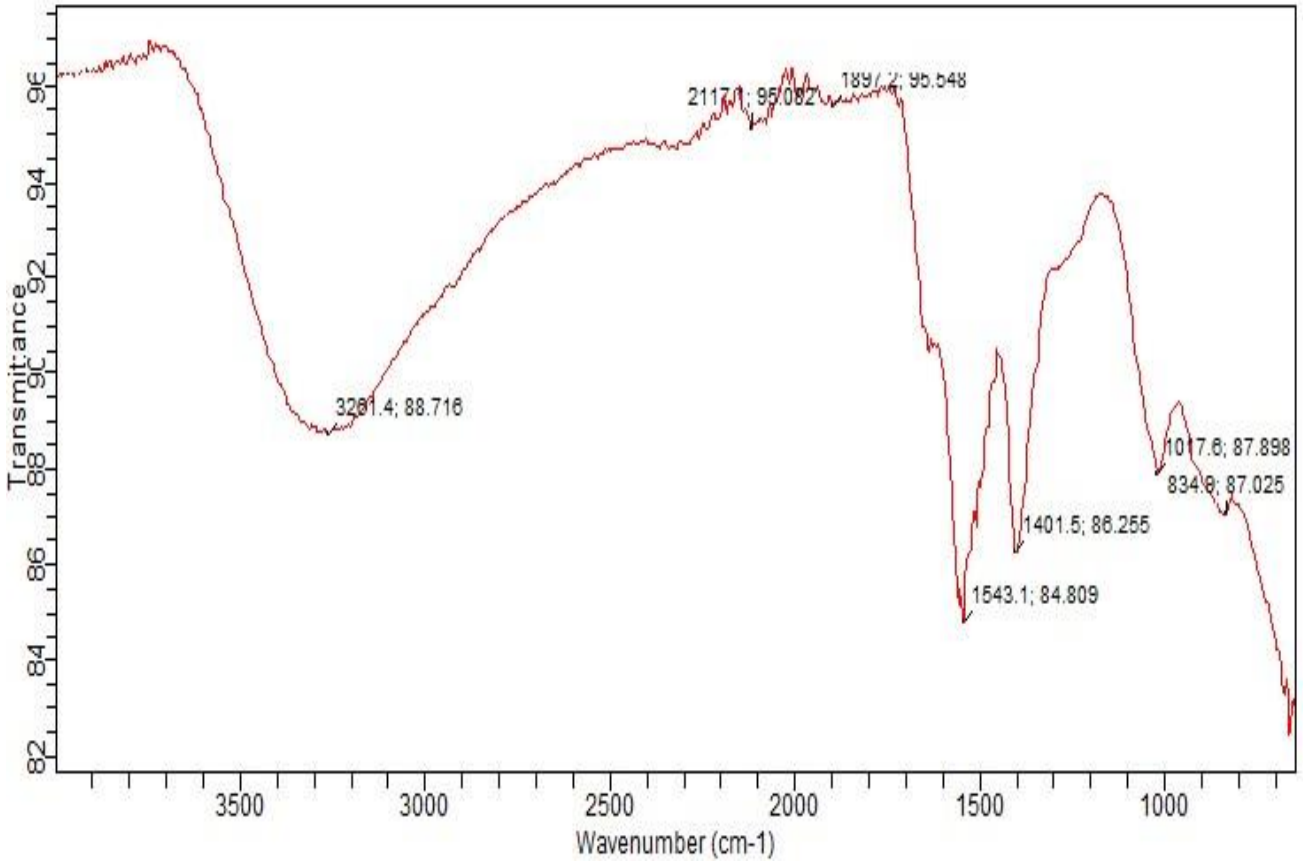


Figure 4.1.4: FTIR of *Pennisetum purpureum* zinc oxide nanoparticles.

**Table 4.1.6: FTIR result of *Pennisetum purpureum* zinc oxide nanoparticles**

| **Characteristic Absorption ($cm^{-1}$) Peak value** | **Bond** | **Functional group** |
|---|---|---|
| 1017.6 | C-O | Ether, Ester |
| | O-H | Alcohol |
| 1401.5 | N=O | Nitro |
| | $-CH_3$ | Alkane |
| 1543.1 | N-O | Nitro |
| 2117 | C≡C | Alkyne |
| 3201 | OH | Alcohol |

#### 4.1.2.3 Transmission Electron Microscopy

Transmission Electron Microscopy confirmed the formation of the size, size distribution, and shape of the synthesised zinc oxide nanoparticles.

The TEM images (Figure 4.1.5 - 4.1.6) showed that the biosynthesised cow dung and *Pennisetum purpureum* zinc oxide nanoparticles were spherical in shape with an average mean particle size of 3.10nm for cow dung zinc oxide nanoparticles and 15.21nm for *Pennisetum purpureum* zinc oxide nanoparticles at 100nm magnification.

**a)** **(b)**

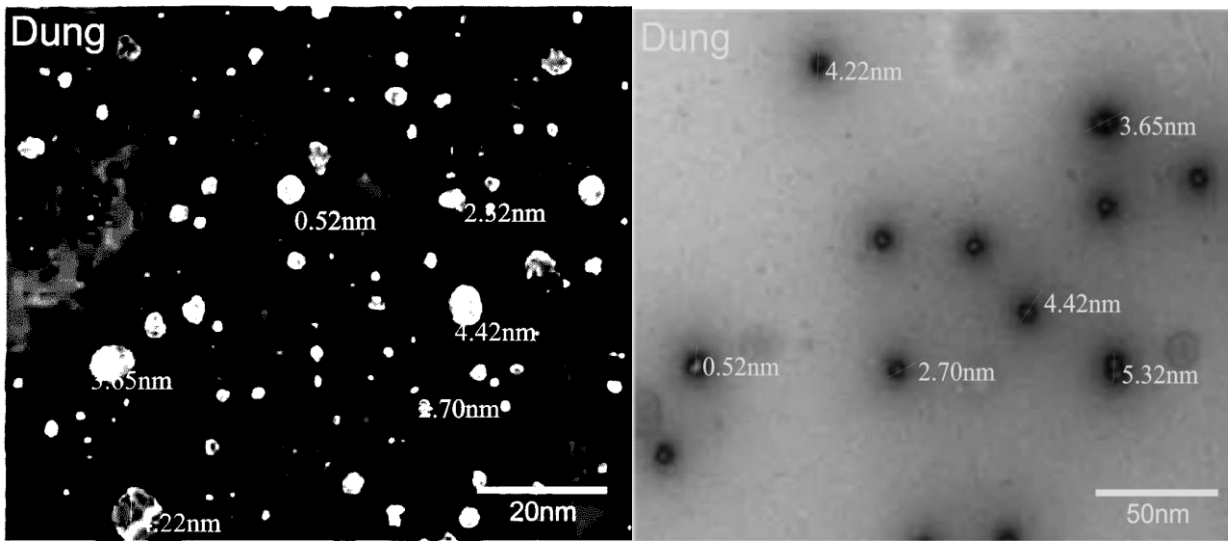


**(c)**

**p**

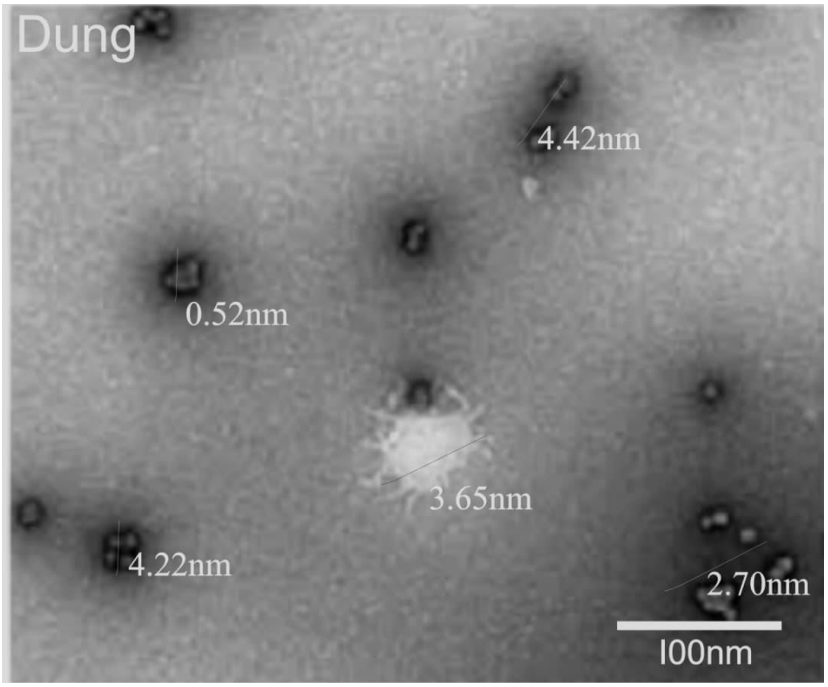


Figure 4.1.5: TEM images of cow dung zinc oxide nanoparticles at different magnifications

**a)** **b)**

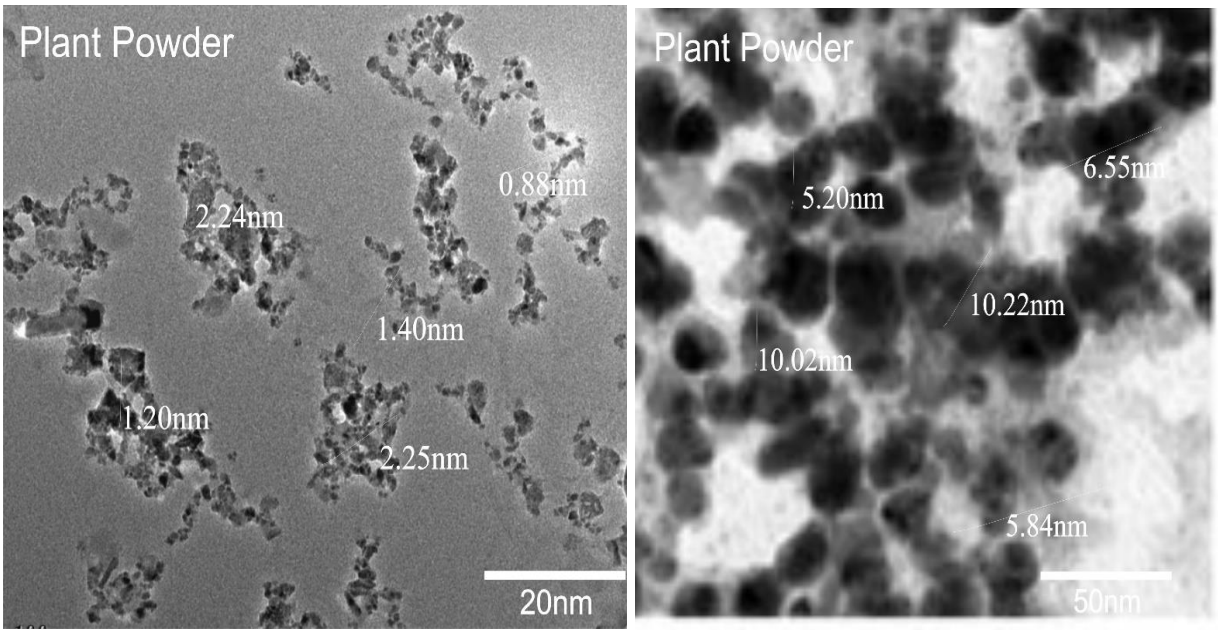


**c)**

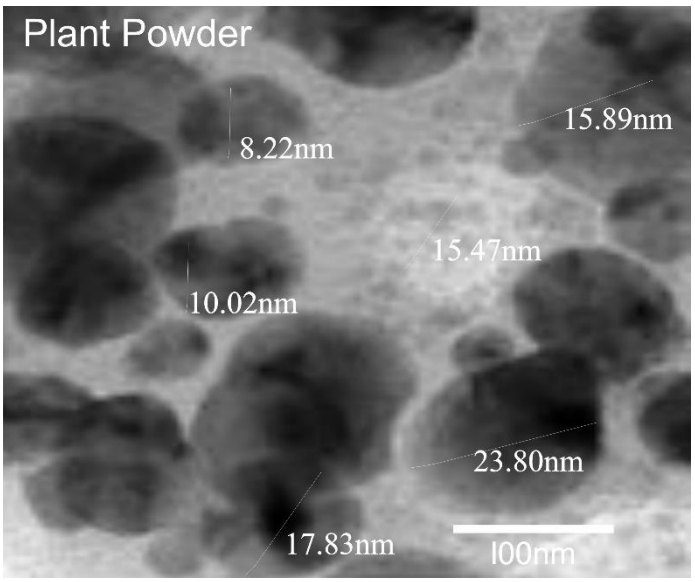


Figure 4.1.6: TEM images of *Pennisetum purpureum* zinc oxide nanoparticles at different magnifications

#### 4.1.2.4 X-ray diffraction of zinc oxide nanoparticles

The XRD spectra showed diffraction peaks for cow dung and *Pennisetum purpureum* zinc oxide nanoparticles in figures 4.1.7 and 4.1.8. The crystallinity of a material was determined from the sharpness of its diffraction peaks.

X-ray diffraction confirmed cow dung and *Pennisetum purpureum* zinc oxide nanoparticle's crystalline structure, peak position and phase composition. The crystalline size of the synthesized cow dung and *Pennisetum purpureum* zinc oxide nanoparticles were calculated using Debye–Scherrer equation. The average crystalline size of cow dung ZnO nanoparticles was 18.17nm and 23.37nm for *Pennisetum purpureum* zinc oxide nanoparticles as shown in table 4.1.7 and table 4.1.8.

The XRD diffractogram showing the diffraction peak intensity of cow dung zinc oxide nanoparticles 2θ values ranged from $28.87^0$ to $68.13^0$ (figure 4.1.7) while the XRD diffractogram showing the diffraction peak intensity of *Pennisetum purpureum* zinc oxide nanoparticle 2θ ranged from $28.56^0$ to $68.02^0$ (figure 4.1.8).

**Table 4.1.7: XRD peak position (2θ) and average crystalline size of cow dung zinc oxide nanoparticles.**

| Peak position 2θ($^0$) | FWHM (degree) | DP (nm) | DP Average (nm) |
|---|---|---|---|
| 28.87 | 0.43 | 19.94 | 18.17 |
| 32.05 | 0.71 | 12.17 | |
| 34.78 | 0.31 | 28.07 | |
| 36.58 | 0.45 | 19.43 | |
| 47.77 | 0.51 | 17.81 | |
| 57.00 | 0.54 | 17.50 | |
| 63.09 | 0.62 | 15.72 | |
| 68.13 | 0.68 | 14.74 | |

**NOTE**

FWHM = Full Width at Half Maximum

Dp = Average Crystallite size

θ = Bragg angle

**Table 4.1.8: XRD peak position (2θ) and average crystalline size of *Pennisetum purpureum* zinc oxide nanoparticles**

| Peak position 2θ(degree) | FWHM (degree) | Dp (nm) | Dp Average (nm) |
|---|---|---|---|
| 28.56 | 0.42 | 20.40 | 23.37 |
| 31.06 | 0.23 | 37.47 | |
| 31.80 | 0.41 | 21.06 | |
| 32.68 | 0.31 | 27.91 | |
| 34.50 | 0.24 | 35.23 | |
| 36.33 | 0.44 | 19.86 | |
| 47.59 | 0.69 | 13.15 | |
| 56.55 | 0.56 | 16.84 | |
| 62.86 | 0.56 | 17.38 | |
| 68.02 | 0.59 | 16.98 | |

**NOTE**

Full Width at Half Maximum (FWHM).

Dp = Average Crystallite size

θ = Bragg angle

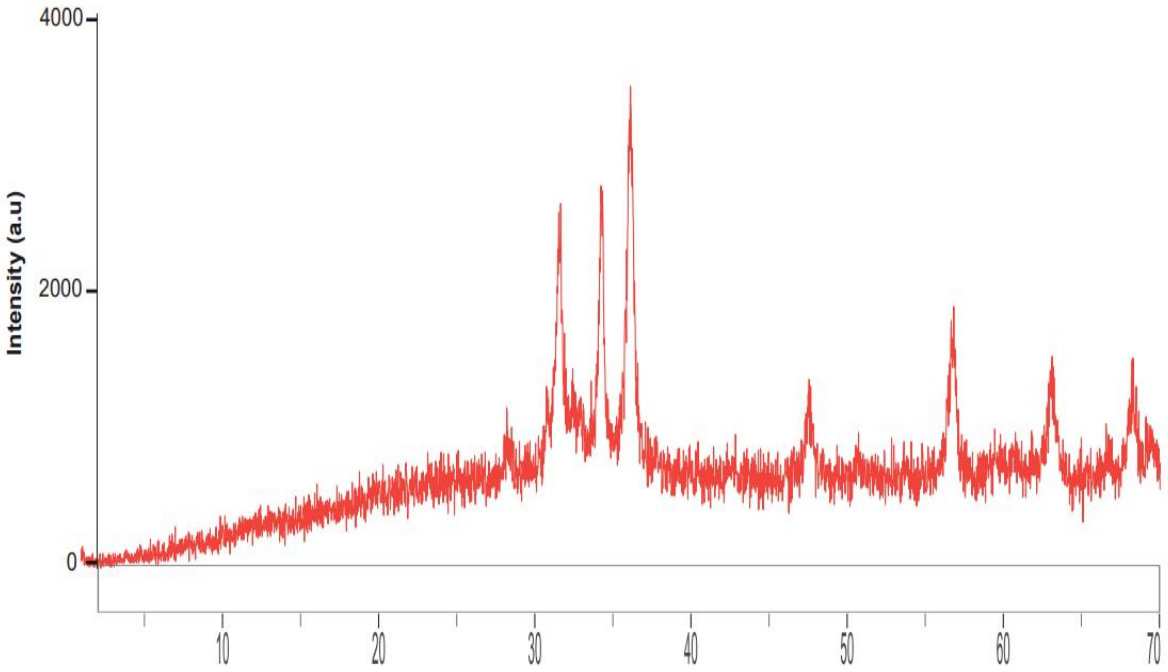


**Figure 4.1.7: XRD image of cow dung zinc oxide nanoparticles**

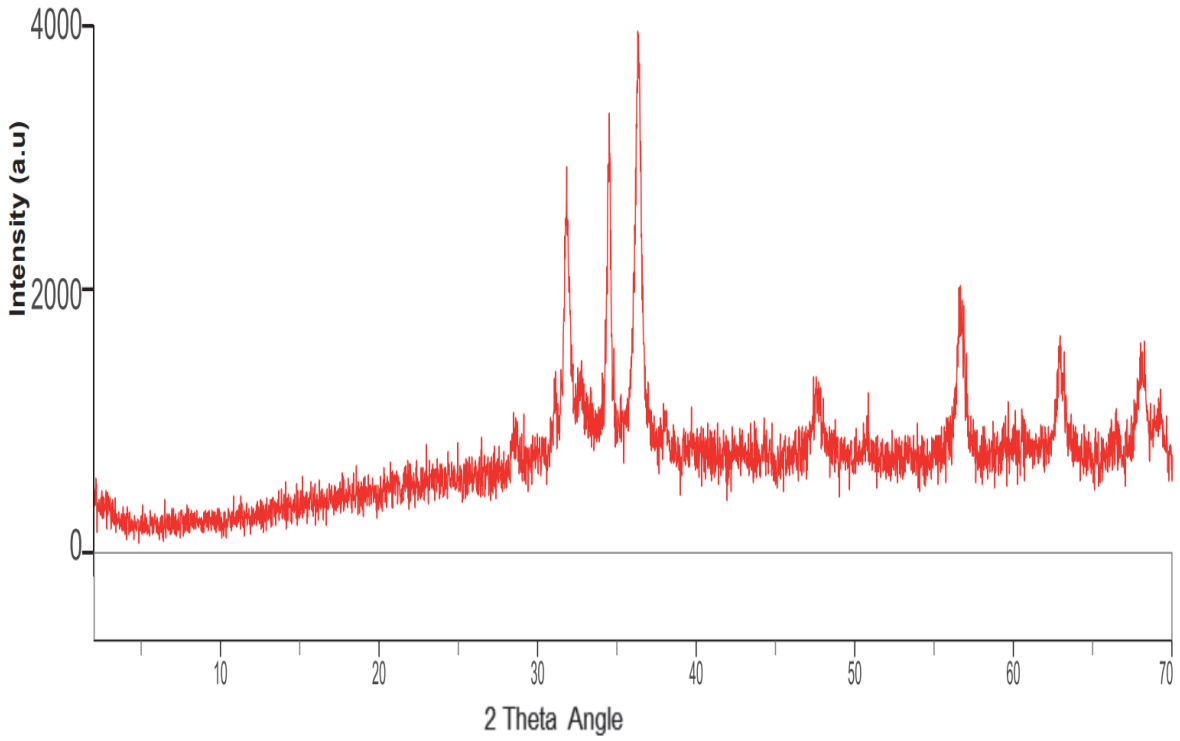


**Figure 4.1.8: XRD image of *Pennisetum purpureum* zinc oxide nanoparticles**

### 4.1.3 Soil Texture

The soil texture presented in table 4.1.9 shows the soil composition and texture. The soil composition are silt 44.5%, clay 44.0% and sand 11.0%. The soil sample texture is silty clay.

**Table 4.1.9: Soil composition and texture**

| PARAMETER | UNIT | CONCENTRATION |
|---|---|---|
| Sand | % | 11.0 |
| Silt | % | 44.5 |
| Clay | % | 44.0 |
| Soil Texture | mg/kg | Silty clay |

### 4.1.4 Total Nitrogen Concentrations (mg/kg)

Table 4.1.10 shows the mean and standard deviation of the concentrations of nitrogen in unpolluted, polluted and remediated soil samples from day 1, 14, 28 and 42. The total nitrogen concentrations in the unpolluted soil remained relatively stable, with only a slight decrease from 0.33 mg/kg on Day 1 to 0.31 mg/kg by Day 42. In the crude oil-polluted soil, the nitrogen concentrations dropped from 0.26 mg/kg to 0.22 mg/kg over the 42-day period, indicating some depletion due to the pollution. For the soil treated with cow dung zinc oxide nanoparticles, both 20g and 40g treatments showed significant reductions in nitrogen concentration, with 40g showing the largest decrease to 0.14 mg/kg by Day 42. The soil treated with *Pennisetum purpureum* zinc oxide nanoparticles also exhibited declines in nitrogen, with the 40g treatment reducing nitrogen content the most, to 0.11 mg/kg, suggesting the higher concentration of nanoparticles effectively reduced nitrogen levels in the soil.

**Table 4.1.10: Total Nitrogen Concentrations (mg/kg) (Day 1 to Day 42)**

| Total Nitrogen (mg/kg) | Day 1 | Day 14 | Day 28 | Day 42 |
|---|---|---|---|---|
| Unpolluted Soil | $0.33\pm0.003^{f}$ | $0.33\pm0.002^{d}$ | $0.32\pm0.001^{f}$ | $0.31\pm0.001^{f}$ |
| Crude Oil Polluted Soil | $0.26\pm0.002^{d}$ | $0.26\pm0.001^{c}$ | $0.24\pm0.001^{d}$ | $0.22\pm0.001^{e}$ |
| 20g cow dung ZnO NP | $0.24\pm0.002^{b}$ | $0.22\pm0.006^{b}$ | $0.18\pm0.001^{c}$ | $0.17\pm0.001^{d}$ |
| 40g cow dung ZnO NP | $0.26\pm0.002^{c}$ | $0.18\pm0.001^{a}$ | $0.15\pm0.001^{b}$ | $0.14\pm0.001^{b}$ |
| 20g *Pennisetum purpureum* ZnO NP | $0.23\pm0.002^{a}$ | $0.26\pm0.002^{c}$ | $0.25\pm0.002^{e}$ | $0.15\pm0.002^{c}$ |
| 40g *Pennisetum purpureum* ZnO NP | $0.29\pm0.001^{e}$ | $0.21\pm0.001^{b}$ | $0.12\pm0.002^{a}$ | $0.11\pm0.001^{a}$ |

Results are Mean±Standard deviation of triplicate determinations. Columns with different alphabets are significantly different at $p\leq0.05$

### 4.1.5 Phosphorus Concentrations (mg/kg)

Table 4.1.11 shows the mean and standard deviation of the concentrations of phosphorous in unpolluted, polluted and remediated soil samples from day 1, 14, 28 and 42. Phosphorus concentrations in the unpolluted soil presented a slight reduction from 0.38 mg/kg to 0.33 mg/kg over the study period. In the crude oil-polluted soil, phosphorus concentration declined from 0.28 mg/kg to 0.20 mg/kg, reflecting the negative impact of pollution on nutrient availability. In the soil treated with cow dung zinc oxide nanoparticles, the phosphorus concentrations decreased significantly, particularly in the 40g treatment, which dropped to 0.10 mg/kg. Similar trends were observed in the *Pennisetum purpureum* zinc oxide treatments, with phosphorus concentrations in the 40g treatment falling to 0.06 mg/kg by Day 42. This suggests that the treatments, especially at higher concentrations, effectively reduced phosphorus content in the soil.

**Table 4.1.11: Phosphorus Concentrations (mg/kg) (Day 1 to Day 42)**

| Phosphorus (mg/kg) | Day 1 | Day 14 | Day 28 | Day 42 |
|---|---|---|---|---|
| Unpolluted Soil | $0.38\pm0.01^{b}$ | $0.36\pm0.01^{d}$ | $0.33\pm0.00^{d}$ | $0.33\pm0.00^{e}$ |
| Crude Oil Polluted Soil | $0.28\pm0.01^{a}$ | $0.24\pm0.01^{ab}$ | $0.23\pm0.00^{c}$ | $0.20\pm0.00^{d}$ |
| 20g cow dung ZnO NP | $0.28\pm0.01^{a}$ | $0.26\pm0.01^{bc}$ | $0.22\pm0.00^{b}$ | $0.15\pm0.00^{c}$ |
| 40g cow dung ZnO NP | $0.28\pm0.01^{a}$ | $0.25\pm0.02^{abc}$ | $0.20\pm0.00^{a}$ | $0.10\pm0.00^{b}$ |
| 20g *Pennisetum purpureum* ZnO NP | $0.27\pm0.01^{a}$ | $0.26\pm0.01^{bc}$ | $0.22\pm0.00^{b}$ | $0.15\pm0.00^{c}$ |
| 40g *Pennisetum purpureum* ZnO NP | $0.27\pm0.01^{a}$ | $0.24\pm0.01^{a}$ | $0.20\pm0.00^{a}$ | $0.06\pm0.00^{a}$ |

Results are Mean±Standard deviation of triplicate determinations. Columns with different alphabets are significantly different at $p\leq0.05$

### 4.1.6 Potassium Concentrations (mg/kg)

Table 4.1.12 shows the mean and standard deviation of the concentrations of potassium in unpolluted, polluted and remediated soil samples from day 1, 14, 28 and 42. The result of potassium concentration in the unpolluted soil, showed gradual decrease from 4.71 mg/kg on Day 1 to 4.24 mg/kg by Day 42. The crude oil-polluted soil also saw a decrease, from 4.57 mg/kg to 3.82 mg/kg, over the same period. The soil treated with cow dung zinc oxide nanoparticles showed a significant reduction in potassium, especially with the 40g treatment, where potassium levels dropped to 1.08 mg/kg by Day 42. In the *Pennisetum purpureum* zinc oxide nanoparticle treatments, the 40g treatment significantly reduced potassium levels to 2.07 mg/kg, indicating that both treatments effectively lowered potassium levels, with the higher nanoparticle concentrations being more effective.

**Table 4.1.12: Potassium Concentrations (mg/kg) (Day 1 to Day 42)**

| Potassium (mg/kg) | Day 1 | Day 14 | Day 28 | Day 42 |
|---|---|---|---|---|
| Unpolluted Soil | 4.71±0.02$^{b}$ | 4.65±0.03$^{a}$ | 4.53±0.02$^{f}$ | 4.24±0.03$^{f}$ |
| Crude Oil Polluted Soil | 4.57±0.01$^{d}$ | 4.66±0.00$^{a}$ | 4.25±0.01$^{e}$ | 3.82±0.02$^{e}$ |
| 20g cow dung ZnO NP | 4.70±0.01$^{b}$ | 4.65±0.00$^{a}$ | 3.67±0.02$^{d}$ | 1.16±0.01$^{b}$ |
| 40g cow dung ZnO NP | 4.92±0.01$^{c}$ | 4.66±0.00$^{a}$ | 2.40±0.01$^{a}$ | 1.08±0.01$^{a}$ |
| 20g *Pennisetum purpureum* ZnO NP | 4.71±0.01$^{b}$ | 4.65±0.01$^{a}$ | 3.26±0.01$^{c}$ | 2.95±0.01$^{d}$ |
| 40g *Pennisetum purpureum* ZnO NP | 4.87±0.02$^{a}$ | 4.66±0.01$^{a}$ | 2.65±0.01$^{b}$ | 2.07±0.01$^{c}$ |

Results are Mean±Standard deviation of triplicate determinations. Columns with different alphabets are significantly different at $p \leq 0.05$

### 4.1.7 Total Organic Carbon (TOC) (%) Concentrations

Table 4.1.13 shows the mean and standard deviation of the concentrations of total organic carbon in unpolluted, polluted and remediated soil samples from day 1, 14, 28 and 42. the total organic carbon (TOC) content in the unpolluted soil, remained relatively constant, with a slight decrease from 0.94% on Day 1 to 0.88% by Day 42. The crude oil-polluted soil initially had significantly higher TOC levels (3.94%), which decreased to 3.74% by Day 42. The treatments with cow dung zinc oxide nanoparticles showed a significant reduction in TOC, with the 40g treatment reducing it to 0.73% by Day 42. A similar trend was observed in the *Pennisetum purpureum* zinc oxide nanoparticles treatments, where the 40g treatment significantly reduced TOC to 0.72%, indicating that the nanoparticles effectively broke down the organic carbon in the soil over time, with higher concentrations yielding better results.

**Table 4.1.13: Total Organic Carbon (TOC) (%) (Day 1 to Day 42)**

| TOC (%) | Day 1 | Day 14 | Day 28 | Day 42 |
|---|---|---|---|---|
| Unpolluted Soil | $0.94\pm0.01^{a}$ | $0.93\pm0.01^{a}$ | $0.91\pm0.00^{a}$ | $0.88\pm0.01^{b}$ |
| Crude Oil Polluted Soil | $3.94\pm0.01^{c}$ | $3.91\pm0.01^{f}$ | $3.88\pm0.02^{f}$ | $3.74\pm0.02^{d}$ |
| 20g cow dung ZnO NP | $3.84\pm0.01^{b}$ | $3.24\pm0.02^{c}$ | $2.55\pm0.04^{d}$ | $0.92\pm0.01^{c}$ |
| 40g cow dung ZnO NP | $3.94\pm0.02^{c}$ | $2.75\pm0.03^{b}$ | $1.90\pm0.01^{c}$ | $0.73\pm0.03^{a}$ |
| 20g *Pennisetum purpureum* ZnO NP | $3.95\pm0.02^{c}$ | $3.73\pm0.02^{e}$ | $2.14\pm0.02^{d}$ | $0.91\pm0.01^{c}$ |
| 40g *Pennisetum purpureum* ZnO NP | $3.95\pm0.01^{c}$ | $3.37\pm0.02^{d}$ | $1.68\pm0.01^{b}$ | $0.72\pm0.01^{a}$ |

Results are Mean±Standard deviation of triplicate determinations. Columns with different alphabets are significantly different at $p\leq0.05$

### 4.1.8 Total Petroleum Hydrocarbon (TPH) Concentrations (mg/kg)

Table 4.1.14 shows the mean and standard deviation of the concentrations of total petroleum hydrocarbon in unpolluted, polluted and remediated soil samples from day 1, 14, 28 and 42. The total petroleum hydrocarbon (TPH) Concentration in the unpolluted soil, remained nearly unchanged, starting at 5.12 mg/kg and decreasing slightly to 5.02 mg/kg by Day 42. In the crude oil-polluted soil, however, TPH concentrations were extremely high initially (5373.85 mg/kg) and showed a significant reduction to 4657.47 mg/kg by the end of the study. Treatment with cow dung zinc oxide nanoparticles presented the most significant reduction in TPH, especially in the 40g treatment, where it significantly reduced to 403.65 mg/kg. The *Pennisetum purpureum* zinc oxide treatments also significantly and effectively reduced TPH concentrations, with the 40g treatment reaching 498.13 mg/kg.

These results indicate that both types of nanoparticles, particularly at higher concentrations, were highly effective in breaking down petroleum hydrocarbons in the polluted soil.

**Table 4.1.14: Total Petroleum Hydrocarbon Concentrations (mg/kg) (Day 1 to Day 42)**

| TPH (mg/kg) | Day 1 | Day 14 | Day 28 | Day 42 |
|---|---|---|---|---|
| Unpolluted Soil | 5.12±0.01[a] | 5.08±0.03[a] | 5.05±0.01[a] | 5.02±0.01[a] |
| Crude Oil Polluted Soil | 5373.85±3.06[c] | 5359.96±0.58[e] | 5345.64±3.46[e] | 4657.47±0.24[f] |
| 20g cow dung ZnO NP | 5367.69±1.50[b] | 4656.47±1.49[d] | 2979.02±0.12[c] | 543.43±0.38[d] |
| 40g cow dung ZnO NP | 5366.81±0.51[b] | 3224.73±0.70[b] | 1992.29±1.17[b] | 403.65±0.08[b] |
| 20g *Pennisetum purpureum* ZnO NP | 5375.52±1.73[c] | 5360.20±0.22[e] | 3195.09±0.57[d] | 673.18±0.79[e] |
| 40g *Pennisetum purpureum* ZnO NP | 5373.31±1.07[c] | 3986.08±0.06[c] | 2979.00±0.94[c] | 498.13±0.21[c] |

Results are Mean±Standard deviation of triplicate determinations. Columns with different alphabets are significantly different at $p \leq 0.05$

### 4.1.9 Polycyclic Aromatic Hydrocarbon (PAH) Concentrations (mg/kg)

Table 4.1.15 shows the mean and standard deviation of the concentrations of polycyclic aromatic hydrocarbon (PAH) in unpolluted, polluted and remediated soil samples from day 1, 14, 28 and 42. PAH concentrations in the unpolluted soil showed minimal change, with values decreasing slightly from 2.17 mg/kg to 2.03 mg/kg. In the crude oil-polluted soil, PAH concentrations were initially very high (722.72 mg/kg), but reduced significantly to 376.65 mg/kg by Day 42. The cow dung zinc oxide nanoparticle treatments, particularly the 40g treatment, resulted in significant reductions in PAH to 18.37 mg/kg by the end of the study. The *Pennisetum purpureum* zinc oxide treatments were similarly effective, with the 40g treatment lowering PAH levels to 7.04 mg/kg by Day 42. This shows that both types of nanoparticles were highly effective at degrading PAH in the soil, with higher concentrations yielding better results.

**Table 4.1.15: Polycyclic Aromatic Hydrocarbon (mg/kg) (Day 1 to Day 42)**

| PAH (mg/kg) | Day 1 | Day 14 | Day 28 | Day 42 |
|---|---|---|---|---|
| Unpolluted Soil | 2.17±0.02[a] | 2.15±0.01[a] | 2.12±0.02[a] | 2.03±0.01[a] |
| Crude Oil Polluted Soil | 722.72±2.22[d] | 526.99±0.92[f] | 438.65±0.21[f] | 376.65±0.34[f] |
| 20g cow dung ZnO NP | 713.27±2.73[c] | 78.21±0.05[d] | 52.19±0.09[e] | 23.55±0.35[e] |
| 40g cow dung ZnO NP | 703.75±5.53[b] | 36.74±0.49[c] | 26.24±0.13[b] | 18.37±0.24[c] |
| 20g *Pennisetum purpureum* ZnO NP | 723.45±2.81[d] | 115.63±0.42[e] | 47.06±0.41[d] | 21.03±0.35[d] |
| 40g *Pennisetum purpureum* ZnO NP | 703.19±2.54[b] | 33.22±0.56[b] | 30.66±0.30[c] | 7.04±0.03[b] |

Results are Mean±Standard deviation of triplicate determinations. Columns with different alphabets are significantly different at $p \leq 0.05$

### 4.1.10 Benzene, Toluene, Ethylene, and Xylene (BTEX) Concentrations (mg/kg)

Table 4.1.16 shows the mean and standard deviation of the concentrations of benzene, toluene, ethylene, and xylene (BTEX) in unpolluted, polluted and remediated soil samples from day 1, 14, 28 and 42. BTEX concentrations in the unpolluted soil, remained fairly stable, decreasing slightly from 2.22 mg/kg to 2.04 mg/kg. The crude oil-polluted soil had high initial BTEX levels (240.55 mg/kg), which reduced to 116.69 mg/kg by Day 42. Treatment with cow dung zinc oxide nanoparticles, especially at 40g, resulted in significant reduction in BTEX, down to 2.80 mg/kg. The *Pennisetum purpureum* zinc oxide nanoparticles treatments were similarly effective, with the 40g treatment reducing BTEX levels to 1.93 mg/kg. These findings suggest that both nanoparticles, particularly at higher concentrations, were very efficient in reducing BTEX concentrations in the soil.

**Table 4.1.16: Benzene, Toluene, Ethylene and Xylene ( BTEX) Concentrations (mg/kg) (Day 1 to Day 42)**

| BTEX (mg/kg) | Day 1 | Day 14 | Day 28 | Day 42 |
|---|---|---|---|---|
| Unpolluted Soil | 2.22±0.02[a] | 2.21±0.02[a] | 2.13±0.01[a] | 2.04±0.01[a] |
| Crude Oil Polluted Soil | 240.55±0.88[d] | 218.57±0.39[f] | 216.34±0.56[e] | 116.69±0.28[e] |
| 20g cow dung ZnO NP | 240.22±1.06[d] | 15.40±0.07[d] | 10.77±0.14[c] | 4.19±0.12[c] |
| 40g cow dung ZnO NP | 238.55±1.31[c] | 5.22±0.04[c] | 3.16±0.09[b] | 2.80±0.04[b] |
| 20g *Pennisetum purpureum* ZnO NP | 238.59±0.93[c] | 25.39±0.05[e] | 14.51±0.42[d] | 5.91±0.02[d] |
| 40g *Pennisetum purpureum* ZnO NP | 234.86±0.28[b] | 3.25±0.03[b] | 3.02±0.02[b] | 1.93±0.03[a] |

Results are Mean±Standard deviation of triplicate determinations. Columns with different alphabets are significantly different at $p \leq 0.05$

### 4.1.11 Arsenic (As) Concentrations (mg/kg)

Table 4.1.17 shows the mean and standard deviation of the concentrations of arsenic in unpolluted, polluted and remediated soil samples from day 1, 14, 28 and 42. In the unpolluted soil, arsenic concentration remained stable at 0.002 mg/kg throughout the study. Crude oil-polluted soil exhibited a significant reduction in arsenic levels, from 0.266 mg/kg on Day 1 to 0.144 mg/kg by Day 42. The 20g and 40g cow dung ZnO nanoparticles treatments significantly reduced arsenic concentration, with the 40g treatment showing a greater reduction to 0.002 mg/kg by Day 42. Similarly, the 20g and 40g *Pennisetum purpureum* ZnO nanoparticles treatments effectively reduced arsenic levels, with the 40g treatment reducing arsenic to 0.002 mg/kg by Day 42, suggesting strong remediation efficiency at higher nanoparticle concentrations.

**Table 4.17: Arsenic (As) Concentrations (mg/kg) (Day 1 to Day 42)**

| As (mg/kg) | Day 1 | Day 14 | Day 28 | Day 42 |
|---|---|---|---|---|
| Unpolluted Soil | 0.002±0.001[a] | 0.002±0.001[a] | 0.002±0.001[a] | 0.002±0.001[a] |
| Crude Oil Polluted Soil | 0.266±0.004[b] | 0.198±0.001[e] | 0.177±0.006[d] | 0.144±0.003[d] |
| 20g cow dung ZnO NP | 0.265±0.003[b] | 0.016±0.001[d] | 0.011±0.001[c] | 0.004±0.001[c] |
| 40g cow dung ZnO NP | 0.263±0.002[b] | 0.012±0.001[c] | 0.007±0.002[bc] | 0.002±0.000[bc] |
| 20g *Pennisetum purpureum* ZnO NP | 0.265±0.001[b] | 0.015±0.001[d] | 0.008±0.001[bc] | 0.004±0.001[bc] |
| 40g *Pennisetum purpureum* ZnO NP | 0.266±0.003[b] | 0.008±0.001[b] | 0.005±0.001[ab] | 0.002±0.001[ab] |

Results are Mean±Standard deviation of triplicate determinations. Columns with different alphabets are significantly different at $p \leq 0.05$

### 4.1.12 Chromium (Cr) Concentrations (mg/kg)

Table 4.1.18 shows the mean and standard deviation of the concentrations of chromium in unpolluted, polluted and remediated soil samples from day 1, 14, 28 and 42. The unpolluted soil showed no significant changes in chromium concentration, remaining constant at 0.001 mg/kg. In crude oil-polluted soil, chromium levels increased slightly from 0.278 mg/kg on Day 1 to 0.266 mg/kg by Day 42. The cow dung ZnO nanoparticles treatments, particularly the 40g treatment, showed a significant reduction in chromium levels, dropping to 0.014 mg/kg by Day 42. The *Pennisetum purpureum* ZnO nanoparticles treatments also reduced chromium concentrations, with the 40g treatment lowering it to 0.014 mg/kg by Day 42, indicating effective chromium remediation by both nanoparticle treatments.

**Table 4.1.18: Chromium (Cr) Concentrations (mg/kg) (Day 1 to Day 42)**

| Cr (mg/kg) | Day 1 | Day 14 | Day 28 | Day 42 |
|---|---|---|---|---|
| Unpolluted Soil | $0.001\pm0.001^{a}$ | $0.001\pm0.001^{a}$ | $0.001\pm0.001^{a}$ | $0.001\pm0.001^{a}$ |
| Crude Oil Polluted Soil | $0.278\pm0.001^{d}$ | $0.315\pm0.001^{c}$ | $0.256\pm0.002^{b}$ | $0.266\pm0.003^{d}$ |
| 20g cow dung ZnO NP | $0.274\pm0.003^{cd}$ | $0.934\pm0.010^{e}$ | $0.583\pm0.001^{d}$ | $0.024\pm0.002^{c}$ |
| 40g cow dung ZnO NP | $0.266\pm0.004^{b}$ | $0.666\pm0.003^{d}$ | $0.445\pm0.043^{c}$ | $0.014\pm0.003^{b}$ |
| 20g *Pennisetum purpureum* ZnO NP | $0.274\pm0.003^{cd}$ | $1.192\pm0.016^{f}$ | $0.615\pm0.019^{d}$ | $0.024\pm0.002^{c}$ |
| 40g *Pennisetum purpureum* ZnO NP | $0.272\pm0.001^{c}$ | $0.296\pm0.003^{b}$ | $0.246\pm0.002^{b}$ | $0.014\pm0.003^{b}$ |

Results are Mean±Standard deviation of triplicate determinations. Columns with different alphabets are significantly different at $p\leq0.05$

### 4.1.13 Mercury (Hg) Concentrations (mg/kg)

Table 4.1.19 shows the mean and standard deviation of the concentrations of mercury in unpolluted, polluted and remediated soil samples from day 1, 14, 28 and 42. In the unpolluted soil, mercury concentrations remained stable between 0.001 and 0.002 mg/kg throughout the study. Crude oil-polluted soil exhibited a reduction in mercury levels, from 0.197 mg/kg on Day 1 to 0.098 mg/kg by Day 42. Both cow dung ZnO and *Pennisetum purpureum* ZnO nanoparticles treatments led to significant decreases in mercury concentration, with the 40g treatments performing better: cow dung ZnO reduced mercury to 0.017 mg/kg and *Pennisetum purpureum* ZnO to 0.025 mg/kg by Day 42. This demonstrates the efficiency of the nanoparticles in mercury remediation.

**Table 4.1.19: Mercury (Hg) Concentration (mg/kg) (Day 1 to Day 42)**

| Hg (mg/kg) | Day 1 | Day 14 | Day 28 | Day 42 |
|---|---|---|---|---|
| Unpolluted Soil | 0.001±0.001[a] | 0.002±0.001[a] | 0.002±0.001[a] | 0.001±0.000[a] |
| Crude Oil Polluted Soil | 0.197±0.002[b] | 0.187±0.001[e] | 0.104±0.001[f] | 0.098±0.001[e] |
| 20g cow dung ZnO NP | 0.197±0.004[b] | 0.138±0.001[d] | 0.075±0.001[e] | 0.035±0.001[d] |
| 40g cow dung ZnO NP | 0.196±0.004[b] | 0.053±0.002[b] | 0.045±0.002[c] | 0.017±0.001[b] |
| 20g *Pennisetum purpureum* ZnO NP | 0.192±0.002[b] | 0.137±0.003[d] | 0.050±0.001[d] | 0.035±0.001[d] |
| 40g *Pennisetum purpureum* ZnO NP | 0.195±0.004[b] | 0.057±0.004[c] | 0.042±0.001[b] | 0.025±0.001[c] |

Results are Mean±Standard deviation of triplicate determinations. Columns with different alphabets are significantly different at $p \leq 0.05$

### 4.1.14 Nickel (Ni) Concentrations (mg/kg)

Table 4.1.20 shows the mean and standard deviation of the concentrations of nickel in unpolluted, polluted and remediated soil samples from day 1, 14, 28 and 42. The unpolluted soil showed a slight reduction in nickel concentrations, from 0.132 mg/kg to 0.107 mg/kg over the study period. Crude oil-polluted soil had much higher nickel concentrations, which decreased from 0.334 mg/kg to 0.264 mg/kg by Day 42. The cow dung ZnO nanoparticles treatments significantly reduced nickel levels, especially the 40g treatment, which significantly reduced nickel concentration to 0.163 mg/kg. Similarly, the *Pennisetum purpureum* ZnO nanoparticles treatments also significantly reduced nickel concentrations, with the 40g treatment reducing it to 0.111 mg/kg by Day 42, indicating the effectiveness of both treatments in nickel remediation.

**Table 4.1.20: Nickel (Ni) Concentrations (mg/kg) (Day 1 to Day 42)**

| Ni (mg/kg) | Day 1 | Day 14 | Day 28 | Day 42 |
|---|---|---|---|---|
| Unpolluted Soil | 0.132±0.001[a] | 0.127±0.001[a] | 0.113±0.002[a] | 0.107±0.001[a] |
| Crude Oil Polluted Soil | 0.334±0.003[b] | 0.298±0.002[f] | 0.286±0.003[f] | 0.264±0.001[f] |
| 20g cow dung ZnO NP | 0.334±0.003[b] | 0.258±0.001[e] | 0.253±0.001[e] | 0.204±0.001[e] |
| 40g cow dung ZnO NP | 0.336±0.004[b] | 0.225±0.004[d] | 0.214±0.001[d] | 0.163±0.002[d] |
| 20g *Pennisetum purpureum* ZnO NP | 0.336±0.001[b] | 0.215±0.002[c] | 0.207±0.001[c] | 0.153±0.000[c] |
| 40g *Pennisetum purpureum* ZnO NP | 0.337±0.003[b] | 0.163±0.003[b] | 0.127±0.001[b] | 0.111±0.001[b] |

Results are Mean±Standard deviation of triplicate determinations. Columns with different alphabets are significantly different at $p \leq 0.05$

### 4.1.15 Zinc (Zn) Concentrations (mg/kg)

Table 4.1.21 shows the mean and standard deviation of the concentrations of zinc in unpolluted, polluted and remediated soil samples from day 1, 14, 28 and 42. The unpolluted soil showed a steady reduction in zinc levels, starting at 1.019 mg/kg and dropping to 0.085 mg/kg by Day 42. In the crude oil-polluted soil, zinc concentrations were initially high at 2.117 mg/kg but decreased to 1.167 mg/kg by Day 42. The cow dung ZnO nanoparticles treatments resulted in significant reductions in zinc levels, with the 40g treatment showing a major significant reduction to 0.257 mg/kg. The *Pennisetum purpureum* ZnO nanoparticles treatments also significantly reduced zinc levels effectively, with the 40g treatment bringing zinc down to 0.211 mg/kg by the end of the study, suggesting both nanoparticle types were effective at reducing zinc concentrations.

**Table 4.1.21: Zinc (Zn) Concentrations (mg/kg) (Day 1 to Day 42)**

| Zn (mg/kg) | Day 1 | Day 14 | Day 28 | Day 42 |
|---|---|---|---|---|
| Unpolluted Soil | 1.019±0.002$^{a}$ | 1.015±0.001$^{c}$ | 0.979±0.001$^{c}$ | 0.085±0.001$^{a}$ |
| Crude Oil Polluted Soil | 2.117±0.002$^{bc}$ | 2.026±0.002$^{f}$ | 1.257±0.001$^{f}$ | 1.167±0.001$^{f}$ |
| 20g cow dung ZnO NP | 2.120±0.001$^{c}$ | 1.162±0.001$^{e}$ | 1.128±0.001$^{d}$ | 1.066±0.003$^{e}$ |
| 40g cow dung ZnO NP | 2.125±0.004$^{d}$ | 0.663±0.001$^{b}$ | 0.357±0.003$^{b}$ | 0.257±0.000$^{c}$ |
| 20g *Pennisetum purpureum* ZnO NP | 2.120±0.002$^{c}$ | 1.126±0.002$^{d}$ | 1.145±0.001$^{e}$ | 0.955±0.004$^{d}$ |
| 40g *Pennisetum purpureum* ZnO NP | 2.115±0.002$^{b}$ | 0.283±0.002$^{a}$ | 0.250±0.001$^{a}$ | 0.211±0.000$^{b}$ |

Results are Mean±Standard deviation of triplicate determinations. Columns with different alphabets are significantly different at $p \leq 0.05$

### 4.1.16 pH Levels

Table 4.1.22 shows the mean and standard deviation of pH in unpolluted, polluted and remediated soil samples from day 1, 14, 28 and 42. The pH of the unpolluted soil was slightly acidic polluted soil was acidic and alkaline in treated soil.The soil pH in the unpolluted soil showed a slight increase, from 6.73 on Day 1 to 7.02 by Day 42, remaining neutral throughout the experiment. Crude oil-polluted soil exhibited consistently low pH values, decreasing from 5.43 to 5.17, indicating acidity. The cow dung ZnO nanoparticle treatments raised the pH towards neutral levels, with the 40g treatment increasing the pH to 7.33 by Day 42. Similarly, the *Pennisetum purpureum* ZnO nanoparticle treatments increased the pH significantly, with the 40g treatment reaching a pH of 7.43, showing the potential of both nanoparticles to neutralize soil acidity.

**Table 4.1.22: pH (Day 1 to Day 42)**

| pH | Day 1 | Day 14 | Day 28 | Day 42 |
|---|---|---|---|---|
| Unpolluted Soil | 6.73±0.06$^{c}$ | 6.97±0.06$^{c}$ | 6.90±0.10$^{c}$ | 7.02±0.03$^{c}$ |
| Crude Oil Polluted Soil | 5.43±0.06$^{a}$ | 5.40±0.17$^{a}$ | 5.47±0.06$^{a}$ | 5.17±0.29$^{a}$ |
| 20g cow dung ZnO NP | 5.73±0.06$^{b}$ | 6.33±0.15$^{b}$ | 6.53±0.25$^{b}$ | 6.53±0.25$^{b}$ |
| 40g cow dung ZnO NP | 5.77±0.06$^{b}$ | 6.90±0.10$^{c}$ | 7.17±0.06$^{cd}$ | 7.33±0.23$^{c}$ |
| 20g *Pennisetum purpureum* ZnO NP | 5.80±0.10$^{b}$ | 7.47±0.06$^{d}$ | 7.00±0.00$^{cd}$ | 7.33±0.29$^{c}$ |
| 40g *Pennisetum purpureum* ZnO NP | 5.77±0.06$^{b}$ | 7.07±0.12$^{c}$ | 7.27±0.21$^{d}$ | 7.43±0.21$^{c}$ |

Results are Mean±Standard deviation of triplicate determinations. Columns with different alphabets are significantly different at $p \leq 0.05$

### 4.1.17 Conductivity (µS/cm)

Table 4.1.23 shows the mean and standard deviation of conductivity (µS/cm) in unpolluted, polluted and remediated soil samples from day 1, 14, 28 and 42. The soil conductivity in the unpolluted soil displayed consistent values, decreasing slightly from 76.67 µS/cm to 74.00 µS/cm over the study. In contrast, crude oil-polluted soil had high conductivity, starting at 224.00 µS/cm and decreasing to 198.67 µS/cm by Day 42, reflecting the presence of pollutants. The cow dung ZnO nanoparticles treatments, particularly the 40g treatment, showed a drastic reduction in conductivity from 1572.67 µS/cm on Day 1 to 600.00 µS/cm by Day 42. The *Pennisetum purpureum* ZnO nanoparticles treatments also showed a substantial drop in conductivity, with the 40g treatment decreasing from 826.67 µS/cm on Day 1 to 93.33 µS/cm by Day 42, demonstrating the nanoparticle treatments' ability to lower soil conductivity over time.

**Table 4.1.23: Conductivity (µS/cm) (Day 1 to Day 42)**

| Conductivity (µS/cm) | Day 1 | Day 14 | Day 28 | Day 42 |
|---|---|---|---|---|
| Unpolluted Soil | 76.67±1.15$^{a}$ | 75.33±0.58$^{a}$ | 75.67±0.58$^{a}$ | 74.00±1.73$^{a}$ |
| Crude Oil Polluted Soil | 224.00±3.61$^{b}$ | 232.67±2.52$^{b}$ | 203.67±3.21$^{b}$ | 198.67±2.31$^{c}$ |
| 20g cow dung ZnO NP | 602.00±2.00$^{c}$ | 600.33±0.58$^{c}$ | 301.67±2.89$^{c}$ | 89.33±1.15$^{b}$ |
| 40g cow dung ZnO NP | 1572.67±0.58$^{f}$ | 1506.00±2.00$^{e}$ | 609.00±1.00$^{e}$ | 600.00±0.00$^{d}$ |
| 20g *Pennisetum purpureum* ZnO NP | 634.67±2.52$^{cd}$ | 602.00±2.00$^{c}$ | 503.00±3.00$^{d}$ | 750.00±0.00$^{e}$ |
| 40g *Pennisetum purpureum* ZnO NP | 826.67±1.15$^{de}$ | 806.33±1.53$^{d}$ | 681.00±1.73$^{f}$ | 93.33±5.77$^{b}$ |

Results are Mean±Standard deviation of triplicate determinations. Columns with different alphabets are significantly different at $p \leq 0.05$

### 4.1.18 Moisture Content (%)

Table 4.1.24 shows the mean and standard deviation of moisture content in unpolluted, polluted and remediated soil samples from day 1, 14, 28 and 42. The percentage moisture content of the unpolluted soil maintained relatively consistent moisture content, starting at 25.00% on Day 1 and fluctuating slightly to 25.33% by Day 42. In crude oil-polluted soil, moisture levels remained high, beginning at 30.00% on Day 1 and returning to 30.00% by Day 42 after a slight drop at Day 14 and Day 28. The cow dung ZnO nanoparticles treatments (both 20g and 40g) resulted in stable moisture content, with values ranging from 21.00% to 24.67% over the study period, indicating that these treatments helped stabilizse moisture levels. Similarly, the 20g and 40g *Pennisetum purpureum* ZnO nanoparticles treatments maintained steady moisture levels, with values between 21.00% and 25.33%, suggesting both nanoparticles helped maintain the soil's moisture balance effectively.

**Table 4.1.24: Moisture content (%) (Day 1 to Day 42)**

| Moisture (%) | Day 1 | Day 14 | Day 28 | Day 42 |
|---|---|---|---|---|
| Unpolluted Soil | 25.00±1.00[a] | 23.33±0.58[b] | 24.67±0.58[a] | 25.33±0.58[a] |
| Crude Oil Polluted Soil | 30.00±1.00[b] | 25.33±0.58[c] | 28.00±1.00[b] | 30.00±1.00[b] |
| 20g cow dung ZnO NP | 25.00±1.00[a] | 21.00±1.00[a] | 23.00±1.00[a] | 24.67±0.58[a] |
| 40g cow dung ZnO NP | 25.00±2.00[a] | 21.33±2.08[ab] | 24.00±1.00[a] | 24.67±0.58[a] |
| 20g *Pennisetum purpureum* ZnO NP | 25.00±2.65[a] | 21.33±0.58[ab] | 24.33±0.58[a] | 25.33±0.58[a] |
| 40g *Pennisetum purpureum* ZnO NP | 24.67±0.58[a] | 21.00±1.00[a] | 24.67±1.15[a] | 25.00±1.00[a] |

Results are Mean±Standard deviation of triplicate determinations

### 4.1.19 Total Heterotrophic Bacteria (THB) Count ( $10^4$ Cfu/g) (Day 1 to Day 42)

Table 4.1.25 shows the mean and standard deviation of total heterotrophic bacteria (THB) count in unpolluted, polluted and remediated soil samples from day 1, 14, 28 and 42. The unpolluted soil exhibited an increase in total heterotrophic bacteria count from 21.03 x $10^4$ Cfu/g on Day 1 to 25.00 x $10^4$ Cfu/g on Day 28, before slightly declining to 21.00 x $10^4$ Cfu/g by Day 42. The crude oil-polluted soil showed a consistent decrease in THB count, starting at 18.00 x $10^4$ Cfu/g on Day 1 and dropping to 10.00 x $10^4$ Cfu/g by Day 42, indicating a detrimental effect of the crude oil on bacterial populations. In contrast, the cow dung ZnO nanoparticles treatments, especially the 40g treatment, significantly boosted the THB count, which increased from 21.00 x $10^4$ Cfu/g on Day 1 to 44.60 x $10^4$ Cfu/g by Day 42. Similarly, the 20g and 40g *Pennisetum purpureum* ZnO nanoparticles treatments increased THB counts, with the 40g treatment showing an increase from 20.00 x $10^4$ Cfu/g on Day 1 to 36.00 x $10^4$ Cfu/g by Day 42. These results suggest that both nanoparticle treatments, particularly at higher concentrations, promote total heterotrophic bacteria in the soil.

**Table 4.1. 25: Total Heterotrophic Bacteria (THB) Count ( $10^4$ Cfu/g) (Day 1 to Day 42)**

| THB (Cfu/g) | Day 1 | Day 14 | Day 28 | Day 42 |
|---|---|---|---|---|
| Unpolluted Soil | 21.03±0.05$^{b}$ | 22.00±1.00$^{b}$ | 25.00±1.00$^{b}$ | 21.00±1.00$^{b}$ |
| Crude Oil Polluted Soil | 18.00±1.00$^{a}$ | 16.00±1.00$^{a}$ | 15.00±1.00$^{a}$ | 10.00±1.00$^{a}$ |
| 20g cow dung ZnO NP | 21.00±1.00$^{b}$ | 22.00±1.00$^{b}$ | 32.00±1.00$^{d}$ | 39.00±1.00$^{e}$ |
| 40g cow dung ZnO NP | 21.00±1.73$^{b}$ | 30.00±1.00$^{d}$ | 35.00±1.00$^{e}$ | 44.60.±1.00$^{f}$ |
| 20g *Pennisetum purpureum* ZnO NP | 19.00±1.00$^{ab}$ | 22.00±1.00$^{b}$ | 25.00±1.00$^{b}$ | 30.00±1.00$^{c}$ |
| 40g *Pennisetum purpureum* ZnO NP | 20.00±1.00$^{ab}$ | 25.00±1.00$^{c}$ | 29.66±1.00$^{c}$ | 36.00±1.00$^{d}$ |

Results are Mean±Standard deviation of triplicate determinations. Columns with different alphabets are significantly different at $p \leq 0.05$

### 4.1.20 Total Hydrocarbon Utilizing Bacteria (THUB) Count ($10^4$ Cfu/g)

Table 4.1.26 shows the mean and standard deviation of total hydrocarbon utilizing bacteria (THUB) count in unpolluted, polluted and remediated soil samples from day 1, 14, 28 and 42. The unpolluted soil expressed increased THUB count from 10.03 x $10^4$ Cfu/g on Day 1 to 19.03 x $10^4$ Cfu/g by Day 42, reflecting the natural resilience of these bacteria. In crude oil-polluted soil, THUB counts were significantly lower, starting at 3.00 x $10^4$ Cfu/g and declining further to 2.00 x $10^4$ Cfu/g by Day 42, suggesting a negative impact of crude oil pollution on hydrocarbon-utilizing bacteria. The cow dung ZnO nanoparticles treatments significantly enhanced THUB counts, with the 40g treatment increasing from 12.03 x $10^4$ Cfu/g on Day 1 to 18.03 x $10^4$ Cfu/g by Day 42, and the 20g treatment showing similar positive trends. The *Pennisetum purpureum* ZnO nanoparticles treatments also boosted THUB counts, particularly the 40g treatment, which increased THUB levels from 8.00 x $10^4$ Cfu/g on Day 1 to 21.03 x $10^4$ Cfu/g by Day 42. This

suggests that both nanoparticle treatments, particularly the 40g concentration, are effective in promoting the growth of hydrocarbon-degrading bacteria in remediated soils.

**Table 4.1.26: Total Hydrocarbon Utilizing Bacteria (THUB) Count ($10^4$ Cfu/g)**

**(Day 1 to Day 42)**

| THUB (Cfu/g) | Day 1 | Day 14 | Day 28 | Day 42 |
|---|---|---|---|---|
| Unpolluted Soil | $10.03\pm0.05^{c}$ | $10.13\pm0.01^{b}$ | $10.83\pm0.01^{b}$ | $19.03\pm0.05^{d}$ |
| Crude Oil Polluted Soil | $3.00\pm0.10^{a}$ | $2.50\pm0.10^{a}$ | $2.50\pm0.10^{a}$ | $2.00\pm0.01^{a}$ |
| 20g cow dung ZnO NP | $11.03\pm0.05^{d}$ | $11.03\pm0.05^{c}$ | $13.70\pm0.10^{c}$ | $15.33\pm0.01^{e}$ |
| 40g cow dung ZnO NP | $12.33\pm0.05^{e}$ | $13.50\pm0.10^{d}$ | $16.66\pm0.01^{d}$ | $18.03\pm0.05^{c}$ |
| 20g *Pennisetum purpureum* ZnO NP | $10.03\pm0.05^{c}$ | $16.03\pm0.05^{e}$ | $19.03\pm0.05^{e}$ | $15.03\pm0.05^{b}$ |
| 40g *Pennisetum purpureum* ZnO NP | $8.00\pm0.10^{b}$ | $17.33\pm0.01^{f}$ | $20.03\pm0.05^{f}$ | $21.03\pm0.05^{f}$ |

Results are Mean±Standard deviation of triplicate determinations. Columns with different alphabets are significantly different at $p\leq0.05$

## 4.2 Discussion

Nanoremediation is an eco-friendly and cost-effective approach that uses nanoparticles to detoxify contaminants in the soil and other environments (Baragano, Forjan, Welte, & Gallego, 2020). Nanoparticles (NPs) exhibit responsiveness, a high surface area-to-mass ratio, distinctive electronic and catalytic properties ( Corsi et al.,2018). Nanoremediation involves the use of different technical processes including, adsorption, heterogeneous catalysis, reduction, deployment of electrical fields (electronanoremediation), photodegradation and involvement of microorganisms (nanobioremediation) to facilitate environmental remediation.

Zinc oxide nanoparticles can be considered a multifunctional material due to its physical and chemical properties (Suwanboon, Amornpitoksuk, Bangrak & Randorn, 2014), namely chemical stability, a broad range of radiation absorption, photocatalyst and low toxicity (Kołodziejczak-Radzimska & Jesionowski 2014; Sirelkhatim et al., 2015). These particles are transparent to

visible light, and they absorb UV light. ZnO is an n-type semiconductor having an energy band gap value of 3.37 eV (Xu, Yuan, Han, Wu, Gao & Jiang, 2012).

Gas chromatography mass spectrometry (GC-MS) analysis revealed phytochemical constituents in aqueous extract of *Pennisetum purpureum*, *Pennisetum purpureum* zinc oxide nanoparticles, cow dung and cow dung zinc oxide nanoparticles that have biological activities and useful component in nanoparticle synthesis.

The GC-MS profile of the volatile phytochemical constituents of the aqueous extract of *Pennisetum purpureum* and *Pennisetum purpureum* zinc oxide nanoparticles revealed various volatile phytochemical compounds. The result indicated that the aqueous extract of *Pennisetum purpureum* was rich in bioactive compounds like 9,12-octadecadienoic acid (linoleic acid) (18.89%), Cis-13-octadecenoic acid (15.74%), 1,2-benzisothiazole (6.69%), 11-octadecenoic acid (5.53%), oleic acid (5.01%). The major constituents in aqueous extract of *Pennisetum purpureum* ZnO are hexadecanoic acid (15.25%), 1-octadene (13.16%), 11-octadecenoic acid (7.14%), cyclopentadecane (6.64%). The major bioactive compounds in aqueous extract of cow dung are trans-13-Octadecenoic acid (12.03%), 8, 11 – octadecadienoic acid (8.29%), 9-octadecanoic acid (8.11%), cycloeisane (7.43%) and the major constituents in aqueous extract of cow dung zinc oxide nano particles are alpha-endosulfan (67.99%), 4-trifluoroacetoxy tetradecane (10.18%), 1-octapdecene (4.83%), 5-bromomethyl-2-chloropyridine (4.46%).

The presence of phytochemicals in *Pennisetum purpureum* and cow dung are responsible for synthesizing nanoparticles. These chemical compounds (linoleic acid, oleic acid, Phthalic acid, 3-chlorophenyl methyl ester, hexadecanoic acid, stearic acid). are useful component in nanoparticle synthesis and perform various functions like stabilizers, capping and coating agents in nanoparticle synthesis (Ovais, 2018; Dong et al., 2016).

In this study, zinc oxide nanoparticles were synthesized using aqueous extracts of *Pennisetum purpureum* , cow dung and zinc acetate dihydrate.

Characterisation of synthesised cow dung zinc oxide nanoparticles and *Pennisetum purpureum* zinc oxide nanoparticles were done using various analytical methods such as UV spectroscopy Fourier-transform infrared spectroscopy (FTIR), Transmission electron microscopy (TEM) and X-ray diffraction (XRD).

The confirmation of zinc oxide nanoparticles formation was realized by visual observation of the reaction mixture and UV-visible spectroscopy. The addition of zinc acetate dihydrate and NaOH to the aqueous extract of cow dung and *Pennisetum purpureum* changed colour from light brown to white colour indicating the formation of zinc oxide nanoparticles for cow dung and dark brown colour to off white for *Pennisetum purpureum* zinc oxide nanoparticles. Cow dung zinc oxide nanoparticles and *Pennisetum purpureum* zinc oxide nanoparticles showed absorption peak at 367nm and 370 nm, respectively, confirming the successful green synthesis of zinc oxide nanoparticles. The distinct peaks centered around 367 and 370 nm is specific for zinc oxide nanoparticles. According to Reuben, Reama & Femi (2023) , the biosynthesis of zinc oxide nanoparticles using aqueous leaf extracts of *Cnidoscolus aconitifolius* showed absorption spectrum peak at 378 nm. The calculated energy band gap value for cow dung zinc oxide nanoparticle was 3.38eV and 3.35eV for *Pennisetum purpureum* zinc oxide nanoparticle. which is consistent with previous research (Ramesh et al., 2021; Saleem et al., 2022).

X-ray diffraction confirmed cow dung and *Pennisetum purpureum* zinc oxide nanoparticles peak position, crystallinity and phase composition. The crystallinity of a zinc oxide nanoparticles were determined from the sharpness of its diffraction peaks (Bigdeli, Morsali, & Retailleau, 2010).The crystalline size of the synthesized cow dung and *Pennisetum purpureum* zinc oxide nanoparticles were calculated using Debye–Scherrer equation ($D = 0.9 \lambda / \beta \cos \theta$). The average crystalline size of cow dung ZnO nanoparticles was 18.17nm and 23.37nm for *Pennisetum purpureum* zinc oxide.

The phase composition of the nanoparticles confirmed the presence of zinc oxide in both cow dung zinc oxide nanoparticles and *Pennisetum purpureum* zinc oxide nanoparticles.

Transmission Electron Microscopy (TEM) confirmed the size and shape of the synthesised zinc oxide nanoparticles. The TEM micrographs showed the homogeneously aggregated spherical biosynthesised cow dung and *Pennisetum purpureum* zinc oxide nanoparticles with an average mean particle size of 3.47nm for cow dung zinc oxide nanoparticles and 15.21nm for *Pennisetum purpureum* ZnO nanoparticles at 100nm magnification.

Fourier Transform Infrared spectroscopic analysis confirmed the presence of various functional groups, which may involve the synthesis of zinc oxide nanoparticles. The Fourier transform infrared spectroscopy (FTIR) showed the presence of biomolecules and functional groups (OH group, alkyne, Nitro, alkene and ether) in both cow dung and *Pennisetum purpureum* zinc oxide nanoparticles that participated in the nanoparticle's synthesis for the capping and reduction process during the green synthesis zinc oxide nanoparticles. The FTIR spectra of the synthesized zinc oxide nanoparticles were within the range of 4000 to 450cm$^{-1}$.

Crude oil polluted soil showed a consistent decrease in total heterotrophic bacteria count and total hydrocarbon utilizing bacteria count throughout the 42 days remediation period. In contrast, the cow dung zinc oxide nanoparticles and *Pennisetum purpureum* zinc oxide nanoparticles treatments showed a significant increase of total heterotrophic bacteria count and total hydrocarbon utilizing bacteria count from day 1 to day 42. The cow dung and *Pennisetum purpureum* mediated synthesized zinc oxide nanoparticles are safe because of the lower toxicity on microbes, Low toxicity of zinc oxide nanoparticle was also reported by Kołodziejczak-Radzimska & Jesionowski (2014) and Sirelkhatim et al. (2015).

The Total Heterotrophic Bacterial isolates from this study are *Bacillus sp, Salmonella Sp, Corynebacterium Sp, Flavobacterium Sp, Streptococcus Sp, Staphylococus Sp, Clostridium Sp,*

*Pseudomonas Sp, Staphylococcus Sp, Escherichia coli, Clostridium Sp, Shigella Sp, Citrobacter species, Micrococcus species.* These results showed that both nanoparticle treatments, particularly at higher concentrations, promote microbial growth in the soil. The hydrocarbon utilizing microbes in the soil was relatively adequate for bioremediation (Ebuehi et al., 2005).

Bacteria are the most effective and promising microorganism in crude oil degradation due to the ability to attack almost any hydrocarbon up to the heaviest paraffin (asphaltic residues) (Lee, Yun, Jang, Kim & Kim, 2015). Total heterotrophic bacteria and total hydrocarbon utilizing bacteria plays an important role in contaminant degradation (McCutcheon & Schnoor, 2003). The increase of total heterotrophic bacteria counts and total hydrocarbon utilizing bacteria in the contaminated soils with treatments could be because the cow dung and *Pennisetum purpureum* zinc oxide nanoparticles provided sufficient carbon and energy (Njoku, Asunmo, Ude, Adesuyi & Oyelami 2020). Lima et al. (2012) showed that high population density of total hydrocarbon utilizing bacteria indicates that the bacteria are able to use crude oil hydrocarbon as the sole source of carbon and energy thus, playing a key role in degradation processes.

The soil pH in the unpolluted soil remained neutral throughout the experiment. Crude oil-polluted soil was slightly acidic. The pH of the crude oil polluted soil treated with cow dung zinc oxide nanoparticles and *Pennisetum purpureum* zinc oxide nanoparticle was initially acidic and finally became neutral. The cow dung and *Pennisetum purpureum* zinc oxide nanoparticle treatments raised the pH towards neutral levels showing the potential of both nanoparticles to neutralize soil acidity. A similar trend was also reported by Ebere, Wokoma & Wokocha (2011) where pH increased averagely from acidity to alkalinity for the remediation of crude oil polluted soil.

The crude oil contamination in the soil showed a significant decrease in the pH range, the acidic nature of the soil is due to the presence of the hydrocarbons in the crude oil which may react with

the soil salts and minerals and change the alkaline minerals to acidic ((Devatha, Vishnu & Purna, 2019).

The nitrogen and phosphorous concentrations in the unpolluted soil remained relatively stable, with only a slight decrease over the 42 days period. In the crude oil polluted soil, the nitrogen concentrations significantly reduced over the 42 days period, indicating some depletion due to the pollution. For the crude oil polluted soil with 20g and 40g treatments of cow dung and *Pennisetum purpureum* zinc oxide nanoparticles showed significant reductions in nitrogen and phosphorous concentrations. 40g showed more reduction on Day 42. The higher concentration of nanoparticles effectively reduced nitrogen levels in the soil.

The decrease in concentrations of nitrogen and phosphorous was due to the fact that they were used in metabolism of organisms in building biomass. However, nitrogen and phosphorous are nutrients for microorganism's to degrade crude oil contaminated soil (Bisht et al., 2015).

The total petroleum hydrocarbon (TPH) concentrations in the unpolluted oil was low and remained unchanged, TPH concentrations were extremely high in crude oil polluted soil, the crude oil polluted soil that was treated with cow dung zinc oxide nanoparticles and *Pennisetum purpureum* zinc oxide nanoparticles was initially high and significantly reduced by the end of the 42 days study especially in the 40g treatment. Treatment with cow dung zinc oxide nanoparticles showed the most significant reduction in TPH.

It was observed that as total petroleum hydrocarbon concentrations decreased during the 42 days study period, the counts/loads of the total hydrocarbon utilising bacteria increased progressively (Frank, Abiye, Ibiene & Ekaette, 2012). This conformed to the results obtained by Tanee and Albert (2011) who observed a decrease in total hydrocarbon content in a crude oil polluted soil.

Cow dung and *Pennisetum purpureum* zinc oxide nanoparticles have energy band gap value of 3.38eV and 3.35eV, as a photocatalyst it can influence the degradation of organic pollutants (Xu et al., 2012).

The total organic carbon (TOC) concentration in the unpolluted soil, remained relatively low and constant, with a slight decrease over the 42 days period. The crude oil-polluted soil was significantly higher initially and significantly decreased by day 42. The treatments with cow dung zinc oxide nanoparticles and *Pennisetum purpureum* zinc oxide treatments showed a significant reduction in TOC indicating that the nanoparticles effectively broke down the organic carbon in the soil over time, with higher concentrations yielding better results. The decreasing rate of TOC with time recorded for the treatment options was attributed to the utilisation of TOC for energy by microorganism (Ukpaka, Uku, Amadi & Dagde, 2020). Nanoparticles, such as zinc oxide exhibit remarkable adsorption capacities, enabling the removal of organic contaminants from soil (Xu et al., 2012).

Benzene, toluene, ethyl benzene and xylene (BTEX) concentrations in the unpolluted soil remained low and fairly stable. The crude oil polluted soil treated with cow dung zinc oxide nanoparticles and *Pennisetum purpureum* zinc oxide nanoparticles reduced significantly by day 42 to the concentration of BTEX in unpolluted soil. Treatment of crude oil with cow dung zinc oxide nanoparticles and *Pennisetum purpureum* zinc oxide nanoparticles especially at 40g resulted in a significant reduction in BTEX by day 42 to the concentration of BTEX in unpolluted soil. These findings suggest that both nanoparticles, particularly at higher concentrations, were very efficient in reducing BTEX concentrations in the soil.

The remediation of BTEX in soil was affected by volatilization, dissolution, adsorption and degradation by microorganism. The bacterial flora in soil has an ability to aerobically degrade the BTEX. This degradation will reduce the of BTEX in soil (Bakker, Casado, Koerselman, Tolls

& Kolloffel, 2004). Cow dung and *Pennisetum purpureum* zinc oxide nanoparticles have energy band gap value of 3.38eV and 3.35eV this shows that the ZnO nanoparticles exhibited remarkable adsorption capacities and are highly active for the photodegradation of BTEX in the crude oil polluted soil. As a photocatalyst it can influence the degradation effect of organic pollutants (Xu et al., 2012).

The concentrations of arsenic, nickel, chromium, mercury, zinc and potassium in unpolluted soil remained stable throughout the study period. Crude oil-polluted soil exhibited a significant reduction in arsenic, nickel, chromium, mercury, zinc and potassium concentrations over the 42 days remediation period. The 20g and 40g cow dung zinc oxide nanoparticles treatments significantly reduced arsenic, nickel, chromium, mercury, zinc and potassium concentrations with the 40g treatment showing a greater reduction over the 42 days period. Similarly, the 20g and 40g *Pennisetum purpureum* zinc oxide nanoparticles treatments effectively reduced the concentrations of arsenic, nickel, chromium, mercury, zinc and potassium, with the 40g treatment significantly reducing the heavy metal concentrations over the 42 days period, suggesting strong remediation efficiency at higher nanoparticle concentrations.

Nanoparticles, such as cow dung and *Pennisetum* zinc oxides with energy band gap value of 3.38eV and 3.35eV exhibits remarkable adsorption capacities, enabling the removal of diverse pollutants including heavy metals from contaminated environments (Xu et al., 2012).

Gong et al. (2018) investigated the soil treatment with $Fe_3 (PO_4)_2$ nanoparticles that successfully immobilized the heavy metals by 70%. This novel remediation technique has proven to be effective in the removal of heavy metals by absorbing them, reducing the toxic valence to a stable metallic state, and catalyzing the reaction (Gil-Díaz et al., 2016).

Polycyclic aromatic hydrocarbons concentrations in the unpolluted soil showed minimal change, with values decreasing slightly. In the crude oil-polluted soil, Polycyclic aromatic hydrocarbons concentrations were initially very high but reduced significantly by day 42. The cow dung zinc oxide nanoparticle treatments, particularly the 40g treatment, resulted in significant reductions in polycyclic aromatic hydrocarbons by the end of the study. The *Pennisetum purpureum* zinc oxide treatments were similarly effective, with the 40g treatment significantly reducing polycyclic aromatic hydrocarbon concentrations by the end of the study. It was observed that as polycyclic aromatic hydrocarbons decreased during the 42 days study period, the counts/loads of the hydrocarbon utilising bacterial increased progressively. This shows that both types of nanoparticles were highly effective at degrading PAH in the soil, with higher concentrations yielding better results.

Polycyclic aromatic hydrocarbons (PAHs) are recognized as potent mutagens or carcinogens and are listed as priority pollutants by the European Commission (EC) and United States Environmental Protection Agency (USEPA). Polycyclic aromatic hydrocarbons enter in soil accidentally or through the intended combustion of various kinds of fuels ( Anyakora & Coker, 2007).

The percentage moisture content of the unpolluted soil maintained relatively consistent moisture content throughout the study period. In crude oil-polluted soil, moisture levels was high and slightly dropped at day 14 and day 28. The cow dung zinc oxide nanoparticles and *Pennisetum purpureum* zinc oxide nanoparticles treatments (both 20g and 40g) over the study period, indicating that these treatments helped stabilize moisture levels. Suggesting both nanoparticles helped maintain the soil's moisture balance effectively. The moisture content in the contaminated soil is a vital feature essential for microbial remediation of hydrocarbons. Sufficient moisture is required to bring the soluble pollutants and microbial cells in contact and their absorption (Ubani, Atagana & Thantsha , 2013).

# CHAPTER FIVE

# CONCLUSION AND RECOMMENDATION

## 5.1 Conclusion

In conclusion, the results in this study revealed that both cow dung and *Pennisetum purpureum* zinc oxide nanoparticles were effective at reducing nitrogen, phosphorus, total organic carbon, heavy metals (As, Cr, Hg, Ni, Zn K), total petroleum hydrocarbon, polycyclic aromatic hydrocarbon, benzene, toluene, ethylbenzene and xylene (BTEX) concentrations in the crude oil polluted soil, with higher concentrations (40g) of nanoparticles being more efficient at soil remediation than lower concentrations (20g). Petroleum pollution can significantly reduce the abundance and diversity of bacteria and fungi in soil. Total hydrocarbon utilising bacterial increased progressively as polycyclic aromatic hydrocarbons, total petroleum hydrocarbon,

benzene, toluene, ethylbenzene and xylene (BTEX) concentrations decreased during the 42 days remediation period. Higher bacterial counts (total heterotrophic bacteria and total hydrocarbon utilizing bacteria) is a good indication of the zinc oxide nanoparticles role in improving microbial population. Petroleum pollution can significantly reduce the soil pH and make the polluted soil acidic. The cow dung and *Pennisetum purpureum* ZnO nanoparticles treatments raised the pH towards neutral levels, showing the potential of both nanoparticles to neutralize soil acidity.

The UV–visible absorption peaks was centered at 367 nm for cow dung zinc oxide nanoparticles and 370 nm for *Pennisetum purpureum* zinc oxide nanoparticles and the energy band gap value for cow dung zinc oxide nanoparticle was 3.38 eV and 3.35 eV for *Pennisetum purpureum* zinc oxide nanoparticle. This shows that cow dung and *Pennisetum purpureum* zinc oxide nanoparticles are photocatalyst and have the potential to degrade pollutants and clean up crude oil polluted soil.

## 5.2 Recommendation

This study was an ex-situ remediation of crude oil polluted soil with cow dung and *Pennisetum purpureum* zinc oxide nanoparticles. I recommend an in-situ remediation of crude oil polluted soil with cow dung and *Pennisetum purpureum* zinc oxide nanoparticles.

## 5.3 Contribution to Knowledge

1. Gas chromatography mass spectrometry (GC-MS) analysis revealed phytochemical constituents in aqueous extract of *Pennisetum purpureum* and cow dung that are bioactive and useful component in nanoparticle synthesis and perform various functions like stabilizers, capping and coating agents in nanoparticle synthesis.

2. Aqueous extracts of cow dung and *Pennisetum purpureum* can be used for the green synthesis of nanoparticles.
3. Cow dung zinc oxide nanoparticles and *Pennisetum purpureum* zinc oxide nanoparticles are ecofriendly.
4. Cow dung zinc oxide nanoparticles and *Pennisetum purpureum* zinc oxide nanoparticles have photocatalytic properties.
5. This study has established that **c**ow dung zinc oxide nanoparticles and *Pennisetum purpureum* zinc oxide nanoparticles have the potential to clean up crude oil polluted soil, reducing clean-up time and hence reducing the contaminants concentration to near zero.

## REFERENCES


Abdel-Shafy, H. I. & Mansour, M. S. (2015). A review on polycyclic aromatic hydrocarbons, source, environmental impact and remediation. *Environmental Science and Pollution Research*, 22 (8), 5501-5517.

Agbor, R. B., Ekpo, I.A., Osuagwu, A. N., Udofia, U. U., Okpako, E. C & Antai, S. P. (2012). Biostimulation of microbial degradation of crude oil polluted soil using cocoa pod husk and plantain peels. *Journal of Microbiology and Biotechnology Research*, 2(3), 464-469.

Ahrens, C.D. (2005). Essentials of meteorology, an invitation to the atmosphere. 3rd Edition, Cambridge University Press, 463.

Akhavan, O., Azimirad, R., Safa, S., & Hasani, E. (2011). Cuprous oxide nanoparticles as well as Cu($Cu_2O$) core-shell nanostructures for elimination of bacteria. *Journal of Materials Chemistry*, 21(19), 9634-9640.

Akuru, U., Akaninwor, J., & Amadi, B. (2015). Phytochemical composition and antidiabetic properties of aqueous stem extract of *Pennisetum purpureum* on Alloxan – induced diabetic Wistar-albino rats. *Open Science Journal of Pharmacy and Pharmacology*, 3 (6), 72-79

Akyuz, H. M. & Cabuk, H. (2010). Gas–particle partitioning and seasonal variation of polycyclic aromatic hydrocarbons in the atmosphere of Zonguldak, Turkey. *Atmospheric Environment*, 44 (10), 1313-1323.

Alagumuthu, G., & Kirubha, R., ( 2012). "Green synthesis of silver nanoparticles using *Cissus quadrangularis* plant extract and their antibacterial activity," *International Journal of Nanomaterials and Biostructures*, 2(3), 30–33

Albrecht, M., Evans, C., & Raston, C. (2006). Green chemistry and the health implications of nanoparticles. *Green Chemistry, 8*(5), 417– 432

Alexis, F., Pridgen, E., Molnar, L., & Farokhzad, O. (2008). Factors affecting the clearance and biodistribution of polymeric nanoparticles. *Molecular Pharmaceutics,* 5(4), 505-515.

Al-Hakkani, M. F. (2020). Biogenic copper nanoparticles and their applications. *SN Applied Sciences*, 2(3), 505.

Alikasturi, A. S., Mokhtar, M. I., Zainuddin, M. A., Serit, M. E., & Rahim, N. S. (2020). Phytoremediation of lead in mineral, distilled and surface water using *Pennisetum purpureum* and *Allium fistulosum*. Materials Today: *Proceedings*, 31, A175-A179.

Altammar, K. A. (2023) A review on nanoparticles, characteristics, synthesis, applications, and challenges. *Front Microbiology,* 14, 1155622.

Anochie, I.C., & Ikpeme, E . E. (2001). Prevalence of sexual activity and outcome among female secondary school students in Port Harcourt, Nigeria. *African Journal of Reproduction Health*, 5(2), 63-71.

Anyakora, C., & Coker. ( 2007). Assessment of polynuclear aromatic hydrocarbon content in four species of fish in the Niger Delta by gas chromatography/mass spectrometry. *African Journal of Biotechnology, 6 (*6), 737-743.

AOAC (1990). Official Method of Analysis of the Association of Official Analytical Chemists. No. 934.06, AOAC, Arlington.

AOAC (1995). Official Methods of Analysis. 16th Edition, Association of Official Analytical Chemists, Washington DC.

AOAC (2012). Official Method of Analysis: Association of Official Analytical Chemists. 19th Edition, Washington DC, 121-130.

Araka, P. P., Okparanma, R. N., & Ayotamuno, J. M. (2019). "Diagnostic screening of organic contaminant level in solidified/stabilized pre-treated oil-based drill cuttings". *Heliyon*. 5 (10), 2644.

Aregbe, A.G. (2017). Natural Gas Flaring—Alternative Solutions. *World Journal of Engineering and Technology*, 5(1), 139-153.

Arey, J., & Atkinson, R. (2003). Photochemical reactions of PAH in the atmosphere. *An Ecotoxicological Perspective, 12,* 47–63

Arpita. R., Apoorva, S., Saanya, Y., Leta, T., & Ramaswamy, K. (2021). Nanomaterials for remediation of environmental pollutants. *Bioinorganic Chemistry and Applications, 3(2), 1-16*

ASTM Standards (2005). Annual Book of ASTM standards. Extraction of solid waste samples for chemical analysis using Soxhlet extraction, environmental assessment, hazardous substances and oil spill responses, Practice for D5369. 11(04), 196-201.

Atagana, H. I. (2010). "Bioremediation of co-contamination of crude oil and heavy metals in soil by phytoremediation using *Chromolaena odorata*. *Water, Air, & Soil Pollution*, 215 (1–4), 261–271.

Atlas, R. M., & Hazen, T. C. (2011). Oil biodegradation and bioremediation. A tale of the two worst spills in U.S. history. *Environmental Science Technology,* 45, 6709-6715.

Atlas, R.M & Cerniglia, C.E. (1995), Bioremediation of petroleum pollutants, *Biological Science*, 45 (5), 332-350.

Azubuike, C. C, Chikere, C. B., Okpokwasili, Gideon, C. (2016). "Bioremediation techniques, classification based on site of application: principles, advantages, limitations and prospects". *World Journal of Microbiology and Biotechnology*, 32(11), 180.

Baig, N., Kammakakam, I., & Falath, W. (2021). Nanomaterials: a review of synthesis methods, properties, recent progress, and challenges. *Material Advances*, 2(6), 1821–1871.

Bakker, M., Casado, B., Koerselman, J., Tolls, J., & Kolloffel, J. (2004). Polycyclic aromatic hydrocarbons in soil and plant samples from the vicinity of an oil refinery. *The Science of The Total Environment, 263(1-3*), 91 – 100.

Balouiri, M., Sadiki, M., & Ibnsouda, S.K. (2016). Methods for in vitro evaluating antimicrobial activity: a review. *Journal of Pharmaceutical Analysis,* 6(2), 71–79.

Baragano, D., Forján, R., Welte, L., & Gallego, J. (2020). Nanoremediation of As and metals polluted soils by means of graphene oxide nanoparticles. *Scientific Rep*orts, *10* (1), 1-10

Barman, G., Maiti, S., & Laha, J. (2013). Bio-fabrication of gold nanoparticles using aqueous extract of red tomato and its use as a colorimetric sensor. *Nanoscale, Environmental Research Letters,* 8, 1–9.

Bhuyan, T., Mishra, K., Khanuja, M., Prasad, R., & Varma, A. (2015). Biosynthesis of zinc oxide nanoparticles from *Azadirachta indica* for antibacterial and photocatalytic applications. *Materials Science in Semiconductor Processing,* 32, 55–61.

Bigdeli, F., Morsali, A., & Retailleau, P., (2010). Syntheses and characterization of different zinc (II) oxide nano-structures from direct thermal decomposition of 1D coordination polymers. *Polyhedron,* 29 (2), 801–806

Bisht, S., Pandey, P., Bhargava, B., Sharma, S., Kumar, V., & Sharma, K (2015). Bioremediation of polyaromatic hydrocarbons (PAH) using rhizosphere technology. *Journal of Microbiology*, 46 (1), 7-21.

Boonmeerati, U., & Sampanpanish, P. (2021). Enhancing Arsenic phytoextraction of dwarf napier grass (*Pennisetum purpureum*) from gold mine tailings by electrokinetics remediation with phosphate and EDTA. *Journal of Hazardous*, *Toxic and Radioactive Waste*, 25(4), 21027

Capelli, S.M., Busalmen, P. J., & De Sanchez, R. S. (2004). Hydrocarbon bioremediation of a mineral base contaminated waste from crude oil extraction by indigenous bacteria. *International Biodeterioration and Biodegradation*, *47* (2001), 233 - 238.

Chaineau, C.H., Rougeux, G., Yepremian, C., & Oudot, J. (2005). Effect of nutrient concentration on the biodegradation of crude oil and associated microbial populations in the soil. *Soil Biology and biochemistry*, *37*(8), 1490-1497

Clemente, A., Anazawa, T., & Durrant, L. (2001). "Biodegradation of polycyclic aromatic hydrocarbons by soil fungi". *Brazilian Journal of Microbiology, 32*(4), 255.

Corsi, I., Winther-Nielsen, M., Sethi, R., Punta, C., Della, C., Torre, G., Libralato, G., Lofrano, L., Sabatini, M., Aiello, L., & Fiordi, F. (2018). Ecofriendly nanotechnologies and nanomaterials for environmental applications: Key issue and consensus recommendations for sustainable and ecosafe nanoremediation. *Ecotoxicology and Environmental Safety*, 154, 237-244.

DAFF, (2014). Elephant grass (*Pennisetum purpureum*). Dept. Agric. Fish. Forest., PP67 Factsheet, Queensland Gov., Australia.

Das, N., & Chandran, P (2010). "Microbial degradation of petroleum hydrocarbon contaminants: an overview". *Biotechnology Research International*, 2011, 941810

Das, N., & Chandran, P. (2011). Microbial degradation of petroleum hydrocarbon contaminants. An overview. – *Biotechnology Research International.* 1-13.

David, T. (1995). Niger Delta Oil Production, Reserves, Field Sizes Assessed. Industry Briefs. *Oil and Gas Journal*. 25(3):105 – 120.

Deepty, M., Srinivas , C., Kumar, E., Mohan, N., Prajapat ,C., & Rao, T. (2019). XRD, EDX, FTIR and ESR spectroscopic studies of co-precipitated Mn-substituted Zn–ferrite nanoparticles. *Ceramics International*, 45(6), 8037–44.

Department of Agriculture Forestry & Fisheries, (2014). Elephant grass (*Pennisetum purpureum*) PP67 factsheet, Queensland Gov., Australia

Devatha, C.P., Vishnu, V., Purna, C., & Rao, J. (2019). Investigation of physical and chemical characteristics on soil due to crude oil contamination and its remediation. *Applied Water Sci*ence, 9 (4), 89.

Dong, C., Zhang, X., Cai, H., Cao, C., Kui, Z., Wang, X., & Xiao, X. (2016). Synthesis of stearic acid-stabilized silver nanoparticles in aqueous solution, *Advanced Powder Technology,* 27 (6), 2416–2423

Ealia, S., & Saravanakumar, M. (2017). A review on the classification, characterisation, synthesis of nanoparticles and their application. *Materials Science and Engineering*, 263 (3), 32019.

Ebere, J. U., Wokoma, E. C. & Wokocha, C. C. (2011) Enhanced Remediation of a Hydrocarbon Polluted Soil. *Research Journal of Environmental and Earth Sciences*, 3(2), 70-74

Eboh, E. C. (1995). Poverty, population growth and environmental Degradation: The Vicious Cycle of Human Misery. Rural Development in Nigeria. Auto-Century Pub. Co. Ibadan.

Ebuehi, O., Abibo, I.., Shekwolo, P., Sigismund, K., Adoki, A., & Okoro, I. C. (2005). Remediation of crude oil contaminated soil by Enhanced natural attenuation technique. *Journal of Applied Environmental Management,* 9(1), 103-106.

Edema, N. E., Obadoni, B. O, Erheni, H., & Osakwuni, U. E. (2009). Eco-phytochemical studies of plants in a crude oil polluted terrestrial habitat located at Iwhrekan, Ughelli North Local Government Area of Delta State. *Natural Science,* 7, 49-52.

EPA, (2013). EPA issues supplemental final rule for new qualifying renewable fuels under the RFS program. US Env. Prot. Agency, Transport. Air Qual., EPA-420-F-13-040, *Feedipedia*.

*EPA, U.S (2012).* Nanotechnology applications for environmental remediation. *"Nanotechnologies for environmental cleanup".*

EPA, U.S. (2007). Nanotechnology solutions, challenges, and implications for superfund. national association of remedial project managers annual training conference. Baltimore, Maryland.

Eze, V. C., Onwuakor, C. E., Orok, F. E. (2014). Microbiological and physicochemical characteristics of soil contaminated with used petroleum products in Umuahia, Abia State, Nigeria. *Journal of Applied & Environmental Microbiology,* 2(6), 281-286.

Ezike, C. U., Igugo, R. U., Uwadiegwu, N., & Felix, E.O. ( 2019). Benzo [a] pyrene- carcinogenic and mutagenic equivalents of fingerlings of *Clarias gariepinus* exposed to water soluble fractions of Nigerian Bonny Light crude oil BLCO. *International Journal of Fisheries and Aquatic Studies,* 7(5), 62-67.

FAO (2015). Grassland Index. A searchable catalogue of grass and forage legumes. FAO, Rome, Italy

FAO (2007). Standard operating procedure for soil organic carbon. Walkley-Black Method. Titration and colorimetric method, A., & Black, I. (2007), Estimation of soil organic carbon by the chromic acid titration method. Soil Science, 37, 29 - 38.

FAO. (2021). Standard operating procedure for soil nitrogen - Kjeldahl method. Rome.

Federal Ministry of Health (Nigeria) (2010). HIV Sero-Prevalence Sentinel Survey. Nigeria:

Federal Ministry of Health (Nigeria). (2003). National HIV/AIDS and Reproductive Health Survey. Nigeria.

Frank, A. O., Abiye, A., Ibiene, & Ekaette, N (2012). Laboratory scale bioremediation of petroleum hydrocarbon – polluted mangrove swamps in the Niger Delta using cow dung. *Malaysian Journal of Microbiology*, *8(*4), 219-228.

Garg, A. K., & Mudgal, V. (2007). Organic and mineral composition of Gomeya (cow dung) from Desi and crossbred cows—a comparative study. *International Journal Cow Science,* 3:1–2.

Gerhardt, K. E., Huang, X., Glick, B. R., & Greenberg, B. M. (2009). Phytoremediation and rhizoremediation of organic soil contaminants. *Plant Science*. 176 (1), 20–30.

Gil-Díaz, M., Diez-Pascual, S González, A., Alonso, J., Rodríguez-Valdés, E., Gallego, J., & Lobo, M. (2016). A nanoremediation strategy for the recovery of an As-polluted soil. *Chemosphere*, 149, 137-145.

Gong, X., Huang, D., Liu, Y., Peng, Z., Zeng, G., Xu, P., Cheng, M., Wang, R., & Wan, J. (2018). Remediation of contaminated soils by biotechnology with nanomaterials: bio-behaviour, applications, and perspectives. *Critical Reviews in Biotechnology,* 38(3), 455-468.

Gupta, K. K., Aneja, K. R. & Rana, D. (2016). Current status of cow dung as a bioresource for sustainable development. *Bioresources Bioprocessing,* 3 (1), 1-11

Han , C., Yang, M.Q., Weng, B., & Xu, Y. J. (2014). Improving the photocatalytic activity and anti-photocorrosion of semiconductor ZnO by coupling with versatile carbon. *Physical Chemistry Physics, 16*(32), 16891- 903.

Hasan, S. (2015). A review on nanoparticles, their synthesis and types. *Research Journal of Recent Sciences,* 4, 9-11.

Holzinger, M., Le Goff , A. & Cosnier, S.(2014).Nanomaterials for biosensing applications. *Frontiers in Chemistry,* 2, 63.

Hudlikar, M., Joglekar, S., Dhaygude, M., & Kodam, K., (2012). Latex mediated synthesis of ZnS nanoparticles: green synthesis approach. *Journal of Nanoparticle Research*, 14(5),1-6

Ikuesan, F. A. (2017): Evaluation of crude oil biodegradation potentials of some indigenous soil microorganisms. *Journal of Scientific Research and Reports,* 13(5), 1-9.

Jahangeer, K. V. (2013): An overview on microbial degradation of petroleum hydrocarbon contaminants. *International Journal of Engineering and Technical Research,* 1, 34-37.

Kalpana, V., Bala, A., Sravani, N., Vigneshwari, T., Panneerselvam, A., & Devi, V. (2018). Biosynthesis of zinc oxide nanoparticles using culture filtrates of *Aspergillus niger,* Antimicrobial textiles and dye degradation studies. *Open Nano*, 3, 48-55.

Kang, D. J., Seo, Y. J., Saito, T., Suzuki, H., & Ishii, Y. (2012). Uptake and translocation of cesium-133 in Napier grass (*Pennisetum purpureum* Schum.) under hydroponic conditions. *Ecotoxicology and environmental safety,* 82, 122-126

Kaur, S., & Roy, A. (2021). Bioremediation of heavy metals from wastewater using nanomaterials. *Environmental Development and Sustainability*, 23 (4), 9617.

Khan, Z. R., Midega, C. A., Wadhams, L. J., Pickett, J. A., & Mumuni, A. (2007). Evaluation of Napier grass (*Pennisetum purpureum*) varieties for use as trap plants for the management of African stemborer (*Busseola fusca*) in a push–pull strategy. *Entomologia Experimentalis et Applicata, 124* (2), 201–211.

Khoso, W., Haleem, N., Baig, M., & Jamal, Y. (2021). Synthesis, characterization and heavy metal removal efficiency of nickel ferrite nanoparticles (NFN's). *Scientific. Reports*, 11 (1), 1-10.

Kim, S.J., Choi, D.H., Sin, D. S., & Oh, Y. (2005). Evaluation of bioremediation effectiveness on crude oil – contaminated sand. *Chemosphere,* 59, 844 – 852

Kołodziejczak-Radzimska, A., & Jesionowski T. Zinc (2014). Oxide-from synthesis to application: A review. *Materials* (Basel), 7(4), 2833-2881.

Kostrz, M., & Satora, P. (2017) . Compounds responsible for air pollution. *Ecological Engineering*, 18 (6), 89–95.

Kuiper, I., Lagendijk, E.L., Bloemberg, G.V., & Lugtenberg, B.J. (2004). Rhizoremediation, a beneficial plant-microbe interaction. *Molecular Plant Microbe Interactions,* 17(1), 6–15

Kumari, S., Raturi, S., Kulshrestha, S., Chauhan, K., Dhingra, S., András, K., Thu, K., & Singh, T. (2023) A comprehensive review on various techniques used for synthesizing nanoparticles. *Journal of Materials Research and Technology, 27(*1), 1739-1763.

Lagopati, N., Gatou, M.A., Gogou, A., & Pavlatou, E. A. (2020). Synthesis of zinc oxide nanoparticles using biological substrates: A review. *United Journal of Nanotechnology and Pharmaceutics*, 1, 1–7.

Lee, H., Yun, S., Jang, S., Kim, G., & Kim, J. (2015). Bioremediation of polycyclic aromatic hydrocarbons in creosote-contaminated soil by *Peniophora incarnata*. *Bioremediation J*ournal, 19 (1), 1-8

Lima, E ., Silva, A., Carvalho, M.,de Souza, S., Dias, P., Silva, F., & Saramago, C. (2012). Heavy metals tolerance (Cr, Ag, and Hg) in bacteria isolated from sewage. *Journal of Microbiology*, 43(4), 1620-1631.

Liu, X., Shen, Y., Lou, L., Ding, C., & Cai, Q. (2009). Copper tolerance of the biomass crops Elephant grass (*Pennisetum purpureum* Schumach), Vetiver grass (*Vetiveria zizanioides*) and the upland reed (*Phragmites australis*) in soil culture. *Biotechnology Advances, 27*(5), 633-640.

Loureiro, A., Azoia, N.G., Gomes, A.C., Cavaco-Paulo. A. (2016). Albumin-based nanodevices as drug carriers. *Curr. Pharm. Des*., 22, 1371-1390

Maduekwe, C., Nwachukwu, E. O., & Joel, O. F. (2016). "Comparative study of rena and mycoremediation techniques in reduction of heavy metals in crude oil impacted soil". Paper presented at the SPE Nigeria Annual International Conference and Exhibition, Lagos, Nigeria.

Mannetje, L., & Jones, R. (1992). *Pennisetum purpureum* Schumach. Record from *Proseabase.* PROSEA (Plant Resources of South-East Asia) Foundation, Bogor, Indonesia.

Manor, J., Feldblum, E., Zanni, M., & Arkin, I. (2012). Environment polarity in proteins mapped noninvasively by FTIR spectroscopy. *J Phys Chem Lett.,* 3 (7), 939–44.

Mason, C., Vivekanandhan, S., Misra, M., & Mohanty, A. (2012). "Switchgrass (*Panicum virgatum*) extract mediated green synthesis of silver nanoparticles," *World Journal of Nano Science and Engineering*, 2, 47–52.

McCutcheon, S.C., & Schnoor, J. L. (2003). Overview of phytotransformation and control of waste and contaminants. Wiley-Interscience Publishers. 3-58.

Meagher, R.B (2000). Phytoremediation of toxic elemental organic pollutants. *Curr Opin Plant Biol*., 3,153–162.

Mukhopadhyay, R., Sarkar, B., Khan, E., Alessi, D., Biswas, J., Manjaiah, K.M., Eguchi, M., Wu, K. C. & Yamauchi, Y.S. (2021). Nanomaterials for sustainable remediation of chemical contaminants in water and soil. *Crit. Rev. Environ. Sci. Technol*. 1-50.

Nadeem, J., & Dirk, L.,(2022). Nanoparticle classification, physicochemical properties, characterization, and applications: a comprehensive review for biologists. *Journal of Nanobiotechnology,* 20, 262.

Naraboyina, D., & Rastogi, A.K. (2014). Remediation techniques for BTEX contamination of groundwater. *International Journal of Engineering Research & Technology,* 3 (3), 1-6.

Neethu, T. M., Dubey, P. K., Kaswala, A. R. & Patel, K.G. (2019). "Cow Dung as a bioremediation agent to petroleum hydrocarbon contaminated agricultural soils". *Current Journal of Applied Science and Technology, 38* (6), 1-9.

Neethu, T. M., Dubey, P. K., Kaswala, A. R., & Patel, K. G. (2019). Cow Dung as a Bioremediation Agent to Petroleum Hydrocarbon Contaminated Agricultural Soils. *Current Journal of Applied Science and Technology,* 38 (6), 1-9.

Njoku, K., Asunmo, M., Ude, E., Adesuyi, A., & Oyelami, A. (2020). The molecular study of microbial and functional diversity of resistant microbes in heavy metal contaminated soil. *Environmental Technology & Innovation*, 17(1), 100606.

Nkwoocha, E. E., & Duru, P. O. ( 2010). Micro-analytic study on the effect of oil pollution on local plant species and food crops. *Advances in Bioresearch,*1 (1), 189-198

Norman, J.H. (2001). Nontechnical Guide to Petroleum Geology, Exploration, Drilling, and Production , 4th edition. *Penn Well*, 1- 4.

Nwankwegu, A. S., Orji, M. U., & Onwosi, C. O. (2016). Studies on organic and in-organic biostimulants in bioremediation of diesel-contaminated arable soil. *Chemosphere,* 162, 148-156.

Nwaogu, L.A., Alisi, C. S., Ibegbulem C. O., & Igwe, C.U (2007). Phytochemical and antimicrobial activity of ethanolic extract of *Landolphia owariensis* leaf. *African Journal of Biotechnology*, 6 (7), 890-893

Nwaoguikpe, R. N. (2011). The effect of crude oil spill on the ascorbic acid content of some selected vegetable species: *Spinach oleraceae*, and *Talinum triangulare* in an oil polluted soil. *Pakistan J Nutr.,*10, 274-81.

Nwauche, C.A., & Akani, C.I. (2006). An assessment of high risk sexual behaviour and HIV transmission among migrant oil workers in the Niger Delta area of Nigeria. *Niger J Clin Pract.,* 9, 48-51. 50.

Nwilo, P. C., & Badejo, O. T. (2001). Impacts of Oil spills along the Nigerian coast. *The Association for Environmental Health and Sciences*. *International Issues,* 119 (1), 2006.

Ociepa-Kubicka, A., & Ociepa, E. (2012). Toxic effects of heavy metals on plants, animals and people. *Environmental Protection Engineering*, 15(2), 169–180.

Okon, O. (2017). "Bioaccumulation of heavy metals in *Cucurbita maxima* duch. and *Telfairia occidentalis* grown on crude oil polluted soil citation". *American Journal of Agricultural Science*. 4, 88–93.

Onwuakor, C. E., & Orok, F. E. (2014). Microbiological and physicochemical characteristics of soil contaminated with used petroleum products in Umuahia, Abia State, Nigeria. *Journal of Applied & Environmental Microbiology,* 2(6), 281-286.

Ordinioha, B., & Sawyer, W. (2008). Food insecurity, malnutrition and crude oil spillage in a rural community in Bayelsa State, South-South Nigeria. *Niger J Med,*17, 304-309

Orisakwe, E. O., Akumka, D. D., Njan, A. A., & Afonne, O. J. (2004). Testicular toxicity of Nigerian Bonny light crude oil in male albino rats. *Reproductive Toxicology*, 18 (3), 439-442.

Osam, M. U., Wegwu, M.O., & Uwakwe, A. A. (2011). The Omoku old pipeline oil spill. Total hydrocarbon content of affected soils and the impact on the nutritive value of food crops. *Archives of Applied Science Research*, 3 (3), 514-521.

Osmana, N. A., Roslana, A. M., Ibrahima, M. F., & Hassana, M. A. (2020). Potential use of *Pennisetum purpureum* for phytoremediation and bioenergy production: A mini review. *Sci. Rep*, 10(1), 6613.

Osuji, L. C., & Nwoye, I. (2007). An appraisal of the impact of petroleum hydrocarbons on soil fertility: The Owaza experience. *Afr J Agric Res.,* 2, 318-24.

Ovais, M. (2018). Role of plant phytochemicals and microbial enzymes in biosynthesis of metallic nanoparticles. *Appl. Microbiol. Biotechnol*., 102, 6799–6814.

Priyanka, K., Kamakhya, P., Saikat, C., Susruta, S. (2021). A brief review on transition metal ion doped ZnO nanoparticles and its optoelectronic applications, *Materials Today*, 43 (5), 3297-3302.

Qu, Z., Liu, P., Yang, X., Wang, F., Zhang, W., & Fei, C. (2016). Microstructure and characteristic of $BiVO_4$ prepared under different ph values: photocatalytic efficiency and antibacterial activity. *Materials*, *9* (3), 129.

Rahman, F., Majed, P., Bakar, S., Bashar, M., Haque, M., Akter, B., Rashid, R., Haque, M., & Royhan, U. (2022). Green synthesis of zinc oxide nanoparticles using Cocos nucifera leaf extract: characterization, antimicrobial, antioxidant and photocatalytic activity. *R. Soc. Open Sci. 9* (1)*, 220858.*

Ramesh, P., Saravanan, K., Manogar, P., Johnson, J., Vinoth, E., & Mayakannan, M. (2021). Green synthesis and characterization of biocompatible zinc oxide nanoparticles and evaluation of its antibacterial potential. *Sens. Biosensing. Res*., 31, 100399.

Ramsden, J. ( 2016). Nanotechnology*,* an introduction. *Nanotechnology and sustainability,* 14 (3), 19–40.

Rana, A., Yadav, K. & Jagadevan, S. A (2020). Comprehensive review on green synthesis of nature-inspired metal nanoparticles: Mechanism, application and toxicity. *J. Clean. Prod.,* 272..

Reed, S. M., & Hutchison, J. E . (2000). "Green Chemistry in the organic teaching laboratory: an environmentally benign synthesis of adipic acid," *Journal of Chemical Education,* 77 (12), 1627–1628.

Remediation of contaminated soils by biotechnology with nanomaterials: bio-behavior, applications, and perspectives. *Critical Review Biotechnol*ogy, 38 (3). 455-468

Resinger, H. J. (1995). Hydrocarbon bioremediation an overview in Department of Applied Microbiology and Brewing, Faculty of Bioscience, Nnamdi Azikiwe University, Awka, Anambra State.

Reuben, S. Dangana, R., Chinedu, G. & Femi, K. (2023). The biosynthesis of zinc oxide nanoparticles using aqueous leaf extracts of *Cnidoscolus aconitifolius* and their biological activities, *Green Chemistry Letters and Reviews*, 16 (1), 2169591.

Rice, A. L., Sacco, L., Hyder, A., Black, R. E.( 2000). Malnutrition as an underlying cause of childhood deaths associated with infectious diseases in developing countries. *Bull World Health Organization,*78,1207-21.

Rogozea, E. A., Petcu, A. R., Olteanu,N. L., Lazar, C. A., Cadar, D., Mihaly, M. (2017).

Ron, E. Z., & Rosenberg, E. (2014): Enhanced bioremediation of oil spills in the sea. *Current Opinion in Biotechnology,* 27, 191-194.

Rufino, R. D., de Luna, J. M., de Campos Takaki, G. M., & Sarubbo, L. A. (2014). Characterization and properties of the biosurfactant produced by *Candida lipolytica*. *Electronic Journal of Biotechnology,* 17, 34-38.

Rupa, S.A, Moni, M.R., Patwary, M., Mahmud, M., Haque, M., Uddin, J., & Abedin, S. (2022). Synthesis of novel tritopic hydrazone ligands: spectroscopy, biological activity, DFT, and molecular docking studies. *Molecules,* 27, 1–22.

Ryu, H., Park, B., Akbar, S. A. & Lee, W., Hong, K., Seo, Y., Shin, D., Park, J., & Choi, G. (2003). ZnO sol–gel derived porous film for CO gas sensing. *Sensors and Actuators B-chemical,* 96 (3), 717-722.

Sabouri, M., Sabouri, M.S., Amiri, M. & Khatami, M. ( 2022). Plant-based synthesis of cerium oxide nanoparticles using *Rheum turkestanicum* extract and evaluation of their cytotoxicity and photocatalytic properties. *Mater Technol*., 37: 555-568.

Saleem, S., Jameel, M.H., Akhtar, N., Nazir, N., Ali, A., Zaman, A., Rehman, A., Butt, S., Sultana, F., Mushtaq, M., Zeng, J.H., Amami, M., & Althubeiti, K.(2022). Modification in structural, optical, morphological, and electrical properties of zinc oxide (ZnO) nanoparticles by metal (Ni, Co) dopants for electronic device applications. *Arabian Journal of Chemistry*, 15 (1), 103518.

Sall, M., Diaw, A., Gningue-Sall, D., Efremova Aaron, S., & Aaron, J. J. (2020). Toxic heavy metals: impact on the environment and human health, and treatment with conducting organic polymers, a review. *Environmental Science Pollution. Res*earch, 27(24), 29927-29942.

Sánchez, A., Rejillas, S., Font, S., Xavier, E., González, E., & Puntes, V. (2011). Ecotoxicity and remediation with engineered inorganic nanoparticles in the environment. *Trends in Analytical Chemistry*. 30(3). 507.

Schrick, B., Hydutsky, B.W., Blough, J.L., & Mallouk, T. E. (2004). Delivery Vehicles for Zerovalent Metal Nanoparticles in Soil and Groundwater. *Chemistry of Materials,* 16 (11), 2187–2193.

Senthamarai, M. D., & Malaikozhundan, B. (2022). Synergistic action of zinc oxide nanoparticle using the unripe fruit extract of *Aegle marmelos* (L.)—Antibacterial, antibiofilm, radical scavenging and ecotoxicological effects. Mater. *Today Commun*. 30, 103228.

Shukla, A & Srivastava, S (2017). Emerging Aspects of Bioremediation of Arsenic, *Green Technologies and Environmental Sustainability*, 395–407,

Silva, L., Solis-Pomar, F., Gutiérrez-Lazos, C., Manuel, F., Meléndrez, E., Martinez, A., Fundora, E., & Pérez-Tijerina. (2014). Synthesis of Fe nanoparticles functionalized with oleic acid synthesized by inert gas condensation. *Journal of Nanomaterials,* 1-6

Singhal, G., Bhavesh, R., Kasariya, K., Sharma, A., & Singh (2011). "Biosynthesis of silver nanoparticles using (Tulsi) leaf extract and screening its antimicrobial activity," *Journal of Nanoparticle Research*, 13 (7), 2981– 2988.

Sirelkhatim, A., Mahmud, S., Seeni, A., Kaus, N., Ann, L.C., Bakhori, S., Hasan, H., & Mohamad, D. (2015). Review on Zinc Oxide Nanoparticles: Antibacterial Activity and Toxicity Mechanism. *Nanomicro Letters,* 7(3), 219-242.

Speight, J. G. (2006). The Chemistry and Technology of Petroleum. CRC Press.

Steiner, R. (2010) Double Standard: Shell Practices in Nigeria Compared with International Standards to Prevent and Control Pipeline Oil Spills and the Deepwater Horizon Oil Spill. Milieudefensie, Amsterdam, 11-15.

Sutradhar, P., & Saha, M. (2016). Green synthesis of zinc oxide nanoparticles using tomato (Lycopersicon esculentum) extract and its photovoltaic application. *J. Exp. Nanosci.,* 11, 314–327.

Suwanboon, S., Amornpitoksuk, P., Bangrak, P., & Randorn, C. (2014). Physical and chemical properties of multifunctional ZnO nanostructures prepared by precipitation and hydrothermal methods. *Ceramics International*. 40(1), 975-983.

Swadeshmukul, Z., Peng, W., Kemin, T., & Rovelyn, T. (2001). Conjugation of biomolecules with luminophore-doped silica nanoparticles for photostable biomarkers. *Anal. Chem*., 73, 4988-4993.

Tanee, F., & Albert, E. (2011). Post-remediation assessment of crude oil polluted site at Kegbara-Dere community, Gokana L.G.A. of Rivers State, Nigeria. *Journal of Bioremediation and Biodegradation*.

The Welding Institute (2024). What are nanoparticles? Definition, size, uses and properties. Retrieved from *https://theweldinginstitute.com*

Todescato, F., Fortunati, I., Minotto, A., Signorini, R., Jasieniak, J., & Bozio, R. (2016). Engineering of semiconductor nanocrystals for light emitting applications. *Materials*, 9, 672.

Tratnyek, P. G., & Johnson, R. L. (2006). Nanotechnologies for environmental cleanup. *Nano Today*, 1, 44-48.

Tundo, P., & Anastas, P. (2000). Green chemistry: Challenging perspectives, Oxford University Press, Oxford, UK.

Ubani O., Atagana, H., & Thantsha, M. (2013). Biological degradation of oil sludge. A review of the current state of development. *African Journal of Biotechnology*. 12, 6544–6567.

Ukpaka, C.P , Uku, P.E, Amadi, S.A ., & Dagde, K.K. (2020). Characteristics of Physicochemical Parameters of Elephant Grass Mixture for the Remediation of Crude Oil Polluted Swampy Soil. *International Journal of Petroleum and Petrochemical Engineering,* 6(4).

United Nations Development Programme (UNDP). (2006). Niger Delta human development report. Abuja, Nigeria. 20.

United Nations Environment Programme (UNEP). ( 2011). The UNEP Environmental Assessment of Ogoniland.

United Nations Environmental Programme (2017). Ogoni land oil assessment reveals extent of environmental contamination and threats to human health.

United States Environmental Protection Agency (USEPA) 3540C (1996). Soxhlet extraction method. Revision 3

United States Environmental Protection Agency (USEPA). (1984). Guidelines establishing Test Procedures for the analysis of pollutants under the clean water Act, method 624.

USEPA. Method 8015. (2007). Non halogenated Organics by Gas chromatography

Varjani, S. J., Rana, D.P., Jain, A.K., Bateja, S. & Upasani, V.N. (2018). Synergistic ex-situ biodegradation of crude oil by halotolerant bacterial consortium of indigenous strains isolated from on shore sites of Gujarat, *India. Int Biodeter Biodegrad.,* 103,116–24.

Vázquez-Núñez, E., Molina-Guerrero, C. E., Peña-Castro, J. M., Fernández-Luqueño, F., & de la Rosa-Álvarez, M. G. (2020). Use of nanotechnology for the bioremediation of contaminants. A Review. *Processes*, *8*(7), 826.

Venetz, J.E., Del Medico, L., Wölfle, A., Schächle, P., Bucher, Y., & Appert, D. (2019). Chemical synthesis rewriting of a bacterial genome to achieve design flexibility and biolo gical functionality. *Proc Natl Acad Sci.,* 116 (16), 8070–9z.

Venosa, A. D., Suidan, M. T., Wrenn, B. A., Strohmeier, K. L., Haines, J. R., Eberhart, B. L., King, D., & Holder, E. (2001). Bioremediation of an experimental oil spill on the shoreline of Delaware Bay. *Environmental Science and Technology*, 30(5), 1764-1775.

Vouillamoz, J., & Milke, M. W. (2001). "Effect of compost in phytoremediation of diesel-contaminated soils". *Water Science and Technology*, 43 (2), 291–295.

Vu, K. A., & Mulligan, C. N. (2022). Utilization of a biosurfactant foam/nanoparticle mixture for treatment of oil pollutants in soil. *Environmental Science and Pollution Research,* 29,88618–88629.

Wackett, L.P. (1996). Co-Metabolism: is the Emperor Wearing any Clothes? *Current Opinion in Biotechnology*, 7, 321-325.

Wang, F.H. & Chang, C.L. ( 2016). Effect of substrate temperature on transparent conducting Al and F co-doped ZnO thin films prepared by magnetron sputtering. *Applied Surface Science, 370*, 83– 91.

Xu, F., Yuan, Y., Han, H., Wu, D., Gao, Z., & Jiang, K. (2012). Synthesis of ZnO/CdS hierarchical heterostructure with enhanced photocatalytic efficiency under nature sunlight. *Cryst Eng Comm*., 14(10), 3615-3622.

Yan, L., & Chuan-sheng, L (2009). Hydro/solvo-thermal synthesis of ZnO crystallite with particular morphology. *Transactions of Nonferrous Metals Society of China,* 19 (2), 399–403

Zulfa, A. D., Samir, J., Dhabia, A.T., Saeed, A.M., & Nabil, Z. (2017). Considering the specific impact of harsh conditions and oil weathering on diversity, adaptation, and activity of hydrocarbon-degrading bacteria in strategies of bioremediation of harsh oily-polluted soils. *BioMed Research International. 3 (1), 99-101.*

## APPENDIX 1

Table 1: XRD phase name and chemical composition of cow dung zinc oxide nanoparticles.

| **2θ($^0$)** | **Phase name** | **Chemical formula** |
|---|---|---|
| 28.87 | Zincite | ZnO |
| 32.05 | Zincite | ZnO |
| 34.78 | Zincite | ZnO |
| 36.58 | Zincite | ZnO |
| 47.77 | Zincite | ZnO |
| 57.00 | Zincite | ZnO |
| 63.09 | Zincite | ZnO |
| 68.13 | Zincite | ZnO |

## APPENDIX 2

Table 2: XRD phase name and chemical composition of *Pennisetum purpureum* zinc oxide nanoparticles.

| **2θ(degree)** | **Phase name** | **Chemical formula** |
|---|---|---|
| 28.56 | Zincite | ZnO |
| 31.06 | Zincite | ZnO |
| 31.80 | Zincite | ZnO |
| 32.68 | Zincite | ZnO |
| 34.50 | Zincite | ZnO |

| | | |
|---|---|---|
| 36.33 | Zincite | ZnO |
| 47.59 | Zincite | ZnO |
| 56.55 | Zincite | ZnO |
| 62.86 | Zincite | ZnO |
| 68.02 | Zincite | ZnO |